UCL INSTITUTE OF CARDVIOVASCULAR SCIENCE

Cardiovascular Magnetic Resonance Augmented Cardiopulmonary Exercise Testing (CMR-CPET) in Exercise Intolerance.

Dr James Thomas Brown

PhD Thesis

University College London

UCL Department of Cardiac MRI, Royal Free Hospital
Pond Street
London
NW3 2QG

2024

DECLARATION

I, James Thomas Brown, confirm that the work presented in my thesis is my own. Where information has been derived from other sources, I confirm that this has been indicated in this thesis.

Signature: [redacted]

Name: Dr James Thomas Brown

Date: 27/08/2024

CONTENTS

Table of Contents

1. ABSTRACT 7

1.1 BACKGROUND 7
1.2 AIMS 8
1.3 RESULTS AND CONCLUSIONS 8

2. IMPACT STATEMENT 9

3. ETHICAL APPROVAL AND FUNDING 11

3.1 ETHICAL APPROVAL 11
3.2 FUNDING 11

4. RESEARCH PAPER DECLARATION FORMS 12

4.1 UCL RESEARCH PAPER DECLARATION FORM 1 12
4.2 UCL RESEARCH PAPER DECLARATION FORM 2 15
4.3 UCL RESEARCH PAPER DECLARATION FORM 3 18

5. ACKNOWLEDGEMENTS 21

6. ABBREVIATIONS 23

7. INTRODUCTION 30

7.1 EXERCISE INTOLERANCE 30
7.2 EXERCISE PHYSIOLOGY UNDER NORMAL CONDITIONS 34
7.2.1 Mitochondria and myocytes *34*
7.2.2 Vascular beds and the heart *37*
7.2.3 Ventilation centres and the lungs *39*
7.3 INVESTIGATING MECHANISMS OF EXERCISE INTOLERANCE 41
7.3.1 The Respiratory System *42*
7.3.2 The Cardiovascular system *44*
7.3.3 Musculoskeletal system *48*
7.3.4 Integrating Tests of Multiple Systems *49*

8. SPECIAL POPULATIONS WITH EXERCISE INTOLERANCE 55

8.1 PULMONARY HYPERTENSION 55
8.1.1 Pulmonary arterial hypertension *57*
8.1.2 Pulmonary arterial hypertension therapies *62*
8.2 LONG-COVID 64

9. RESEARCH AIMS AND OBJECTIVES 66

10. METHODS AND MATERIALS 67

10.1 PHASE CONTRAST MR 67
10.2 VENTRICULAR VOLUMETRIC ASSESSMENT 72
10.3 EXERCISE CMR 75
10.4 CPET-CMR EQUIPMENT 75
10.5 IMAGE RECONSTRUCTION AND ANALYSIS 76

11. RESULTS - COMPARING THE MECHANISMS OF EXERCISE LIMITATION IN SYSTEMIC SCLEROSIS, SYSTEMIC SCLEROSIS-ASSOCIATED PULMONARY HYPERTENSION AND NON-CONNECTIVE TISSUE-ASSOCIATED PULMONARY HYPERTENSION 78

11.1 INTRODUCTION 78
11.2 METHODS 80

11.2.1 Study population ... *80*
11.2.2 CMR-augmented cardiopulmonary exercise testing ... *82*
11.2.4 Exercise protocol ... *82*
11.2.5 Data analysis ... *84*
11.2.6 Statistical analysis ... *85*
11.3 RESULTS ... 86
11.3.1 Demographics and clinical data ... *86*
11.3.2 Resting CMR-CPET ... *89*
11.3.3 Exercise feasibility ... *91*
11.3.4 Exercise CMR-CPET metrics ... *92*
11.3.5 Relationship between exercise metrics and lung function and haemoglobin ... *95*
11.3.6 Relationship between exercise metrics and myocardial T1 and T2 ... *95*
11.4 DISCUSSION ... 96
11.5 LIMITATIONS ... 99
11.6 CONCLUSIONS ... 100

12. RESULTS - COMPARING THE MECHANISMS OF ONGOING EXERCISE INTOLERANCE IN COVID-19 PATIENTS. ... **101**

12.1 INTRODUCTION ... 101
12.2 METHODS ... 103
12.2.1 Study Population ... *103*
12.2.2 Clinical Assessment ... *104*
12.2.3 MR-Augmented Cardiopulmonary Exercise Testing ... *105*
12.2.4 MR Imaging Techniques (Real-Time Flow and Volume Imaging) ... *105*
12.2.5 Respiratory Gas Analysis ... *106*
12.2.6 Exercise Protocol ... *106*
12.2.7 Data Processing ... *107*
12.2.8 Statistical Analysis ... *108*
12.3 RESULTS ... 109
12.3.1 Demographics and Clinical Data ... *109*
12.3.2 Resting CMR-CPET ... *112*
12.3.3 Exercise Feasibility ... *114*
12.3.4 Exercise MR-CPET Metrics ... *115*
12.3.6 Disease Severity and CMR-CPET Metrics ... *118*
12.4 DISCUSSION ... 118

13. RESULTS - THE PROGNOSTIC UTILITY OF EXERCISE CMR IN INTERMEDIATE RISK SYSTEMIC SCLEROSIS ASSOCIATED PULMONARY HYPERTENSION ... **125**

13.1 INTRODUCTION ... 125
13.2 METHODS ... 127
13.2.1 Patient population ... *127*
13.2.2 Clinical data ... *128*
13.2.3 CMR-augmented cardiopulmonary exercise testing ... *128*
13.2.4 CMR imaging techniques (real-time flow and volume imaging) ... *129*
13.2.5 Respiratory gas analysis ... *129*
13.2.6 Exercise protocol ... *130*
13.2.7 Data analysis ... *130*
13.2.8 Statistics ... *131*
13.3 RESULTS ... 132
13.3.1 Study population ... *132*
13.3.2 Resting CMR-CPET ... *134*
13.3.3 Exercise feasibility ... *136*
13.3.4 Predictors of mortality ... *140*
13.4 DISCUSSION ... 142
13.4.1 Limitations ... *145*
13.5 CONCLUSIONS ... 146

14. DISCUSSION AND CONCLUSIONS 147

14.1 MECHANISMS OF EXERCISE LIMITATION IN SYSTEMIC SCLEROSIS, SYSTEMIC SCLEROSIS-ASSOCIATED PULMONARY ARTERIAL HYPERTENSION AND NON-CONNECTIVE TISSUE ASSOCIATED PULMONARY HYPERTENSION. 148
14.2 MECHANISMS OF ONGOING EXERCISE INTOLERANCE IN COVID-19 PATIENTS 149
14.3 PROGNOSTIC UTILITY OF EXERCISE CMR IN INTERMEDIATE RISK SYSTEMIC SCLEROSIS ASSOCIATED PULMONARY ARTERIAL HYPERTENSION 149
14.4 FUTURE WORK 150

15. PUBLICATIONS 153

15.1 PUBLICATIONS ARISING FROM RESEARCH FELLOWSHIP 153
15.2 PRESENTATIONS AND POSTERS 157

16. BIBLIOGRAPHY 158

Tables

TABLE 1. GRADING OF EXERCISE INTOLERANCE 31
TABLE 2. SUBJECT DEMOGRAPHICS. 86
TABLE 3. SUBJECT CHARACTERISTICS. 87
TABLE 4. HEMODYNAMIC MEASUREMENTS FOR PULMONARY HYPERTENSION GROUPS, CLINICAL MEASUREMENTS FOR ALL PATIENT GROUPS. 88
TABLE 5. RESTING CPET AND CMR METRICS. 90
TABLE 6. EXERCISE METRICS FOR ALL GROUPS. 91
TABLE 7. PEAK EXERCISE CPET AND CMR METRICS 92
TABLE 8. SUBJECT CHARACTERISTICS. 110
TABLE 9. CLINICAL DATA FOR PATIENT GROUPS. 111
TABLE 10. RESTING CMR-CPET DATA. 113
TABLE 11. METRICS OF EXERCISE PERFORMANCE. 114
TABLE 12. EXERCISE CMR-CPET DATA 116
TABLE 13. CLINICAL DETAILS OF THE STUDY COHORT. 133
TABLE 14. DIFFERENCES IN CLINICAL DATA, PAH RISK STRATIFICATION DATA AND RESTING CMR-CPET IN DEAD COMPARED TO ALIVE PATIENTS 135
TABLE 15. CHANGES IN CMR-CPET METRICS WITH EXERCISE. 137
TABLE 16. DIFFERENCES BETWEEN INTERMEDIATE-LOW RISK AND INTERMEDIATE-HIGH RISK PATIENTS IN REST AND EXERCISE CMR METRICS 138
TABLE 17. DIFFERENCES IN EXERCISE CMR-CPET METRICS IN DEAD COMPARED TO ALIVE PATIENTS. 139

Figures

FIGURE 1. SCHEMATIC OF THE ROLE OF WORKLOAD AND DURATION IN EXERCISE INTOLERANCE. 30
FIGURE 2. THE ATP-DEPENDENT MECHANISM OF SKELETAL MUSCLE CONTRACTION 35
FIGURE 3. AEROBIC VS. ANAEROBIC RESPIRATION. 36
FIGURE 4. INCREASE IN CARDIAC OUTPUT AND CHANGES TO BLOOD FLOW DISTRIBUTION DURING EXERCISE. 39
FIGURE 5. COUPLING OF CELLULAR AND RESPIRATORY RESPIRATION 40
FIGURE 6. CARDIOPULMONARY EXERCISE TEST EQUIPMENT 50
FIGURE 7. FLOWCHART FOR DIFFERENTIAL DIAGNOSIS OF EXERTIONAL DYSPNOEA AND FATIGUE. 51
FIGURE 8. EXERCISE CMR MODALITIES. 53
FIGURE 9. COMPARISON OF CMR-CPET VO_2 VALUES OBTAINED AT PEAK EXERCISE VERSUS CONVENTIONAL CPET VO_2 54
FIGURE 10. CLASSIFICATION, PREVALENCE AND THERAPEUTIC STRATEGIES OF PULMONARY HYPERTENSION GROUPS 57
FIGURE 11. SCHEMATIC OF CHANGES IN PULMONARY ARTERIES AND RIGHT VENTRICLE IN PAH. 58
FIGURE 12. DETECT ALGORITHM 61
FIGURE 13. THERAPEUTIC TARGETS IN PULMONARY ARTERIAL HYPERTENSION 64

Figure 14. Proton magnetic moments 68
Figure 15. Magnetic field gradients within a MRI scanner. 68
Figure 16. Representation of phase contrast MR. 69
Figure 17. Measurement of aortic flow and cardiac output using PC-MR 71
Figure 18. Assessment of ventricular volumes. 74
Figure 19. CMR-CPET equipment. 76
Figure 20. Exercise protocol 83
Figure 21. CMR-CPET Metrics at rest and peak-exercise for each subject group 93
Figure 22. Stroke volume, heart rate and ventricular ejection fraction at rest and peak-exercise for each subject group 94
Figure 23. Exercise protocol and cumulative workload. 107
Figure 24. CMR-CPET metrics at rest and peak exercise for each subject group. 117
Figure 25. Forest plot of resting CMR and CPET variables to predict all-cause mortality on univariable Cox regression analysis. 140
Figure 26. Forest plot of peak exercise CMR and CPET variables to predict all-cause mortality on univariable Cox regression analysis. 141
Figure 27. Kaplan-Meier plots 142

Equations

Equation 1. The Fick equation 42
Equation 2. Cardiac Output 44
Equation 3. Phase shift of hydrogen nuclei in a gradient magnetic field. 69

1. ABSTRACT

1.1 Background

Exercise intolerance is common to many diseases. Investigation of exercise intolerance frequently isolates the respiratory and/or cardiovascular systems, but this approach neglects other systems that can contribute significantly. Furthermore, many investigations are performed in the *resting* state. Without assessing all relevant systems in the *exercise* state, any understanding of exercise intolerance would be incomplete.

Combining Cardiovascular Magnetic Resonance Imaging (CMR) and Cardiopulmonary Exercise Testing (CPET) - "CMR-CPET" - allows *simultaneous and comprehensive* measurement of physiological metrics that determine exercise capacity. CPET allows measurement of oxygen consumption (VO_2) and carbon dioxide production (VCO_2), and derivation of various metrics associated with respiratory and metabolic function. CMR allows accurate measurement of cardiac output (CO) and ventricular size and function. From these two tests, arteriovenous blood oxygen content gradients (ΔavO_2) can be calculated. This metric represents tissue oxygen extraction at the skeletal muscle level. A comprehensive assessment of the respiratory, cardiovascular and musculoskeletal system function is therefore possible with this technique at rest, and importantly, during exercise.

1.2 Aims

In this thesis, using CMR-CPET, I aimed to assess the mechanisms affecting exercise tolerance in different patient groups. Firstly, I measured these CMR-CPET metrics at rest and at peak exercise, examining differences between groups. Secondly, I assessed if these metrics provided prognostic information in patients with systemic sclerosis-associated pulmonary arterial hypertension (SSc-PAH).

1.3 Results and Conclusions

I demonstrated that there are differences in tissue oxygen extraction at peak exercise which may explain exercise capacity differences between subtypes of pulmonary arterial hypertension, and differences in stroke volume augmentation during exercise in patients with prolonged COVID-19 symptoms. Finally, I showed that in SSc-PAH, right ventricular contractile reserve provides additional prognostic information to current risk stratification tools. CMR-CPET aids our understanding of the mechanisms causing exercise intolerance, provides novel biomarkers and identifies potential treatment targets.

2. IMPACT STATEMENT

Cardiac magnetic resonance augmented cardiopulmonary exercise testing ("CMR-CPET") is a technique that has shown promise in identifying mechanisms contributing to exercise intolerance (EI) in paediatric pulmonary hypertension and adult haemoglobinopathy populations in proof-of-concept studies. This thesis builds on that work, performing CMR-CPET in larger adult populations with conditions where EI is a predominant feature.

Firstly, this work confirms that CMR-CPET is a safe, well-tolerated investigation. I performed CMR-CPET in 20 healthy volunteers and 137 patients without complication. Using CMR-CPET, I performed maximal exercise tests on 97 patients with pulmonary hypertension (PH) - including 6 on intravenous therapy, a population traditionally considered high risk for exercise testing. With appropriate selection, PH should not preclude exercise testing in an MRI environment.

Secondly, harnessing the comprehensive assessment of respiratory, cardiovascular and musculoskeletal physiology that CMR-CPET allows, I investigated patients with the rare but debilitating condition, systemic sclerosis (SSc). Exercise intolerance is a predominant symptom in this multisystem inflammatory disorder and causes reduced quality of life. My work shows that SSc patients have reduced skeletal oxygen extraction at peak exercise, and this finding contributes to exercise intolerance. Furthermore, CMR-CPET provides a biomarker (non-invasive avO_2) to assess the effect of interventions targeting improved skeletal muscle oxygen uptake, (e.g. exercise programmes or skeletal muscle anti-inflammatory therapy).

Thirdly, a subset of SSc patients develop associated pulmonary arterial hypertension (SSc-PAH). This form of PAH can be less severe (in terms of pulmonary arterial pressures and vascular resistance) than other forms of PAH, but is paradoxically associated with worse symptoms and poorer prognosis. My thesis identified that reduced right ventricular contractile reserve at peak exercise is a putative mechanism of exercise intolerance in two groups of pulmonary hypertension patients. Whilst this finding was anticipated, the combination of SSc *and* PAH (SSc-PAH) resulted in a "double hit" of decreased skeletal muscle oxygen extraction *and* reduced RV contractile reserve causing exercise intolerance, which is a novel finding and explains the paradoxical findings above.

Fourthly, most patients with SSc-PAH are graded as being at "intermediate risk" of death at 1 year using contemporary guideline-directed risk scores. Together with more reassuring pulmonary haemodynamics, this may result in less intensive therapy than might be warranted. Work in this thesis identifies a group of these intermediate risk SSc-PAH patients in whom uncoupling of the right ventricle and pulmonary artery is unmasked by exercise CMR testing (at an earlier stage of their disease than would otherwise be detected with conventional testing), a finding associated with worse prognosis (and which potentially explains the "prognosis paradox" above). Furthermore, I define a cut-off for RV contractile reserve that might promote earlier, more intensive treatment.

Finally, my work during the COVID-19 pandemic allowed identification of the likely putative mechanism behind prolonged exercise intolerance post-infection, namely a reduction is venous pre-load. This raised the prospect of a possible treatment which would have the benefits of simple administration, minimal side-effects and low cost, namely promoting fluid/electrolyte intake.

3. ETHICAL APPROVAL AND FUNDING

3.1 Ethical Approval

All participants whose data was used in the research studies described in this thesis gave explicit informed consent by signing a consent form whilst visiting the centre. The research was approved by national ethics committee (IRAS project ID 226101; REC reference 17/LO/1499, National Health Service Health Research Authority UK CRN 058274).

3.2 Funding

This work was supported by a grant from the British Heart Foundation (Dr Knight and Prof Muthurangu; Project Grant Number PG/17/47/32963) and my salary was met by research funding from Actelion/Janssen/Johnson & Johnson. I have no conflict of interests to declare regarding the work in this thesis.

4. RESEARCH PAPER DECLARATION FORMS

4.1 UCL Research Paper Declaration Form 1

For a research manuscript that has already been published

a) **What is the title of the manuscript?**

Reduced exercise capacity in patients with systemic sclerosis is associated with lower peak tissue oxygen extraction: a cardiovascular magnetic resonance-augmented cardiopulmonary exercise study.

b) **Please include a link to or doi for the work**

https://jcmr-online.biomedcentral.com/articles/10.1186/s12968-021-00817-1

c) **Where was the work published?**

Journal of Cardiovascular Magnetic Resonance

d) **Who published the work?**

BMC

e) **When was the work published?**

28th October 2021

f) **List the manuscript's authors in the order they appear on the publication**

James T Brown, Tushar Kotecha, Jennifer A Steeden, Marianna Fontana, Christopher P Denton, J Gerry Coghlan, Daniel S Knight, Vivek Muthurangu.

g) **Was the work peer reviewed?**

Yes

h) **Have you retained the copyright?**

Yes

i) **Was an earlier form of the manuscript uploaded to a preprint server?**

No

If 'No', please seek permission from the relevant publisher and check the box next to the below statement:

☒

*I acknowledge permission of the publisher named under **1d** to include in this thesis portions of the publication named as included in **1c**.*

1. **For multi-authored work, please give a statement of contribution covering all authors**

James Brown – study design, patient recruitment and scanning, data and image collection and analysis, statistical analysis and manuscript preparation

Tushar Kotecha – patient scanning, manuscript review

Jennifer Steeden – image sequence development

Marianna Fontana – manuscript review

Christopher Denton – patient recruitment, manuscript review

Gerry Coghlan – study design, patient recruitment, manuscript review

Daniel Knight – study design, patient scanning, image analysis, manuscript preparation

Vivek Muthurangu – study design, statistical analysis, manuscript preparation

2. **In which chapter(s) of your thesis can this material be found?**

Chapter 11

3. **e-Signatures confirming that the information above is accurate**

Candidate

James Brown

Date:

23/08/24

Supervisor/ Senior Author

Daniel Knight

Date:

25/08/24

4.2 UCL Research Paper Declaration Form 2

For a research manuscript that has already been published

a) What is the title of the manuscript?

Ongoing Exercise Intolerance Following COVID-19: A Magnetic Resonance-Augmented Cardiopulmonary Exercise Test Study.

b) Please include a link to or doi for the work

- 10.1161/JAHA.121.024207

c) Where was the work published?

Journal of the American Heart Association

d) Who published the work?

American Heart Association

e) When was the work published?

26th April 2022

f) List the manuscript's authors in the order they appear on the publication

James T Brown, Anita Saigal, Nina Karia, Rishi K Patel, Yousuf Razvi, Natalie Constantinou, Jennifer A Steeden, Swapna Mandal, Tushar Kotecha, Marianna Fontana, James Goldring, Vivek Muthurangu, Daniel S Knight.

g) Was the work peer reviewed?

Yes

h) Have you retained the copyright?

Yes

i) Was an earlier form of the manuscript uploaded to a preprint server?

No

If 'No', please seek permission from the relevant publisher and check the box next to the below statement:

☒

*I acknowledge permission of the publisher named under **1d** to include in this thesis portions of the publication named as included in **1c**.*

1. For multi-authored work, please give a statement of contribution covering all authors

James Brown – study design, patient recruitment, patient scanning, image and data analysis, manuscript preparation

Anita Saigal – patient recruitment

Nina Karia – patient recruitment, clinical measurements

Rishi K Patel – clinical measurements

Yousuf Razvi – clinical measurements

Natalie Constantinou – clinical measurements

Jennifer Steeden – imaging sequence development

Swapna Mandal – patient recruitment, manuscript review

Tushar Kotecha – patient scanning, manuscript review

Marianna Fontana – manuscript review

James Goldring – patient recruitment, manuscript review

Vivek Muthurangu – study design, statistical analysis, manuscript preparation

Daniel Knight – study design, patient scanning, image analysis, manuscript preparation

2. In which chapter(s) of your thesis can this material be found?

Chapter 12

3. **e-Signatures confirming that the information above is accurate**

Candidate

James Brown

Date:

23/08/24

Supervisor/ Senior Author

Daniel Knight

Date:

25/08/2024

4.3 UCL Research Paper Declaration Form 3

1. For a research manuscript that has already been published

a) What is the title of the manuscript?

Prognostic utility of exercise CMR in intermediate risk patients with systemic sclerosis-associated pulmonary arterial hypertension.

b) Please include a link to or doi for the work

- 10.1093/ehjci/jeae177

c) Where was the work published?

European Heart Journal Cardiovascular Imaging

d) Who published the work?

Oxford University Press

e) When was the work published?

19th August 2024

f) List the manuscript's authors in the order they appear on the publication

James T. Brown, Ruta Virsinskaite, Tushar Kotecha, Jennifer A. Steeden, Marianna Fontana, Nina Karia, Benjamin E. Schreiber, Voon H. Ong, Christopher P. Denton, J. Gerry Coghlan, Vivek Muthurangu, Daniel S. Knight

g) Was the work peer reviewed?

Yes

h) Have you retained the copyright?

Yes

i) Was an earlier form of the manuscript uploaded to a preprint server?

No

If 'No', please seek permission from the relevant publisher and check the box next to the below statement:

☒

*I acknowledge permission of the publisher named under **1d** to include in this thesis portions of the publication named as included in **1c**.*

For multi-authored work, please give a statement of contribution covering all authors

James Brown - study design, patient recruitment, patient scanning, image and data analysis, manuscript preparation

Ruta Virsinskaite – data collection

Tushar Kotecha – patient scanning, manuscript review

Jennifer Steeden – imaging sequence development

Marianna Fontana – manuscript review

Nina Karia – patient recruitment, data collection, manuscript review

Benjamin Schreiber – patient recruitment, manuscript review

Voon Ong - patient recruitment, manuscript review

Christopher Denton - patient recruitment, manuscript review

J. Gerry Coghlan - patient recruitment, manuscript review

Vivek Muthurangu - study design, statistical analysis, manuscript preparation

Daniel Knight - study design, patient scanning, image analysis, manuscript preparation

2. In which chapter(s) of your thesis can this material be found?

Chapter 13

3. e-Signatures confirming that the information above is accurate

Candidate

James Brown

Date:

23/08/24

Supervisor/ Senior Author

Daniel Knight

Date:

25/08/24

5. ACKNOWLEDGEMENTS

I would like to thank all the participants who gave their time to undergo the CMR-CPET tests, often during the evenings and weekends. Some travelled great distances to participate, and I am grateful to the Royal Free Charity for meeting the costs of their travel and accommodation.

I would also like to thank all of the members of the Pulmonary Hypertension team at the Royal Free Hospital, in particular Dr Coghlan, Dr Handler and Dr Schreiber and the Nurse Specialists (Adele, Javier and Gaby) for helping with patient recruitment and preparation.

Thank you to the CMR team at the Royal Free Hospital for allowing me use of the scanner and department, particularly Prof Marianna Fontana. Especial thanks to Sarah Anderson for teaching me how to scan patients well, and with compassion. Thank you to my colleagues for making the time in the department so enjoyable including Dr Liza Chacko, Dr Ana Martinez-Naharro, Dr Rishi Patel, Dr Yousuf Razvi and Dr Adam Ioannou.

I am indebted to those who helped me scan the participants and gave up so much of their free time, principally Dr Dan Knight and Dr Tushar Kotecha. Dr Jenny Steeden's work allowed imaging to be made possible during exercise and was essential for this work. Prof Vivek Muthurangu is an exemplary teacher of MR physics and statistics who has furthered my understanding immeasurably. Further thanks to my supervisor, Dan Knight, whose vision for this project allowed me this opportunity to undertake research. His mentoring and guidance during difficult times was the motivation to complete this work.

Thank you to all my colleagues at the Royal Free Hospital who I had the honour of working with during the COVID-19 pandemic.

Finally, thank you to my wife, Mary, for her love, support and understanding:

> "We shall not cease from exploration
> And the end of all our exploring
> Will be to arrive where we started
> And know the place for the first time." *Little Gidding, T.S. Eliot*

This research is dedicated to the memory of Karl Norrington.

6. ABBREVIATIONS

ΔavO_2	Arteriovenous Oxygen Content Gradient
ΔCO_2	Carbon Dioxide Content Gradient
2D	2 Dimensional
3D	3 Dimensional
6MWT	6 Minute Walk Test
ACA	Anti-Centromere Antibodies
ANA	Anti-Nuclear Antibodies
ANOVA	Analysis of Variance
APAH	Associated Pulmonary Arterial Hypertension (in Connective Tissue Disease)
AT	Anaerobic Threshold
ATP	Adenosine Tri-Phosphate
BNP	Brain Natriuretic Peptide
BSA	Body Surface Area
bSSFP	Balanced Steady State Free Precession
CAD	Coronary Artery Disease
cAMP	Cyclic Adenosine Monophosphate
cGMP	**Cyclic Guanosine Monophosphate**
CI	Chronotropic Incompetence
CI	Cardiac Index (Cardiac Output indexed to body surface area)
CK	Creatinine Kinase
cm	Centimetre
CMR	Cardiovascular Magnetic Resonance

CMR-CPET	Cardiovascular Magnetic Resonance-augmented Cardiopulmonary Exercise Test
CO	Cardiac Output
COi	Cardiac Output Indexed (to body surface area)
CO_2	Carbon Dioxide
COPD	Chronic Obstructive Pulmonary Disease
COVID-19	SARS-CoV-2/Severe Acute Respiratory Syndrome Coronavirus 2
CPET	Cardiopulmonary Exercise Test
CPET-SE	Cardiopulmonary Exercise Test with Stress Echocardiography
CRP	C-Reactive Protein
CS	Compressed Sensing
CT	Computed Tomography
CTD	Connective Tissue Disease
CTEPH	Chronic Thromboembolic Pulmonary Hypertension
CVD	Cardiovascular Disease
dcSSc	Diffuse Cutaneous Systemic Sclerosis
DICOM	Digital Imaging and Communications in Medicine
DLCO	Diffusing Capacity for Carbon Monoxide
E	Early left ventricular diastolic filling velocity
E'	Early diastolic velocity of the mitral annulus
ECG	Electrocardiogram
ECV	Extracellular Volume
EDV	End Diastolic Volume
EF	Ejection Fraction
eGFR	Estimated Glomerular Filtration Rate

EI	Exercise Intolerance
ERA	Endothelin Receptor Antagonist
ESC/ERS	European Society of Cardiology/European Respiratory Society
ESV	End Systolic Volume
Ex-CMR	Exercise-Cardiovascular Magnetic Resonance
FAD (H)	Flavin Adenine Dinucleotide
FBC	Full Blood Count
FEV1	Forced Expiratory Volume in 1 Second
FVC	Forced Vital Capacity
GTP	Guanosine-5'--triphosphate
Hb	Haemoglobin
HF	Heart Failure
HFpEF	Heart Failure with Preserved Ejection Fraction
HFrEF	Heart Failure with Reduced Ejection Fraction
HR	Heart Rate
iCPET	Invasive Cardio-Pulmonary Exercise Testing
IP	Prostacyclin
IPAH	Idiopathic Pulmonary Arterial Hypertension
IQR	Interquartile Range
IRAS	Integrated Research Application System
IV	Intravenous
iVO_2	Oxygen Consumption Indexed (to body surface area)
IVS	Interventricular Septum
LA	Left Atrium
LAA	Left Atrial Area

LBBB	Left Bundle Branch Block
lcSSc	Limited Cutaneous Systemic Sclerosis
LGE	Late Gadolinium Enhancement
LH	Left Heart
LV	Left Ventricle
LVEDV	Left Ventricular End Diastolic Volume
LVEDVi	Left Ventricular End Diastolic Volume Indexed (to body surface area)
LVEF	Left Ventricular Ejection Fraction
LVESV	Left Ventricular End Systolic Volume
LVESVi	Left Ventricular End Systolic Volume Indexed (to body surface area)
LVH	Left Ventricular Hypertrophy
LVOT	Left Ventricular Outflow Tract
MAPSE	Mitral Annular Plane Systolic Excursion
METS	Estimated Metabolic Equivalents
MI	Myocardial Infarction
min	Minutes
MOLLI	Modified Look Locker Inversion (Recovery)
mPAP	Mean Pulmonary Arterial Pressure
MR-CPET	Magnetic Resonance-augmented Cardiopulmonary Exercise Test
MRI	Magnetic Resonance Imaging
msec	Milliseconds
NAD (H)	Nicotinamide adenine dinucleotide (+Hydrogen)
NC-PH	Non-Connective Tissue disease associated Pulmonary Hypertension
NHS	National Health Service
NMR	Nuclear Magnetic Resonance

NO	Nitric Oxide
NT-proBNP	N-Terminal Brain Natriuretic Peptide
NYHA	New York Heart Association
PAH	Pulmonary Arterial Hypertension
PAH-CTD	Connective Tissue Disease-associated Pulmonary Arterial Hypertension
PAP	Pulmonary Arterial Pressure
PADP	Pulmonary Arterial Diastolic Pressure
PASP	Pulmonary Arterial Systolic Pressure
PC-CMR	Phase Contrast Cardiac Magnetic Resonance
PCH	Pulmonary Capillary Haemangiomatosis
PAWP	Pulmonary Arterial Wedge Pressure
PCWP	Pulmonary Capillary Wedge Pressure
PDE5I	Phosphodiesterase Type 5 Inhibitor
PH	Pulmonary Hypertension
PVOD	Pulmonary Veno-Occlusive Disease
PVR	Pulmonary Vascular Resistance
REC	Research Ethics Committee
RER	Respiratory Exchange Ratio
RF	Radiofrequency
RHC	Right Heart Catheterisation
RNA	Ribonucleic Acid
RNP	Ribonuclear Protein
ROI	Region of Interest
RPM	Revolutions Per Minute
RV	Right Ventricle

RVEDV	Right Ventricular End Diastolic Volume
RVEDVi	Right Ventricular End Diastolic Volume Indexed (to body surface area)
RVEF	Right Ventricular Ejection Fraction
RVESV	Right Ventricular End Systolic Volume
RVESVi	Right Ventricular End Systolic Volume Indexed (to body surface area)
RVH	Right Ventricular Hypertrophy
s	Seconds
SD	Standard Deviation
sGC	Soluble Guanylate Cyclase
sGCS	Soluble Guanylate Cyclase Stimulator
ShMOLLI	Shortened Modified Look Locker Inversion (Recovery)
SLE	Systemic Lupus Erythematosus
SSc	Systemic Sclerosis
SSc-PAH	Systemic Sclerosis-associated Pulmonary Arterial Hypertension
SSFP	Steady State Free Precession
SV	Stroke Volume
SVi	Stroke Volume Indexed (to body surface area)
TAPSE	Tricuspid Annular Plane Systolic Excursion
T1	Longitudinal Relaxation Time
T2	Transverse Relaxation Time
TE	Echo Time
TI	Inversion Time
VCO_2	Carbon Dioxide Output
VE	Ventilation
VE/VCO_2	Ventilatory Equivalents for Carbon Dioxide

VENC	Velocity Encoding
VO_2	Oxygen Consumption
VO_2max	Maximal Oxygen Consumption
W	Watts
WHO-FC	World Health Organisation Functional Class

7. INTRODUCTION

This thesis builds on the work of Nathaniel Barber, Jennifer Steeden, Karl Norrington, Daniel Knight and Vivek Muthurangu.

7.1 Exercise Intolerance

The syndrome of exercise intolerance (EI) results from the inability of the body to deliver sufficient oxygen to meet the demands of respiring skeletal muscles during exercise(1). It results in the symptoms of exertional dyspnoea and/or fatigue. It is present in many chronic diseases (2-4), and results in reduced quality of life(5). Additionally, exercise intolerance is a predictor of mortality(6-12).

Exercise intolerance may refer to either attaining a decreased *maximal workload* (compared to what would be expected for that individual; this is a measure of anaerobic capacity), or decreased *exercise duration* for a submaximal workload (so called functional capacity, a measure of aerobic capacity (13)).

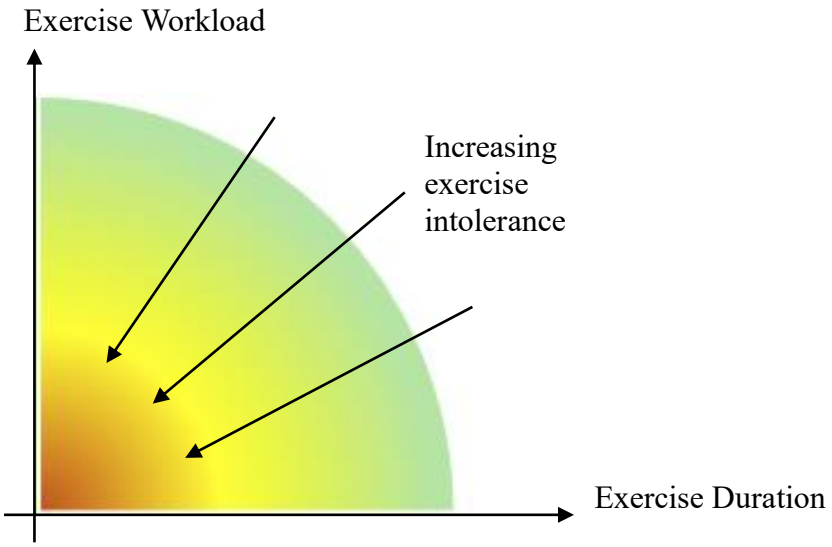

Figure 1. Schematic of the role of workload and duration in exercise intolerance.

The symptoms of exercise intolerance can be subtle and are frequently understated by patients. It therefore requires skilled history-taking to assess their presence and severity. Changes in severity over time can similarly be difficult to pinpoint – patients may gradually avoid situations where they are required to exert themselves, and thereby not volunteer any deterioration in symptoms. Due to this subjectivity, various efforts have been made to provide objective assessments of exercise intolerance. One method is by using semi-quantitative scores such as the New York Heart Association Function Class (NYHA)(14), widely used in heart failure populations, and the related World Health Organization Function Class (WHO-FC) which was adapted from the NYHA system in 1998 for use in pulmonary hypertension populations(15) – see Table 1. Formal objective assessments of submaximal exercise capacity can be made using tests such as the 6-minute walk test distance (6MWT), whilst maximal workload can be assessed using various treadmill- or bicycle ergometer-based techniques.

Class	NYHA – Patient Symptoms	NYHA – Objective Assessment	WHO-FC
I	No limitation of physical activity. Ordinary physical activity does not cause undue fatigue, palpitation, dyspnoea (shortness of breath).	**A** - No objective evidence of cardiovascular disease. No symptoms and no limitation in ordinary physical activity.	Patients with pulmonary hypertension but without resulting limitation of physical activity. Ordinary physical activity does not cause undue dyspnoea or fatigue, chest pain or near syncope.
II	Slight limitation of physical activity. Comfortable at rest. Ordinary physical activity results in fatigue, palpitation, dyspnoea (shortness of breath).	**B** - Objective evidence of minimal cardiovascular disease. Mild symptoms and slight limitation during ordinary activity. Comfortable at rest.	Patients with pulmonary hypertension resulting in slight limitation of physical activity. They are comfortable at rest. Ordinary physical activity causes undue dyspnoea or fatigue, chest pain or near syncope.
III	Marked limitation of physical activity. Comfortable at rest. Less than ordinary activity causes fatigue, palpitation, or dyspnoea.	**C** - Objective evidence of moderately severe cardiovascular disease. Marked limitation in activity due to symptoms, even during less-than-ordinary activity. Comfortable only at rest.	Patients with pulmonary hypertension resulting in marked limitation of physical activity. They are comfortable at rest. Less than ordinary activity causes undue dyspnoea or fatigue, chest pain or near syncope.
IV	Unable to carry on any physical activity without discomfort. Symptoms of heart failure at rest. If any physical activity is undertaken, discomfort increases.	**D** - Objective evidence of severe cardiovascular disease. Severe limitations. Experiences symptoms even while at rest.	Patients with pulmonary hypertension with inability to carry out any physical activity without symptoms. These patient manifest signs of right heart failure. Dyspnoea and/or fatigue may even be present at rest. Discomfort is increased by any physical activity.

Table 1. Grading of exercise intolerance.

NYHA=New York Heart Association Functional Class. WHO-FC=World Health Organization Functional Class.

For the purposes of this thesis, I will treat exercise intolerance as being synonymous with exertional dyspnoea and/or fatigue. Symptoms of chest pain, palpitation or syncope during exertion signify a severe form of exercise intolerance that would be difficult to safely perform research of this nature on, or even an additional diagnosis (e.g. coronary artery disease in chest pain, dysrhythmias in palpitation, and valvular heart disease or heart muscle disease in syncope). These potential additional diagnoses would confound research results and should prompt clinical investigation in their own right.

Due to the complex and sophisticated interactions between multiple body systems that are needed to undertake exercise, exercise intolerance has the potential to be multifactorial. The NYHA functional class (which implies the limitation is due to heart failure) or WHO functional class (which implies the limitation is due to pulmonary hypertension) should not be taken to imply that all the limitation is due to one aetiology. Identifying one specific (and treatable) cause of EI can be challenging, and if a single cause is identified from investigations, this may lead to "satisfaction of search" for the physician. Other contributory (but no less treatable) causes of EI may then be overlooked if the treatment is simply focussed on the first abnormality detected. Similarly, extrapolating potential causes of exercise intolerance from investigations performed at rest risks overlooking important factors that only manifest during exercise.

Exercise intolerance can be quantified objectively with widely available and reproducible tests. Submaximal exercise tests such as the Six-Minute Walk Test (6MWT(16)) give prognostic information and allow serial measurements over time (e.g. to assess clinical worsening or response to treatments). The 6MWT distance is used as a clinical endpoint in many trials for pulmonary hypertension and heart failure populations, yet it does not usually identify the cause of the limitation to exercise. It also has limitations insofar as it does not consider important

variables such as age, sex, height and weight, all of which are known to contribute to exercise capacity.

More sophisticated maximal exercise tests (including treadmill- or bicycle-ergometer exercise tolerance tests and cardiopulmonary exercise tests) may yield useful information about exercise duration, workload and METs, and the adaptations during exercise including respiratory rate, oxygen consumption and carbon dioxide production, the transition between aerobic and anaerobic respiration, heart rate and blood pressure responses. They may identify the main cause of the exercise intolerance, but as they do not comprehensively assess all relevant systems simultaneously, they cannot identify all contributory causes.

Inherent in the physiological definition of exercise intolerance is a focus on the respiratory, cardiovascular and musculoskeletal systems, and it is the interaction between these systems that this thesis necessarily focusses on. Clearly there is more to exercise intolerance than just these three systems. For instance, the role of mood, motivation, and the wider psychosocial environment in which a person finds themself will have a potentially large, yet potentially unquantifiable, contribution to their ability to perform exercise. It may even change on a day-to-day, or hour-by-hour basis. Other sequelae of chronic disease, including anaemia, pain, inflammation, infection and even bowel and urinary habits, can affect the timing and intensity of exercise a person may feel capable of carrying out. This thesis does not overlook the contribution to exercise intolerance from such symptoms but acknowledges that these factors cannot be fully addressed in this piece of work.

7.2 Exercise Physiology Under Normal Conditions

A discussion of the mechanisms contributing to exercise intolerance must begin with an understanding of the normal physiological responses to exercise. Following from this, I will review the available methods by which these responses (or components thereof) can be quantified in a clinical setting. Finally, I will discuss the combination of Cardiopulmonary Exercise Testing and Cardiovascular Magnetic Resonance Imaging (CMR-CPET) that I have used to investigate specific populations where exercise intolerance is a key feature of the disease.

7.2.1 Mitochondria and myocytes

During exercise, skeletal muscle contraction and relaxation results in mechanical work being performed, and this process is ATP-dependent (see Figure 2). The oxidative phosphorylation of ADP to ATP within mitochondria which underpins this process requires oxygen. At rest and during submaximal exercise, oxygen delivery meets the demand of this cellular respiration, and the phosphorylation can be performed aerobically. With inadequate oxygen supply or maximal exercise, cellular respiration switches from aerobic to anaerobic pathways (see Figure 3). The anaerobic process yields ATP quickly, but in a metabolically costly manner (2 ATP per molecule of glucose versus 38 ATP per molecule of glucose for aerobic respiration). Due to the accumulation of pyruvate and ultimately lactate, during anaerobic cellular respiration marked acidosis can result within the myocytes. This produces muscle pain in the short term with persistent acidosis resulting in myocyte damage. Anaerobic respiration is a useful mechanism, as it can permit short periods of high-intensity activity, yet for most daily activities it is not the optimal pathway to utilise chemical energy in order to perform mechanical work.

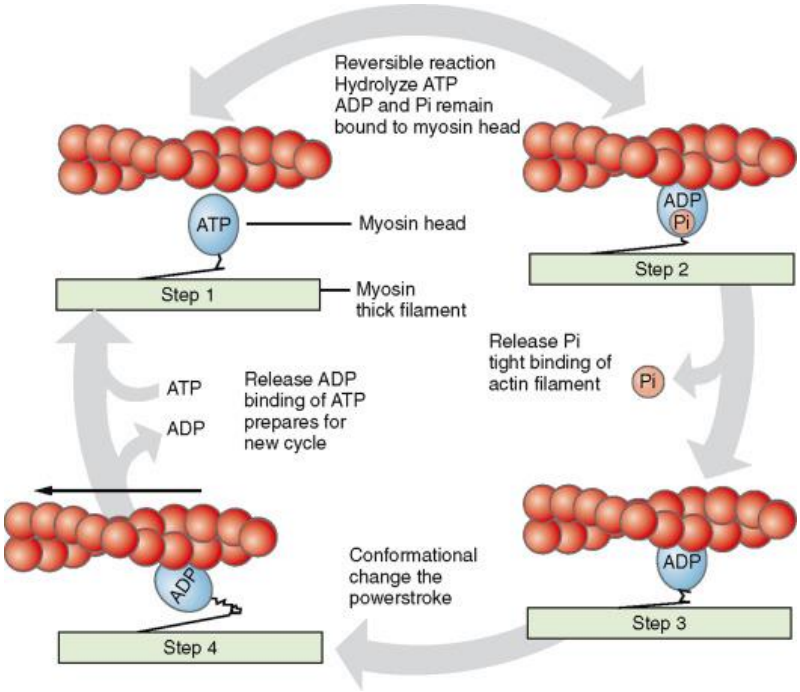

Figure 2. The ATP-dependent mechanism of skeletal muscle contraction.

The binding of ATP to a myosin head group causes release from the actin filament (Step 1). The hydrolysis of ATP to ADP+Pi readies the myosin head to contact an actin filament (Step 2). The initial contact of the myosin with an actin filament causes the release of Pi and a tight binding of the actin filament (Step 3). This tight binding induces a change in conformation of the myosin head, such that it pulls against the actin filament, the power stroke (Step 4). This change in conformation is accompanied with the release of ADP. The binding of an additional ATP causes a release of the actin filament and a return of the myosin head to a position ready for another cycle. ADP = adenosine diphosphate, ATP = adenosine triphosphate, Pi = phosphate. Adapted from (17).

To permit the more sustainable aerobic cellular respiration during submaximal exercise, a sophisticated sequence of events is coordinated by the body to deliver oxygen to skeletal muscles when the demand for ATP, and therefore oxygen, increases. The extent to which the body can deliver oxygen to respiring skeletal muscle is in healthy individuals the key determinant of exercise tolerance. There are conditions, however, where exercise intolerance may be caused not by cardiorespiratory (central) limitations, but rather due to the peripheral limitation of oxygen extraction by skeletal muscle, driven by factors including capillary function and density, skeletal muscle architecture and composition, and mitochondrial function and density (18). For instance, how soon during exercise the switch from aerobic to anaerobic cellular respiration occurs (which depends on the relative proportions of type 1 skeletal muscle

fibres [slow twitch or oxidative] versus type 2 fibres [fast twitch or glycolytic], as well as the total amount of both), and how able the myocytes are to tolerate anaerobic respiration(19) can impact both maximal and submaximal exercise. Early switching to anaerobic respiration is seen in many chronic conditions where exercise intolerance is a prominent symptom. Sarcopenia, or decreased skeletal muscle mass, can also result in exercise intolerance. Finally, any dysfunction of capillaries that increases oxygen diffusion distances from blood stream to respiring cells will have similar effects.

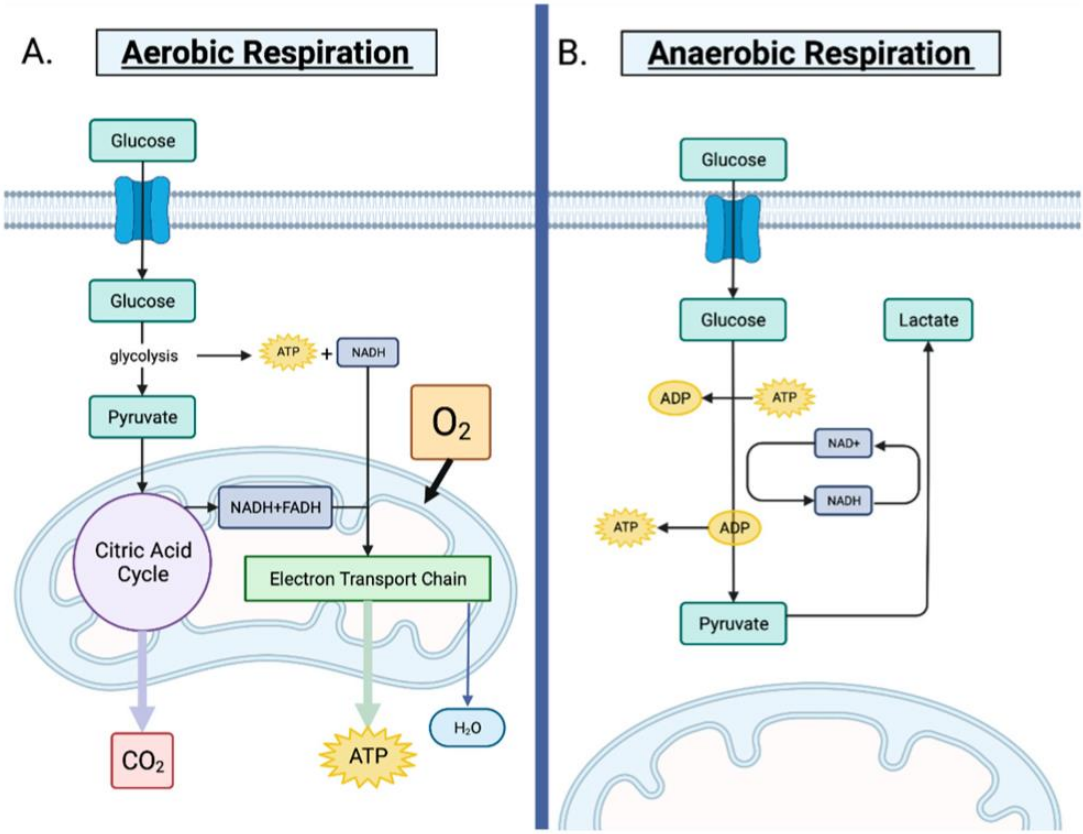

Figure 3. Aerobic vs. anaerobic respiration.

(A). Aerobic respiration, which occurs in the presence of oxygen. The conversion of glucose to pyruvate is facilitated by glycolysis. The citric acid cycle then transforms pyruvate to acetyl-CoA in the mitochondria, also creating ATP, NADH and FADH. ATP is produced via oxidative phosphorylation of NADH and FADH, which fuels the electron transport chain. (B). When oxygen is scarce, cells switch to anaerobic respiration to generate ATP. Pyruvate cannot enter the citric acid cycle after glycolysis and is instead converted to lactate to avoid its accumulation. The NADH produced during glycolysis is converted back to NAD+ allowing glycolysis to continue, when oxygen levels return to baseline, cells resume aerobic respiration. Adapted from (20).

The uptake of oxygen from the bloodstream by respiring tissues can be quantified by the arterio-venous oxygen difference, ΔavO_2. This can be measured directly by sampling arterial and venous oxygen saturations of the blood supplying a specific vascular bed. In practice, it would be arterial and central venous blood that would be sampled. Central venous blood is a composite of blood from skeletal muscle and other vascular beds such as the splanchnic and renal circulation (see Figure 4), with the relative proportions of each varying between rest and exercise, such that during exercise skeletal muscle accounts for the vast majority of the venous return and therefore central venous oxygen saturations would closely align with that of skeletal muscle venous blood. However, to sample arterial and venous blood simultaneously during exercise in a safe manner poses technical problems and would never normally be performed outside of a research setting, minimizing this technique's clinical utility.

As an alternative, arterio-venous oxygen differences can be calculated indirectly if the appropriate measurements of oxygen consumption and cardiac output are available (see 7.3 Investigating Mechanisms of Exercise Intolerance).

Arterio-venous oxygen differences can increase 2.5-fold between rest and peak exercise in healthy young to middle-aged men during a maximal exercise test on an upright bicycle ergometer(21), with similar findings seen in women(22).

7.2.2 Vascular beds and the heart

The effect of increased metabolism at the level of skeletal myocytes results in increased carbon dioxide levels and reduced pH in the vascular beds that supply the muscles. This promotes vasodilation of afferent arterioles allowing increased blood (and oxygen) flow to the skeletal muscles. The net effect of this is a reduction in systemic vascular resistance. In order to

maintain systemic blood pressures, the autonomic nervous system coordinates a complex response to:

a). increase vascular tone and resistance in (and hence decrease blood flow to) non-essential vascular beds, such as the splanchnic circulation (see Figure 4).

b). increase cardiac output (CO), first by increasing heart rate, then by increasing left ventricular stoke volume (SV). At low intensity exercise, SV increases due to the Frank-Starling mechanism, with increases in ventricular end diastolic volumes (EDV). There are minimal increases in the pulmonary capillary wedge pressure associated with this. At higher levels of exercise intensity, the SV increases due to increased ventricular contractility, resulting in lower ventricular end systolic volumes (ESV).

Cardiac index (CI, cardiac output indexed to body surface area) has been found to increase 3.2-fold between rest and peak exercise. This increase in cardiac output resulted from a 2.5-fold increase in heart rate and a 1.4-fold increase in stroke volume(21).

As important as increasing cardiac output is the control of venous return. A decrease in venous return to the right heart will necessarily result in a reduction in the cardiac output that the left heart can generate. Venous return is determined by the gradient between mean systemic filling pressure (resulting from venous sympathetic tone and circulating blood volume) and right atrial pressures (which will be affected by pre- and after-load), and the resistance to venous return (which will be affected by the skeletal muscle pumps and the pressure changes from respiratory movements).

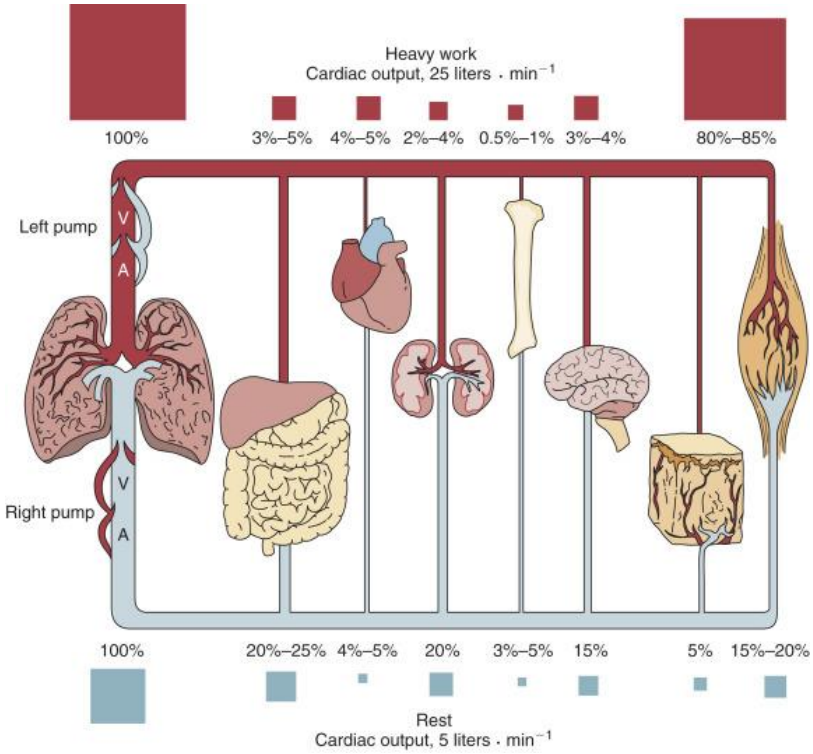

Figure 4. Increase in cardiac output and changes to blood flow distribution during exercise.

The parallel circuits of flow through the various systems of organs, both at rest and during peak exercise. Note that the cardiac output increases by approximately five-fold from rest to strenuous exercise. The relative distribution of flow to the various systems, in contrast, is significantly different from rest to peak exercise. In both states, the red squares are proportional to the percentage of cardiac output received by the particular system. Note that the flow of blood to the muscle increases from between approximately 15% to 20% of cardiac output at rest to 80% to 85% of the cardiac output at peak exercise. Adapted from (23).

7.2.3 Ventilation centres and the lungs

Finally, central and peripheral chemoreceptors detect increased carbon dioxide levels/decreased pH in the blood stream and effect an increase in respiratory rate and ventilatory volumes. This promotes gas exchanges at the level of the alveoli in the lungs, such that CO_2 diffuses from blood stream to air, and O_2 absorption from air to bloodstream increases. The increase in oxygen uptake, VO_2, between rest and peak exercise was shown to be 7.7-fold in the young to middle-aged healthy men.

All of these processes are required, and coordination between them is essential.

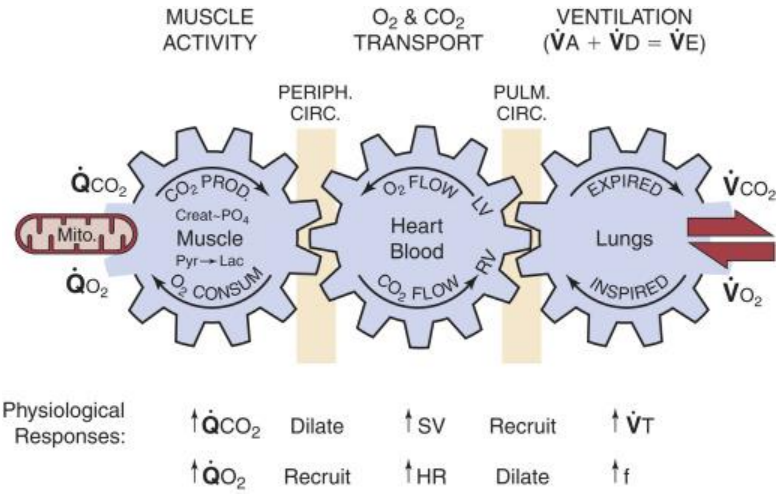

Figure 5. Coupling of cellular and respiratory respiration.

Gas transport mechanisms coupling cellular (internal) respiration to pulmonary (external) respiration. CO2 = carbon dioxide, Consum = consumption, Creat = creatinine, Lac = lactate, HR = heart rate, Mito = mitochondria, O2 = oxygen, Periph = peripheral, PO4 = phosphate, Prod = production, Pulm = pulmonary, Pyr = pyruvate, $\dot{Q}CO2$ = carbon dioxide production, $\dot{Q}O2$ = oxygen consumption, SV = stroke volume, $\dot{V}A$ = minute alveolar ventilation, $\dot{V}D$ = minute dead space ventilation, $\dot{V}E$ = minute ventilation, Vf = breathing frequency, VT = tidal volume, $\dot{V}CO2$ = carbon dioxide output, $\dot{V}O2$ = oxygen uptake. Adapted from (24).

7.3 Investigating Mechanisms of Exercise Intolerance

Exercise intolerance could have many potential causes and whilst some may appear intuitive, such as severe fixed airways disease (e.g. COPD) limiting the ventilatory reserve to meet the increased oxygen demand during exercise, other causes may be less obvious as they may depend on an interplay between more than one body system. For example patients with chronic heart failure that *also* demonstrate structural and function changes to skeletal muscle (e.g. a decrease in the mass of oxidative muscle fibres (type 1), an alteration in the ratio of oxidative versus glycolytic muscle fibres (type 1 *v.* type 2), and mitochondrial down-regulation(25)), may only have treatment directed at the reduced cardiac output, whilst the reduced arteriovenous oxygen difference is not appreciated.

Despite exercise intolerance being a common presenting complaint, it is often under-appreciated, and due to its multifactorial nature, it is frequently incompletely investigated. Many investigative strategies will involve testing one body system under static, resting conditions. Pulmonary function tests or resting transthoracic echocardiography might detect obvious resting abnormalities, but unless the patient has symptoms at rest, they are unlikely to be informative about the responses during exercise. Dynamic tests such as cardiovascular stress imaging or cardiopulmonary exercise testing are better but may lead to ascribing all symptoms to one positive finding, a form of “search-satisfaction” or confirmation bias. A comprehensive assessment of the limitations to exercise from the respiratory, cardiovascular *and* skeletal muscle systems would be the most informative test and should in theory highlight the areas where treatment might be directed to achieve most symptomatic benefit.

In this section I will outline the most common clinical tests used to investigate exercise intolerance, exertional dyspnoea or fatigue. The Fick principle, specifically for oxygen, can be used to identify where the limitation to exercise arises. The principle was first used to calculate cardiac output prior to safe and accurate non-invasive methods being available. It states that the total oxygen consumption by the body, $\dot{V}O2$, is equal to the oxygen delivered to the respiring tissues less the oxygen that is returned from them. The amount of oxygen delivered to the respiring tissues is given by the product of the cardiac output and the arterial oxygen concentration (C_a). The amount of oxygen returned is the product of cardiac output and the venous oxygen concentration (C_v).

$$\dot{V}O_2 = (CO \cdot C_a) - (CO \cdot C_v)$$

$$\dot{V}O_2 = CO \cdot (C_a - C_v) \qquad CO = \dot{V}O_2 / (C_a - C_v) \qquad (C_a - C_v) = \dot{V}O_2 / CO$$

$$\dot{V}O_2 = CO \cdot avO_2 \qquad CO = \dot{V}O_2 / avO_2 \qquad avO_2 = \dot{V}O_2 / CO$$

Equation 1. The Fick equation

avO_2=arteriovenous oxygen difference
C_a=arterial oxygen concentration
C_v=venous oxygen concentration
CO=cardiac output per minute
$\dot{V}O_2$ =minute ventilation, or oxygen consumption per minute

7.3.1 The Respiratory System

7.3.1.1 Limitations of the Respiratory System

In health, the respiratory system allows for highly efficient gas exchange and is never normally the limiting factor to exercise capacity. Limitations of the respiratory system can be divided into impaired ventilation, impaired diffusion, and impaired perfusion.

Impaired ventilation is reduced gas movement into and out of the alveoli and can result from mechanical obstruction of the airways (external compression of the airways, foreign body), obstructive airways disease (asthma, COPD), or decreased diaphragmatic or chest wall movement due to deformity, injury, nerve or muscle disorders, or dysregulation of respiratory drive due to e.g. sedative medications.

Impaired diffusion of gases across the alveoli can result from disorders that affect the alveoli themselves (architecture or number), the lung parenchyma, or the lung vasculature. The number of alveoli (or the total surface area), or the diffusion distance, or both, can be affected so as to reduce the diffusion of O_2 from the alveoli into the pulmonary capillaries and the diffusion of CO_2 from the capillaries into the alveoli.

Finally, the perfusion of blood to ventilated lung may place limits on the amount of blood that can be fully oxygenated. For example, a pulmonary embolism can effectively occlude the flow of blood to lung segments, lobes or even whole lungs, rendering any ventilation to the affected lung unrealised.

7.3.1.2 Investigating the Respiratory System

Imaging: Modalities such as plane radiography (X-ray) or computed tomography (CT) can provide macroscopic information about the appearance of lung parenchyma. Perfusion of the lungs can be assessed with computed tomography or magnetic resonance pulmonary angiography, invasive pulmonary angiography or nuclear medicine ventilation/perfusion scans.

Functional Tests: Pulmonary functions tests (PFTs) are widely available, safe and non-invasive. They can provide volumetric data (including total lung capacity, tidal volume, vital capacity), and spirometry (expiratory flow rates) can provide information about restrictive and

obstructive lung conditions. Measures of gas diffusion (diffusion capacity of the lung for carbon monoxide, DLCO) provide information about the efficiency of alveolar gas exchange. These investigations are performed at rest. If major abnormalities are detected, this is important. However, it does not predict to what extent the abnormality will cause exercise intolerance, nor does it exclude further abnormalities becoming apparent during exercise.

Arterial/Capillary Blood Gas Sampling: Taking small sample of blood from an artery, e.g. the radial artery, or capillaries, e.g. from the earlobe, gives oxygen and carbon dioxide levels, as well as bicarbonate levels which gives information about chronic acid/base states in the body (e.g. chronic CO_2 retention). Samples can be taken at rest, but for exercise sampling, an arterial line is usually required.

Pulse Oximetry: Non-invasive measurement of peripheral oxygen saturations can be obtained using light spectrometry for oxygenated and deoxygenated haemoglobin using widely available devices that can be attached to a patient's finger or earlobe. It is possible to use this technique during exercise, although if oxygen desaturations are observed, the mechanism may not be identified.

7.3.2 The Cardiovascular system

7.3.2.1 Limitations from the Cardiovascular System

The cardiovascular system's role is to deliver oxygenated blood from the lungs to actively respiring tissues via the arterial system, then return deoxygenated blood via the venous system to the right side of the heart where it is pumped through the pulmonary arteries. Cardiac output quantifies the cardiovascular system's delivery of blood to the body:

Cardiac Output = Stroke Volume x Heart Rate

Equation 2. Cardiac Output

Stroke Volume: Central to the cardiovascular system's role is the left ventricle's ability to generate forward flow. The left ventricle must be compliant during diastole to allow adequate filling, with both passive filling and active priming from left atrial contraction playing important roles. It must also be able to contract effectively during systole. The difference between end diastolic volume and end systolic volume gives the stroke volume.

Adequate filling and priming of the LV may be prevented in restrictive cardiomyopathy, constrictive pericarditis, mitral stenosis or in the absence of coordinated atrial activity (e.g. atrial fibrillation). Systemic hypertension and diabetes mellitus are risk factors for diastolic dysfunction/heart failure with preserved ejection fraction (HFpEF), where effective diastolic filling of the LV is impaired.

During low intensity exercise, where increased end diastolic volumes enable the Frank-Starling mechanism to increase LV contractility, limitations of diastolic function may be unmasked, as either the stroke volume may not be augmented satisfactorily to maintain the required cardiac output, or LV end diastolic pressures may increase to such an extent that pulmonary capillary pressures result in pulmonary oedema.

The systolic function of the LV may be impaired in ischaemic heart disease or cardiomyopathies. Aortic stenosis provides mechanical obstruction, and systemic hypertension provides haemodynamic obstruction to forward flow; mitral regurgitation will reduce forward flow by directing a proportion of the cardiac output back to the left atrium.

The right ventricle is similarly affected by systolic and diastolic dysfunction and valvular lesions. Its role in priming the left ventricle is important. For instance, decreased venous return to the right side of the heart (due to autonomic dysfunction or vasoactive drugs) or pulmonary

hypertension can alter the loading conditions of the right ventricle, with consequential decrease in flow through the pulmonary arterial system, and potential under-filling of the left heart.

Heart Rate: Failure to increase heart rate during exercise, so called chronotropic incompetence may be due to intrinsic disease of the cardiac conduction system, or as a result of external influences from rate-limiting medications, electrolyte abnormalities or thyroid disease.

Vascular system: The aorta, and to a certain extent the pulmonary artery, play an important role in producing, through their distensibility, a smoothing of the systolic pressures generated by the respective ventricles, and enabling forward flow of blood throughout the cardiac cycle. Effective distribution of blood flow to the requisite vascular beds requires appropriate neuromuscular control of the arteries and arterioles. Venous tone is essential in returning the blood to the right heart. Vascular tone can be decreased or inappropriately controlled in diseases that affect the autonomic system, including diabetes, inflammatory and auto-immune conditions.

Adequate blood volume is necessary for exercise. In an underfilled system, some or all of the mechanisms described above will already be employed at rest to maintain blood pressure and cardiac output, and therefore there would be less reserve to augment them during exercise. The renin-angiotensin-aldosterone system regulates fluid and electrolyte management by the kidneys and thirst regulation.

Oxygen is carried in the blood mostly by haemoglobin molecules within red blood cells (although small amounts are diffused within the plasma, this is physiologically negligible until anaemia is profound). Anaemia will result in lower oxygen delivery for a given cardiac output.

7.3.2.2 Investigating the Cardiovascular System

ECG and Exercise ECG: The resting 12-lead ECG gives basic information about heart rate and the conduction system and can give clues about myocardial injury. The exercise ECG, with a

treadmill being the usual mode of exercise, will be useful to detect exercise heart rate response, and if there is chronotropic incompetence (CI). Its use to detect myocardial ischaemia has decreased with the advent of more sensitive and specific anatomical and functional tests.

Imaging: Transthoracic Echocardiography can assess ventricular systolic and diastolic function, as well as detect haemodynamically significant valvular lesions. There are patient-related factors such as body habitus and lung disease that might make echocardiography challenging. Alternative modalities include Cardiac MRI (CMR), which is excellent for assessment of ventricular volumes and flows through the great vessels, and Cardiac Computed Tomography, including CT Coronary Angiography (CTCA), which can provide assessment of coronary artery disease anatomy and severity.

Functional Assessments: Combining cardiac imaging with exercise (or pharmacological stress, eg dobutamine, adenosine), for instance with exercise stress echo or adenosine stress-perfusion CMR, allows assessment of cardiac output augmentation and identification of inducible ischaemia (either by detecting regional wall motion abnormalities directly, or by detecting decreased perfusion of contrast agents through the myocardium).

In exercise echocardiography, the Doppler mitral inflow and tissue indices give information about LV diastolic function. The ratio of early left ventricular diastolic filling velocity (E) to the early diastolic velocity of the mitral annulus (E'), E/E', correlates with invasively measured end diastolic left ventricular pressures(26). Resting E/E' correlates with submaximal(27) and maximal(28) exercise intolerance, and increased E/E' during exercise correlates with exercise intolerance(29).

Invasive assessments: Invasive coronary angiography can give anatomical and physiological assessments of coronary lesions. Right heart catheterisation is necessary to diagnose pulmonary hypertension.

Blood tests: Haemoglobin concentration is important factor in oxygen-carrying ability of blood; biomarkers of cardiomyocyte stretch, particularly Brain Natriuretic Peptide (BNP, or its precursor N-Terminal pro-BNP) are elevated in conditions of elevated ventricular pressures, with higher levels conferring poor prognosis for a range of cardiovascular and pulmonary conditions(30, 31).

7.3.3 Musculoskeletal system

7.3.3.1 Limitations from the Musculoskeletal System

There may be particular structural or anatomical considerations affecting the skeletal muscles that could limit exercise capacity, whilst the myocytes themselves are functionally normal. There are numerous muscular dystrophies that result in abnormal myocyte architecture, usually through abnormal protein synthesis, and several myopathies resulting from abnormal mitochondrial function. Systemic autoimmune conditions and medications can result in skeletal muscle inflammation, and vasculopathies can impair the blood flow to skeletal muscles, a situation that is compounded when the oxygen requirements of the muscles increase as in exercise. Finally, the changes in muscle fibre ratio as a result of, for instance, low cardiac output states, alters the response of the skeletal muscles to exercise.

7.3.3.2 Investigating the Musculoskeletal System

Directly investigating the function of skeletal muscle poses problems at rest, and assessment of function during exercise adds further complexity. In theory, measuring tissue oxygen extraction by comparing simultaneous arterial and central venous blood samples could be performed, but this is rarely, if ever, done outside a research environment. Muscle biopsy can inform about inflammatory conditions and skeletal muscle architecture.

7.3.4 Integrating Tests of Multiple Systems

Simultaneous assessment of respiratory, cardiovascular and skeletal muscle systems during exercise would identify limitation(s) and guide therapeutic interventions. Here, I will discuss the methodologies that have attempted to address this problem.

Six-Minute Walk Test: As previously discussed, this is a self-paced, sub-maximal exercise test that measures the distance walked by a patient within the allotted time. Patients can stop and rest during the test if required. It is widely available, requires little in the way of specific equipment, and is reproducible. Being a submaximal test, it does not assess peak oxygen consumption, but it may more accurately reflect a patient's ability to perform daily activities and appears more closely associated with quality of life indices(32). In certain conditions, for example end-stage lung disease, there is good correlation between 6MWD and peak oxygen consumption(33). It provides prognostic information across a range of cardiovascular conditions(34). However, as the American Thoracic Society statement states, the 6MWT does not determine the cause of dyspnoea or fatigue on exertion or evaluate the mechanism of exercise limitation; furthermore, it suggests that the fact investigators have used the test in clinical trials does not suggest that the test is clinically useful (or the best test) for determining function capacity or changes in functional capacity following an intervention. Rather, having been a tool utilised in early clinical trials due to its ubiquity, it then became a legacy test which all subsequent trials have employed.

Cardiopulmonary Exercise Test (CPET): Cardiopulmonary exercise testing (CPET) can be used to assess the respiratory system under exercise conditions non-invasively, with the aim of quantifying functional capacity(35) by way of a symptom-limited maximal test. Inferences can also be made about cardiovascular function. This technique measures the concentration of O_2

and CO_2 in expired gas, together with expired air volume and flow. From these data, $\dot{V}CO_2$, $\dot{V}O_2$ and $\dot{V}_E$ (O_2 consumption [per minute], VCO_2 production [per minute] and minute ventilation respectively) can be calculated.

Figure 6. Cardiopulmonary Exercise Test Equipment.

A cardiopulmonary exercise testing machine using an upright cycle ergometer. A non-rebreathe valve is connected to the mouthpiece. There is continuous ECG and blood pressure monitoring. Adapted from (36).

CPET allows determination of the following metrics:

(1). Peak $\dot{V}O_2$, the most reproducible measurement of cardiopulmonary functional capacity with prognostic data for cardiovascular diseases(10, 37-42);

(2). Anaerobic threshold (AT), the highest (the $\dot{V}O_2$ without increase in blood lactate concentration);

(3). Respiratory Exchange Ratio (RER), a metric for quantifying effort (RER = $\dot{V}CO_2/\dot{V}O_2$; <1.0 = poor effort, 1.0-1.1 =fair effort; 1.1-1.2 = good effort; >1.2 = excellent effort);

(4). Ventilatory efficiency for carbon dioxide, $\dot{V}_E/\dot{V}CO_2$. It is a metric of ventilation/perfusion, with a normal range of 25-30, and higher values in respiratory disease and low-output heart failure. This metric has been shown to be prognostic independent of $\dot{V}O_2$ in chronic heart failure (43).

Assuming a maximal exercise test, CPET can identify limitations in exercise physiology as follows:

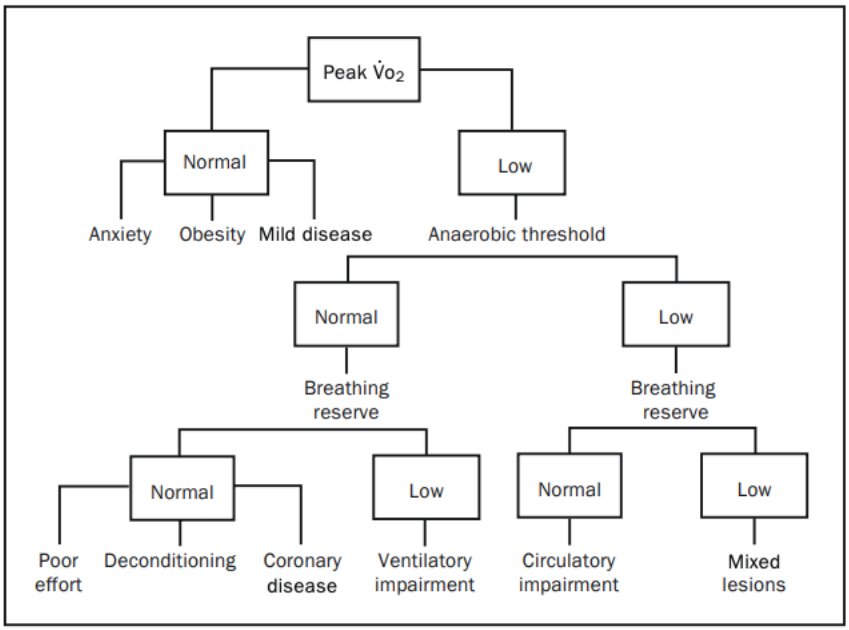

Figure 7. Flowchart for differential diagnosis of exertional dyspnoea and fatigue.

Breathing reserve is the ratio of maximal voluntary ventilation to maximal exercise ventilation. Adapted from (44, 45).

Invasive CPET – "iCPET" -(46, 47), which adds invasive measurements of pulmonary haemodynamics (that can include pulmonary capillary wedge pressure, pulmonary arterial pressure, and pulmonary vascular resistance derived from *estimates* of cardiac output) can resolve further between peripheral and central causes of exercise intolerance, but the procedure requires a motivated patient, and the invasive nature increases procedural risk.

By knowing VO_2 plus one of either CO or avO_2, the Fick principle (Equation 1) could be used to allow assessment of all components of the responses to exercise, and therefore isolation of the limitation to a specific abnormality (or group of abnormalities). CPET readily gives VO_2 data, and whilst it would be possible to perform simultaneous arterial and central venous blood

sampling during exercise (this has been done in small proof-of-principle studies but would be hard to justify for larger studies), it would be more practicable to combine CPET with simultaneous, non-invasive, cardiac imaging to obtain cardiac output data. This would have the potential to resolve between central and peripheral causes of exercise intolerance non-invasively without the technical difficulties of iCPET.

Using CPET in isolation does allow *inference* of cardiac output. The O_2 pulse, the ratio of $\dot{V}O_2$ to HR, provides an estimate of LV stroke-volume *changes* during exercise, but not the diastolic or systolic volumes that produce the stroke volume. Furthermore, assumptions are made to allow this inference, including the assumption that arteriovenous difference (ΔavO_2**)** is maximal, and that there is no anaemia(48). Both assumptions may be unsafe in chronic disease resulting in the very exercise intolerance being investigated.

The combination of CPET with Stress Echocardiography – CPET-SE -(49, 50) has the potential to estimate cardiac output at different stages of exercise, by multiplying the left ventricular outflow tract area (measured at rest), by the LV outflow tract velocity–time integral measured by pulsed-wave Doppler during each activity level(51). This method of CO calculation requires good echocardiographic windows that remain relatively consistent during exercise, requires accurate measurement of the left ventricular outflow tract diameter (a term which is multiplied by itself, therefore potentially introducing significant error) and assumes no change in LVOT geometry during exercise. Independently, stress echocardiography gives useful information pertinent to investigating central causes of exercise intolerance including atrial function, valve function and estimated pulmonary arterial systolic pressure.

An alternative imaging modality, which does not require such geometric assumptions when calculating cardiac output is cardiovascular MRI – CMR. CMR is the gold standard for assessing ventricular volumes and cardiac output non-invasively (52). Exercise-CMR – Ex-CMR - techniques have been developed primarily for ischaemia assessment, yet the technique is also useful for a wider range of indications, not least assessment of exercise intolerance. Exercise has been undertaken either with treadmill exercise immediately adjacent to the CMR scanner(53, 54), or with in-scanner exercise using supine bicycle(55, 56) or stepper(57, 58) ergometers.

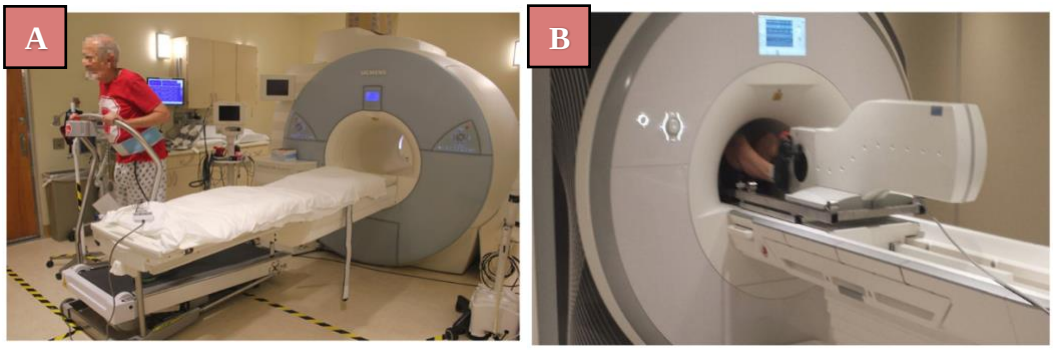

Figure 8. Exercise CMR modalities.

Panel A: Treadmill adjacent to CMR scanner. Panel B: Supine bicycle ergometer with patient in bore of scanner.

When Ex-CMR is combined with CPET – CMR-CPET(39) – accurate and reproducible measurements of VO_2 and cardiac output are possible at all stages of exercise, allowing derivation of peripheral tissue (skeletal muscle) oxygen extraction non-invasively. This additional information is useful as it has long been understood that in other chronic conditions characterised by dyspnoea and exercise intolerance, particularly heart failure, at least some of the limitation in exercise may be due to peripheral mechanisms, including the inability of skeletal muscle to utilise the oxygen delivered to it.

Direct comparisons between upright or semi-recumbent exercise and the supine forms of exercise are not possible due to changes in ventilation mechanics and venous return/loading of the right ventricle associated with the supine position. Furthermore, more emphasis is placed on hip flexor and extensors, and there is less engagement of upper body and core muscles during supine cycling. However, although overall VO_2 is lower for equivalent workloads, there is good correlation between supine and conventional CPET tests(59).

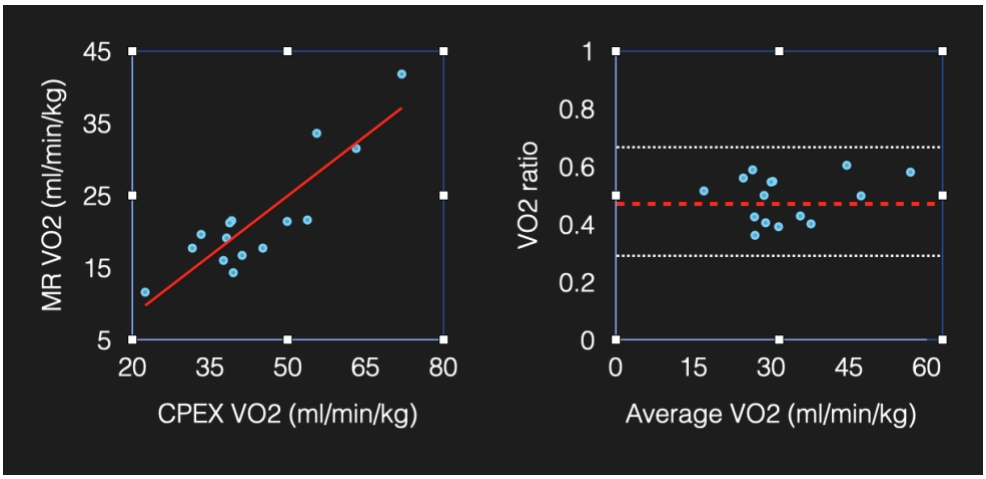

Figure 9. Comparison of CMR-CPET VO_2 values obtained at peak exercise versus conventional CPET VO_2

(n=15 healthy volunteers; r=0.94, p*<0.001, bias ratio = 0.48) Adapted from (58)*

8. SPECIAL POPULATIONS WITH EXERCISE INTOLERANCE

8.1 Pulmonary hypertension

Pulmonary hypertension is diagnosis made when raised pulmonary arterial pressures are detected at right heart catheterisation. At the time of applying for ethical approval, funding and patient recruitment, the haemodynamic definition of pulmonary hypertension required mean pulmonary arterial pressures (mPAP) of ≥25mmHg(60); measurements of pulmonary artery wedge pressure (PAWP, a surrogate for left atrial pressure) of >15mmHg implied a post-capillary component (i.e. due to left heart disease), whilst calculation of pulmonary vascular resistance (PVR) would determine the presence of pre-capillary pulmonary hypertension (PVR >3 Woods Units = pre-capillary involvement). The combination of pre- and post-capillary pulmonary hypertension is well recognised. The 2015 European Cardiology Society/European Respiratory Society guidelines on pulmonary hypertension did recognise that the diagnostic cut-off of 25mmHg for the diagnosis of pulmonary hypertension was arbitrary and suggested that a definition based on population mean and standard deviations (mean = 14mmHg, 2 SDs = +/- 6mmHg) might be adopted in future.

Indeed, the current haemodynamic definition of pulmonary hypertension, as per the 6th World Symposium on Pulmonary Hypertension in 2018(61), and adopted by the 2022 European Cardiology Society/European Respiratory Society guidelines (62) utilise the new haemodynamic criteria. As such, pulmonary hypertension is now defined by mPAP of >20mmHg at rest, with pre-capillary PH defined as also demonstrating PAWP ≤15mmHg and PVR > 2WU, and isolated post-capillary PH demonstrating PAWP >15mmHg and PVR ≤2WU. Combined pre- and post-capillary PH was formally defined as mPAP >20mmHg with PAWP >15mmHg and PVR >2WU. These changes were implemented during the time when

the data for this project was gathered, and such my results pertain to the previous definition of PH, and the conclusions cannot readily be applied to subjects with mean pulmonary pressures of 21-24mmHg.

Pulmonary hypertension affects around 1% of the global population, and in the UK has a prevalence of 125 cases/million population, with increased prevalence in older people(63). Accurate diagnosis and classification are essential so that the underlying aetiology is treated, and potentially harmful treatments avoided (e.g. pulmonary vasodilators, which produce prognostic benefit in pulmonary arterial hypertension, may worsen post-capillary pulmonary hypertension due to left heart disease).

Regardless of the cause of the pulmonary hypertension, the cardinal symptoms are of exercise intolerance, namely exertional dyspnoea fatigue. This is felt to be largely a manifestation of right-ventricular dysfunction.(62)

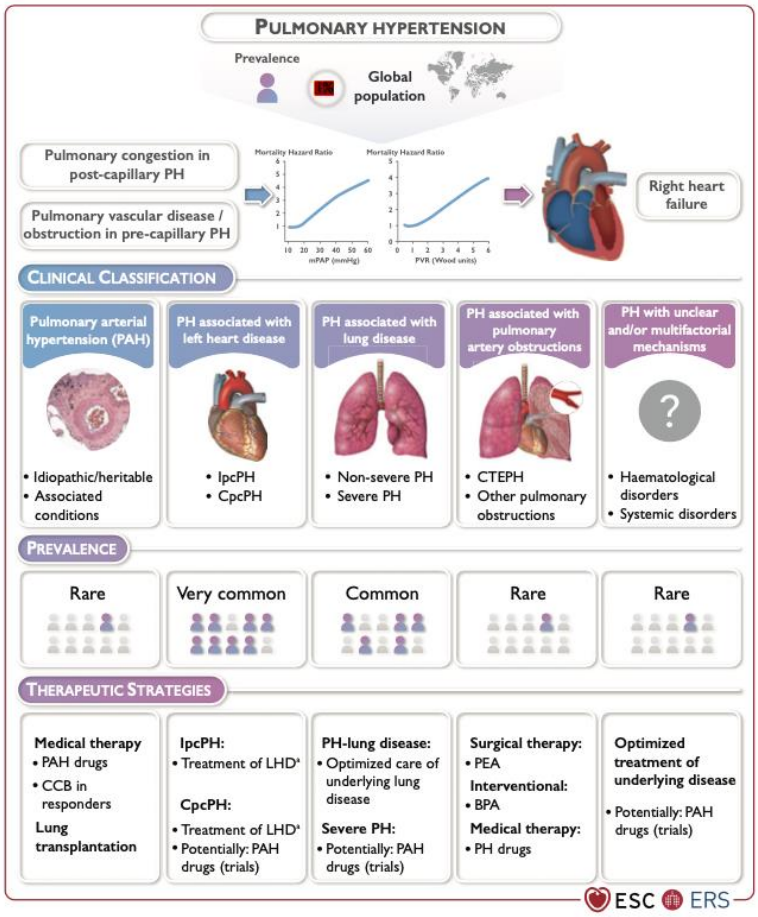

Figure 10. Classification, prevalence and therapeutic strategies of pulmonary hypertension groups.

BPA=balloon pulmonary angioplasty, CCB=calcium channel blocker, CTEPH=chronic thromboembolic pulmonary hypertension, CpCPH=combined pre- and post-capillary pulmonary hypertension, IpcPH=isolated post-capillary pulmonary hypertension, LHD=left heart disease, PAH=pulmonary arterial hypertension, PEA=pulmonary endarterectomy, PH=pulmonary hypertension, From European Cardiology Society/European Respiratory Society Pulmonary Hypertension Guidelines 2022(62)

8.1.1 Pulmonary arterial hypertension

This group of pulmonary hypertension demonstrates increased pulmonary arterial pressures and pulmonary vascular resistance, due to adverse remodelling of the vascular smooth muscle and endothelial proliferation of the pulmonary arteries. Most cases are idiopathic, with connective tissue disease (particularly systemic sclerosis), drugs/toxins (especially anorexigens) and porto-pulmonary hypertension making significant contributions.

8.1.1.1 Idiopathic pulmonary hypertension

Idiopathic pulmonary hypertension is diagnosed when the requisite haemodynamic criteria are met, and other causes of PAH are excluded(64). Traditionally thought to primarily affect young females without cardiovascular disease risk factors(65), it is increasing described in older individuals(66, 67). A form of the disease with capillary (pulmonary capillary haemangiomatosis, PCH) or venous (pulmonary veno-occlusive disease, PVOD) affects around 10% of IPAH patients, resulting in a severe and rapidly-progressive form of the disease. Heritable forms are described, particularly in mutations of the EIF2AK4 gene. Response to standard therapies is poor in this group. I did not recruit subjects with clinical suspicion of PCH/PVOD.

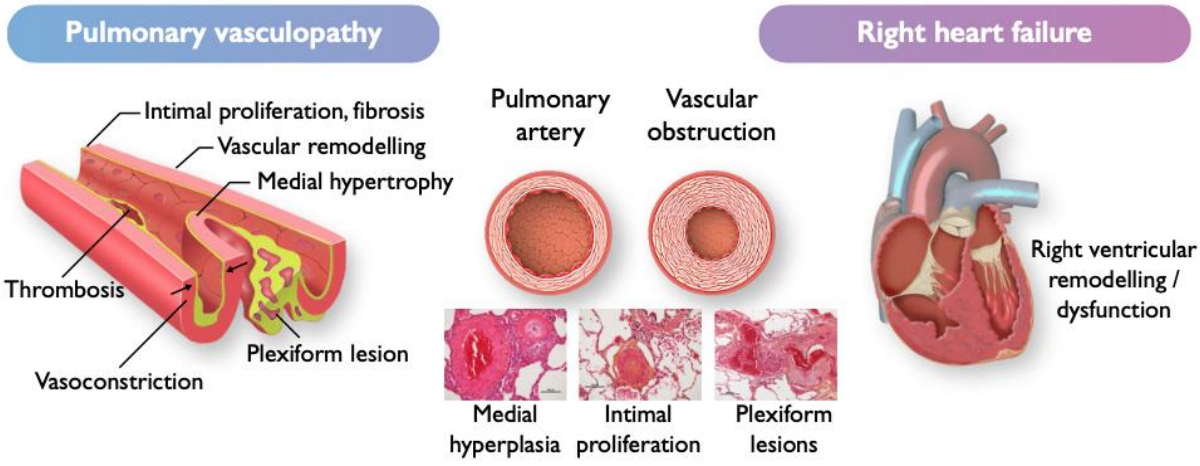

Figure 11. Schematic of changes in pulmonary arteries and right ventricle in PAH.

From(62)

8.1.1.2 Systemic sclerosis

Systemic sclerosis (SSc) is a connective tissue disease characterised by dysregulation of the immune system with autoantibody production, endothelial dysfunction resulting in microvascular injury and vasculopathy, and abnormal fibroblast proliferation and extracellular matrix deposition which produces the fibrosis responsible not only for the

pathognomonic skin thickening, but also that of multiple internal organs(68). Traditionally the extent and distribution of skin thickening allows classification of systemic sclerosis into limited cutaneous (lcSSc) and diffuse cutaneous (dcSSc) forms(69).

Systemic sclerosis is associated with a high burden of morbidity and premature mortality. Meta-analysis of cohort studies including patients with systemic sclerosis suggests that their pooled standardised mortality ratio is 3.5 times that of the general population, a figure that has persisted over the last 40 years despite advances in therapies targeted at limiting end-organ damage(70).

A significant proportion of this disease burden is attributable to pulmonary and cardiovascular involvement.

Direct pulmonary involvement, more common in the diffuse subset, manifests as interstitial lung disease (ILD), which is itself often severe enough to cause pulmonary hypertension (Group 3 PAH, due to lung disease). The pulmonary vasculature can be affected even in the absence of interstitial disease, causing pulmonary *arterial* hypertension(71). This form of the disease appears more common in the limited subset. Often, there is a mixed picture of pulmonary vascular and lung parenchymal components, and as many as 7-13% of SSc patients will develop pulmonary hypertension of some form(72, 73).

Cardiovascular involvement can take the form of left ventricular failure due to acute myocardial inflammation, chronic myocardial fibrosis and microvascular dysfunction; pericardial disease including effusions; conduction disease; and right ventricular dilation and failure as a consequence of pulmonary hypertension(74).

Renovascular disease including renal crises, esophageal dysmotility with resultant risk of recurrent aspiration pneumonias, skeletal myositis and restrictive deformities of joints and chest wall due to skin thickening can all compound the situation regarding exercise intolerance. Systemic sclerosis-related vasculopathy and muscle inflammation may, by impairing muscle oxygen extraction, add another limitation to exercise capacity.

A prominent feature of systemic sclerosis is exertional dyspnoea. Subtler forms of this, such as exercise intolerance or avoidance, and early fatigue, may be overlooked unless specifically sought. The 6-minute walk test, although not validated specifically in the scleroderma population, can quantify the severity of the exercise limitation. However, the multi-system nature of the disease makes identifying the predominant cause of the exercise limitation a diagnostic challenge. Serial biochemical, radiological, spirometric and echocardiographic assessments are required to assess the relative potential contributions of the respiratory and cardiovascular systems to the dyspnoea.

8.1.1.3 Systemic sclerosis-associated pulmonary hypertension

When indicated right heart catheterisation is required to assess the pulmonary pressures invasively(75) – see Figure 12.

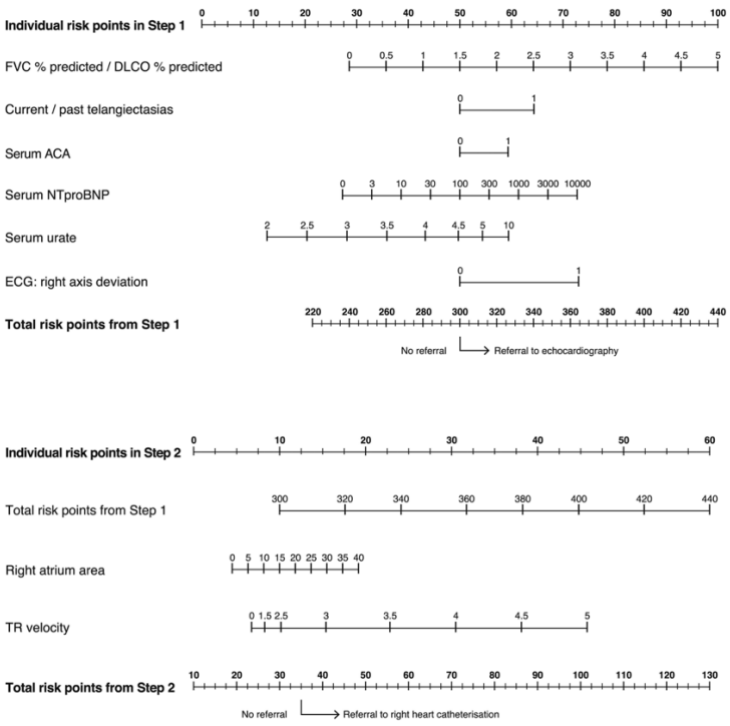

Figure 12. DETECT Algorithm

Nomograms for practical application of the DETECT algorithm: determination of the likelihood of pulmonary arterial hypertension and cut-off points for decision to refer a patient to echocardiography (Step 1) and subsequent right heart catheterisation (Step 2). At Step 1 (top panel), risk points for each of the six non-echocardiographic variables are calculated by reading from 'Individual risk points in Step 1' and adding them up to obtain a total. If the 'Total risk points from Step 1' is >300 (corresponding to a sensitivity of 97% as selected by the Study Scientific Committee) the patient is referred to echocardiography. Similarly, at Step 2 (bottom panel), risk points for the carried forward 'Total risk points from Step 1' and the two echocardiographic variables are calculated by reading from the 'Individual risk points in Step 2'. If the 'Total risk points from Step 2' is >35 (corresponding to a specificity of 35% as selected by the Study Scientific Committee) the patient is referred to right heart catheterisation. Alternatively, being less conservative (65% predefined specificity at Step 2), the patient would be referred to right heart catheterisation if 'Total risk points from Step 2' is >40. Note that all variables will always contribute risk points irrespective of the measured value; for example, a negative serum ACA will contribute 50 risk points. Exclusion of any single variable from the DETECT algorithm has only a small impact on model performance. If a single Step 1 variable is missing it should be assigned 50 risk points, with the exception of current/past telangiectasias which should be assigned 65 points. If a single Step 2 variable is missing it should be assigned 10 points. The nomograms cannot be reliably used if more than one variable out of the eight total variables is missing. ACA, anticentromere antibody; DLCO, pulmonary diffusing capacity for carbon monoxide; FVC, forced vital capacity; NTproBNP, N-terminal pro-brain natriuretic peptide; TR, tricuspid regurgitant jet. Adapted from Coghlan et(75).

Interestingly, despite usually presenting with better pulmonary haemodynamics (lower mean pulmonary artery pressure) than patients with idiopathic pulmonary hypertension, those with SSc-associated pulmonary arterial hypertension are found to have less pronounced

haemodynamic and symptomatic response to pulmonary vasodilator therapy, and also worse mortality outcomes(76). Some of this observation may be explained by the SSc-PAH patients being older on average, and undoubtedly the involvement of other organ systems will contribute. To a certain extent, the modest pulmonary pressures may be a reflection of reduced cardiac output in SSc-PAH patient, either due to disease involvement of the cardiac muscle, or genuinely higher pulmonary vascular resistance against which the right ventricle of SSc-PAH patient is somehow less able to compensate against, but factors other than the pulmonary hypertension and right ventricular function may set the limit to exercise tolerance in SSc-PAH patients.

The use of cardiopulmonary exercise testing (CPET) has been highlighted recently as a promising tool to delineate which part of the cardio-respiratory axis is limiting in SSc patients. One study retrospectively analysed CPET data from 78 SSc patients without known pulmonary hypertension to assess if the limitation was due to respiratory limitation, left ventricular dysfunction or pulmonary vasculopathy(77). CPET has been proposed to better screen SSc patients as being at risk of having PAH, with the aim of more judicious use of right heart catheterisation(78). Exercise metrics derived from CPET, namely VO_2 and V_E/VCO_2 have been shown to predict survival and time to clinical worsening in IPAH patient, and also in patients with other types of PAH(8). However, whether this adds significantly to the prognostic information from 6MWT in PH patients is unclear(79).

8.1.2 Pulmonary arterial hypertension therapies

Current therapeutic strategies for pulmonary arterial hypertension aim to promote pulmonary artery vasodilation. Whilst termed “targeted therapies” or “pulmonary vasodilators”, all agents invariably contribute to systemic vasodilation as well, so their dosage must be titrated to

balance improvement in pulmonary haemodynamics and symptoms against systemic side effects.

Calcium channel blockers, including nifedipine and amlodipine, can be used in the ~10% of patients with IPAH who demonstrate response to acute vasodilator therapy.

Endothelin receptor antagonists reduce the binding of endothelin-1 to endothelin receptors on pulmonary arterial smooth muscle cells, and thereby reduced smooth muscle proliferation and constriction. Examples include ambrisentan, bosentan and macitentan, which are all available as oral agents.

Agents that result in a net increase of cyclic-GMP will increase GMP formation in pulmonary arterial smooth muscle cells, promoting vasodilation. Phosphodiesterase 5 inhibitors (PDE5i) achieve this by reducing the breakdown of nitric oxide by phosphodiesterase, stimulating soluble guanylate cyclase (sGC). The sGC then promotes conversion of GTP to cGMP. Examples of PDE5is include sildenafil and tadalafil. Direct stimulation of sGC can be achieved using riociguat.

The final pathway exploited by current strategies uses the prostacyclin pathway. Prostacyclin promotes vasodilation and is under expressed in patients with PAH. Prostacyclin analogues can be administered intravenously (epoprostenol), subcutaneously (treprostinil), via inhalation (iloprost, treprostinil) or orally (treprostinil, beraprost). Selexipag is a selective prostacyclin receptor agonist available orally.

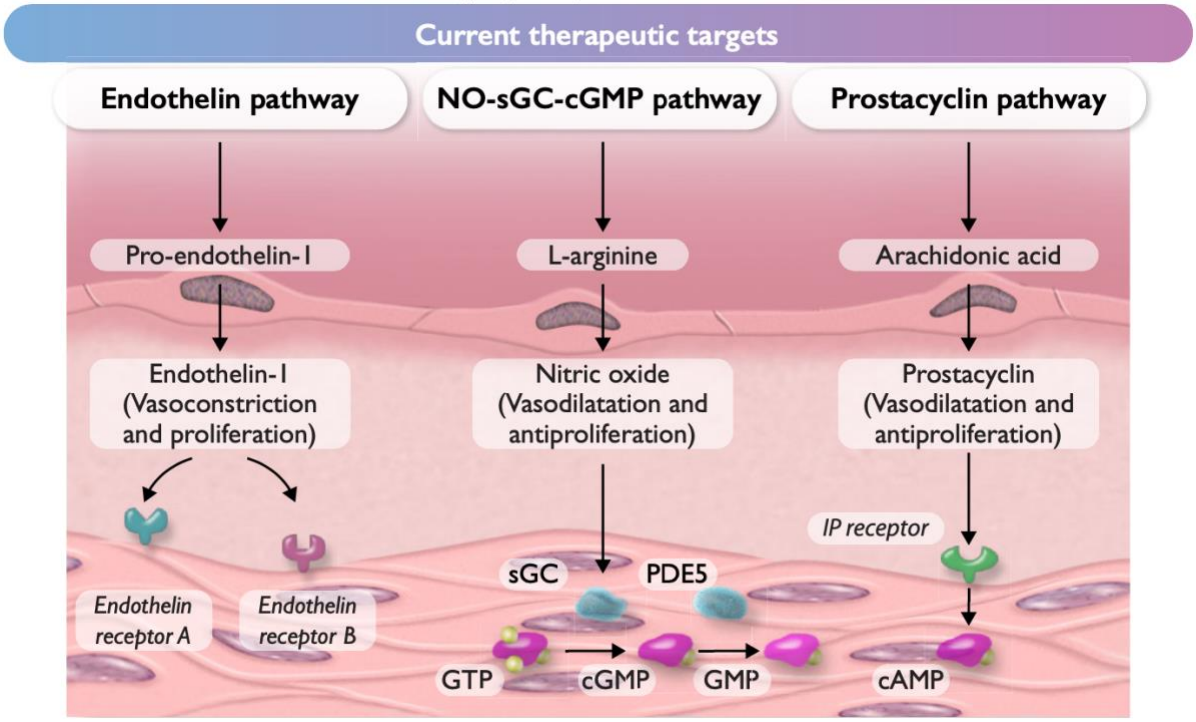

Figure 13. Therapeutic targets in pulmonary arterial hypertension

Current therapeutic targets of pulmonary arterial hypertension (group 1). cAMP, cyclic adenosine monophosphate; (c) GMP, (cyclic) guanosine monophosphate; GTP, guanosine-5'-triphosphate; IP receptor, prostacyclin I2 receptor; NO, nitric oxide; PDE5, phosphodiesterase 5; sGC, soluble guanylate cyclase. From (62).

8.2 Long-COVID

During the COVID-19 pandemic, I was unable to recruit patient with pulmonary hypertension on an outpatient basis because their clinically highly vulnerable status required them to shield. I did endeavour to recruit pulmonary hypertension patients with other reasons to attend hospital, but necessarily these numbers were limited.

After the first wave of COVID-19, reports of persistent dyspnoea and exercise intolerances were published(80, 81). It was clear that the multi-system effects of COVID-19 might give rise to multiple causes for exercise intolerance after acute infection had resolved. Direct myocardial

injury (myocarditis and myocardial infarction), lung parenchymal injury and thromboembolic disease were all potential mechanisms. However, there were patients with no evidence of central limitation to exercise who still experienced profound symptoms(82), and I was ideally placed to comprehensively assess these patients using CMR-CPET.

9. RESEARCH AIMS AND OBJECTIVES

This thesis investigates the utility of CMR-CPET in investigating patient groups with exercise intolerance. My aims were:

1. To measure CMR-CPET metrics at rest and at peak exercise in systemic sclerosis associated pulmonary hypertension patients, with a control group for systemic sclerosis, a control group for pulmonary hypertension, and a healthy volunteer control group, examining differences between groups to identify mechanism for exercise intolerance in SSc-PAH.
2. To measure CMR-CPET metrics at rest and at peak exercise in patients with exercise limitation after COVID-19 infection, with a control group for patients with no limitation after COVID-19 infection, and a healthy volunteer group; examining differences between groups to identify mechanism for exercise intolerance after COVID-19.
3. To assess if CMR-CPET provides prognostic information in patients with systemic sclerosis-associated pulmonary arterial hypertension (SSc-PAH).

10. METHODS AND MATERIALS

I will discuss the techniques I used to obtain data about cardiac output (phase contrast CMR measuring aortic flow) and ventricular volumes, and how exercise CMR was performed. I will also outline how I used CPET to measure VO_2 during exercise. Finally, I will discuss how the data were integrated and analysed.

Imaging was performed on a 1.5 Tesla MR scanner (Magnetom Aera, Siemens Healthcare, Erlangen, Germany) in a temperature-controlled suite. Full resuscitation facilities were available. Peripheral venous access was sited in case of emergency, with blood samples taken where indicated, and the ECG was continuously monitored on the MR scanner.

10.1 Phase Contrast MR

Phase contrast magnetic resonance is a technique that allow measurement of blood flow through vessels. Inherent in the information encoded in the voxels by this magnetic resonance imaging technique is velocity. By prescribing the desired image plane, perpendicular to vessel of interest, it is possible to define the cross section of the vessel. The volume of flow through the vessel can then be measured. Phase contrast can measure blood flow in the pulmonary artery and the aorta, allowing calculation of Qp:Qs ratios to quantify intracardiac shunts non-invasively. It can also be used to compare retrograde flow versus anterograde flow across a valve to quantify regurgitant volumes and fractions. In this context, phase refers to the spin phase of hydrogen nuclei present in free water and lipid molecules. In the presence of the homogenous B_0 magnetic field within an MRI scanner, the intrinsic nuclear spin of the vast majority of these hydrogen nuclei aligns with the B_0 field (see Figure 13).

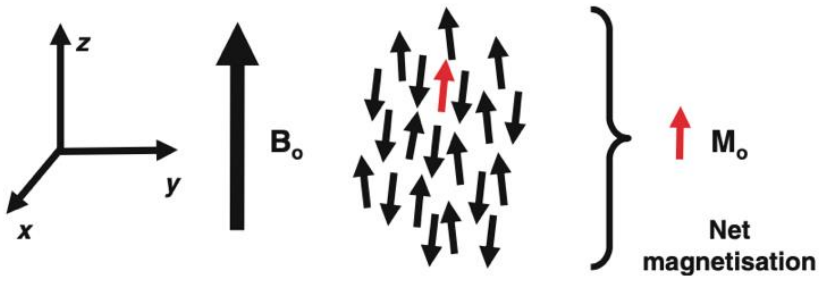

Figure 14. Proton magnetic moments.

Hydrogen nuclei magnetic moments (represented by small arrows) align either with or against the direction of magnetic field B_0, i.e. the z-axis. In this example, there is an excess of just one proton (shown in red) aligned with the field, giving rise to the Net Magnetization M_0. Adapted from (83).

Other magnetic fields can be applied, in addition to B_0, with gradients in field strength along the x-, y- or z-axes, or a combination thereof (see Figure 14).

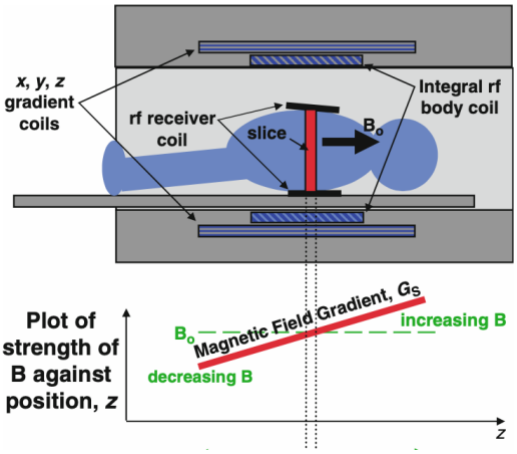

Figure 15. Magnetic field gradients within a MRI scanner.

The x, y and z gradient coils can create magnetic fields with gradients in strength along each of the respective axes. In this example, the gradient is along the z-axis. Adapted from (83).

By applying a magnetic field gradient that increases in strength parallel to the direction of flow of the vessel to interrogated, hydrogen nuclei that are moving in the direction of flow with accrue more phase than stationary hydrogen nuclei in surrounding tissue the further along the gradient they travel. By then reversing the magnetic field by an equal amount after a specified period of time, the phase of the stationary hydrogen nuclei will return to the original orientation but the moving nuclei, moving to a region of greater magnetic field strength, will now accrue phase in the opposite direction overall. The amount of phase accrued by these moving nuclei is proportional to both the velocity of flow and the strength of the applied magnetic field. Given that then strength of the applied magnetic field is known, velocity can be calculated:

$$\Delta\phi = \gamma G V T^2$$

Equation 3. Phase shift of hydrogen nuclei in a gradient magnetic field.

Φ = phase shift, γ = gyromagnetic ratio, G = amplitude of applied magnetic field gradient, V = hydrogen nuclei velocity, T = application time for one gradient.

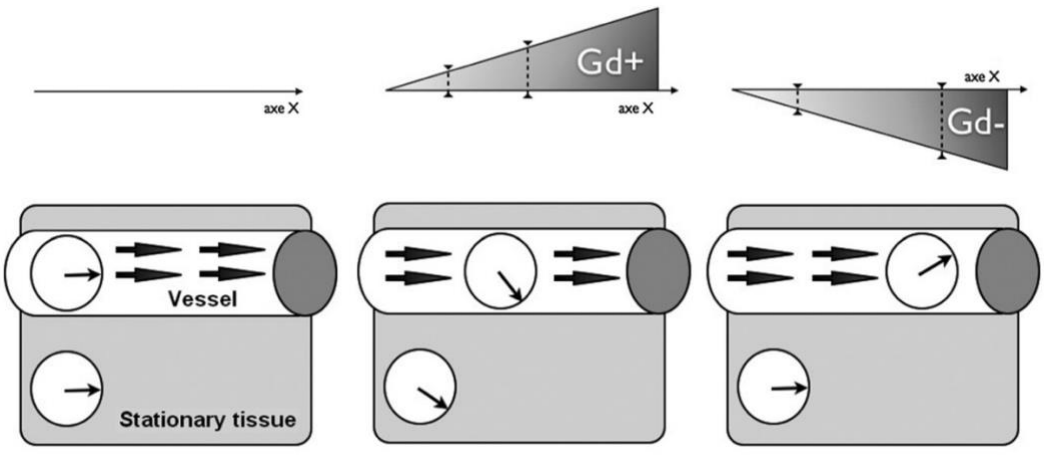

Figure 16. Representation of phase contrast MR.

When the first phase of the bipolar gradient (Gd+) is applied, spins shift phase depending on their position on the x-axis. When the second, same intensity and duration but reverse polarity, gradient (Gd−) is applied, the phase shift of stationary protons is cancelled out whereas the phase shift of moving protons becomes proportional to their speed. Adapted from (84).

For my experiments, aortic flow was measured using real-time phase-contrast (PC) CMR (PC-CMR) using a uniform density golden-angle spiral sequence, with a compressive sensing (CS) reconstruction(85). The following parameters were used:

(1) matrix = 192×192

(2) slice thickness = 7 mm

(3) TR/TE = 9.8/1.6 ms

(4) flip angle = 25°

(5) velocity encoding = 300 cm/s

(6) temporal resolution = ~ 41 ms

(7) spatial resolution = 2.3 × 2.3 mm

(8) acceleration factor = 6.

By integrating the aortic flow across the cardiac cycle, stroke volume can be calculated, with cardiac output being the product of stroke volume and heart rate (see Figure 16).

This technique can be used, within reason, even where there is some movement of the body, as it relies on the relative motion *between* the sampled structures (eg blood within a vessel, and surrounding tissues). This is of obvious benefit during exercise, where movement of the region of interest may occur due to respiratory motion and from the action of the exercise itself, eg pedalling or stepping, during which physical restraint would be undesirable.

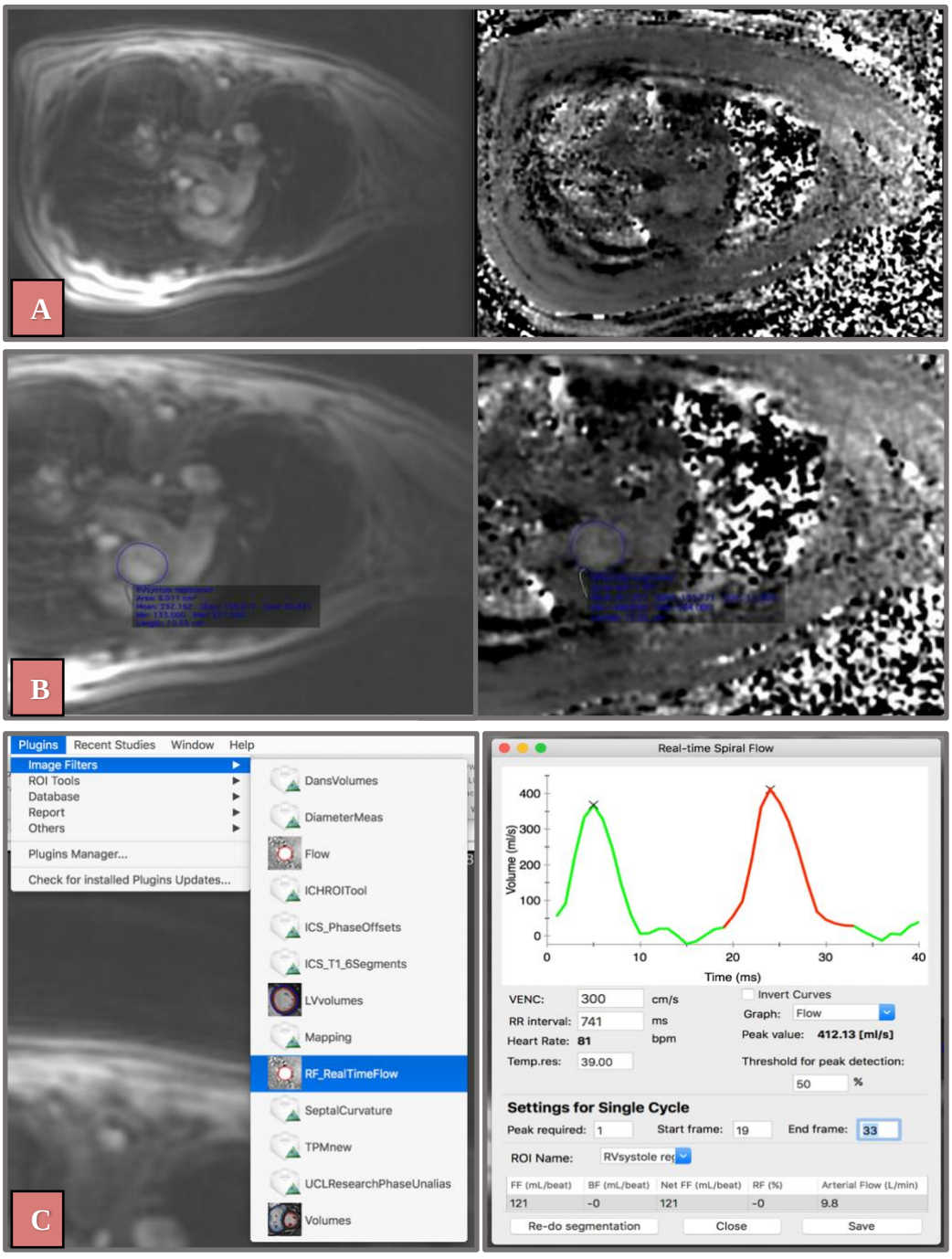

Figure 17. Measurement of aortic flow and cardiac output using PC-MR

Panel A. Phase (left) and magnitude (right) images of phase-contrast imaging through the ascending aorta. Panel B. Aorta identified, and region of interest (ROI) drawn for all images in series using semi-automated tool. Panel C. Measurement of forward flow through aorta, and cardiac output calculated by integrating flow across the cardiac cycle. In this example, forward flow = 121ml, heart rate = 81bpm and cardiac output = 9.8L/min.

10.2 Ventricular Volumetric Assessment

Real-time assessment of left ventricular (LV) and right ventricular (RV) volumes was performed immediately after each real-time flow acquisition using a 2D multi-slice real-time tiny golden-angle spiral CS balanced steady state free precession (bSSFP) sequence(86). The following parameters were used:

(1) matrix = 208×208

(2) slice thickness = 8 mm

(3) TR/TE = 3.4/0.7 ms

(4) flip angle = 67°

(5) temporal resolution = ~31 ms

(6) spatial resolution = 1.7×1.7 mm

(7) acceleration factor = 8

Fourteen slices were used in each acquisition. This allowed the whole volume of the heart to be imaged, allowing for motion from exercise and respiration. Each slice was acquired over 2 R-R intervals. All real-time imaging was acquired during free breathing.

LV and RV endocardial borders were traced manually on the short-axis images at end diastole and end systole, identified by visual assessment of the largest and smallest cavity areas, respectively. Papillary muscle and trabeculae were excluded from the blood pool, a convention adhered to in our department for reporting of clinical scans, and our research group. This method is applied consistently and therefore complies with the guidance from the Society for Cardiovascular Magnetic Resonance (SCMR)(87, 88) . Ventricular stroke volumes were

calculated as the difference between the end diastolic volume (EDV) and end systolic volume (ESV), and ejection fraction (EF) was determined as (SV/EDV)×100.

Where relevant, LV and RV myocardial mass are reported. RV myocardial mass is not routinely reported for clinical scans in our institution, due to its limited thickness and propensity for error. In pulmonary hypertension populations, it has not been found to convey extra prognostic information beyond the pulmonary haemodynamics (89).

Postprocessing of SV data obtained by aortic phase-contrast MR flow imaging and by volumetry of cine images was performed in tandem to maintain internal consistency as suggested by Society for Cardiovascular Magnetic Resonance Task Force recommendations(90)

Figure 18. Assessment of ventricular volumes.

Panel A. Selection of volume tool.
Panel B. Identification of endocardial borders of LV and RV at end diastole (left) and end systole (right).
Panel C. Example ventricular volumes, stroke volume, ejection fraction and cardiac output.

10.3 Exercise CMR

Subjects performed exercise on a supine MR-compatible cycle ergometer (MR Cardiac Ergometer Pedal, Lode, Groningen, Netherlands) – see Figure 18-A. This attaches to the MRI table and allows the participant's body to be in the bore of the MRI scanner with their legs outside the scanner and feet placed in the pedals of the ergometer. The participant would have their range of movement whilst pedalling assessed, and then would be positioned with their heart as close to isocentre in the MRI scanner as possible without restricting their ability to pedal.

The ergometer allowed exercise workload (power measured in Watts, W) to be controlled manually by as little as 1W increments. A target cadence of between 60-70 revolutions per minute would result in the specified resistance (lower cadences would result in increased apparent workload, whilst higher cadences would result in decreased apparent workload). Each experiment had a ramped workload protocol, with workload increments appropriate for the population under investigation.

Systolic blood pressure was recorded at rest and peak using a MR-compatible blood pressure monitor (Expression MR400, Philips Healthcare, Best, The Netherlands). Peripheral oxygen saturations were monitored using the pulse oximeter supplied with the CMR scanner.

10.4 CPET-CMR Equipment

Cardiopulmonary exercise testing was performed with breath-by-breath gas exchange analysis using a commercial CPET system (Ultima, MedGraphics, St Paul, Minnesota, USA). The analyser was placed in the CMR control room and attached to the patient facemask (Hans

Rudolph, Kansas City, Kansas, USA) via a set of CMR-compatible sampling tubes (umbilicus) passed through the waveguide. This bespoke umbilicus was modified as previously described(58) increasing the overall length from the standard 234 cm to 1000 cm, and removing ferromagnetic components – Figure 18-B. It was thoroughly tested by the manufacturer, meeting all quality control standards. Gas and flow calibrations were performed before each test and at least 30 minutes after system initiation to allow the device components to reach the required working temperature. All measurements were taken at body temperature and ambient pressure.

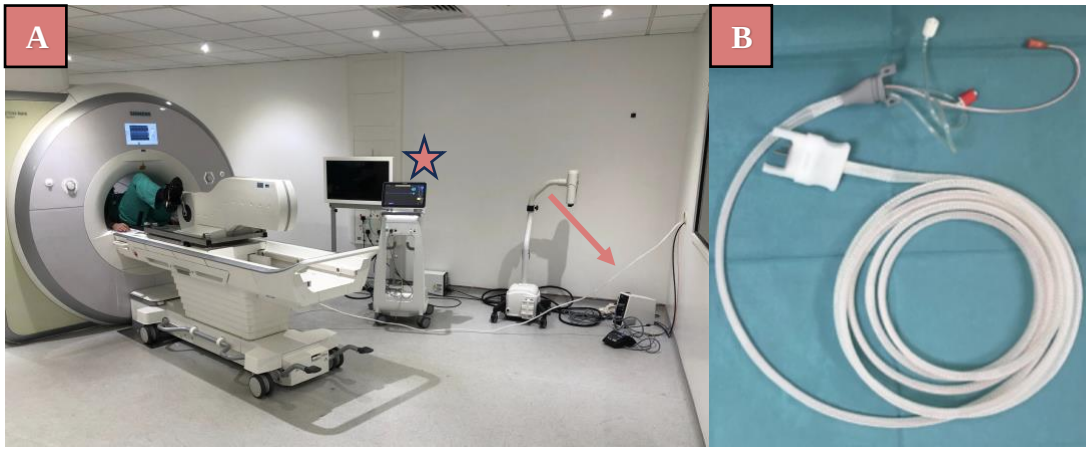

Figure 19. CMR-CPET equipment.

Panel A. CPET Umbilicus (arrow) passing through waveguide from CMR control room to patient in bore of CMR scanner. MR-compatible cycle ergometer attached to MR table, with patient's feet in pedals. Blood pressure monitor (star).
Panel B. CPET Umbilicus.

10.5 Image Reconstruction and Analysis

The aortic flow and short-axis image data were reconstructed off-line (MATLAB R2018a, MathWorks Inc, Natick, Massachusetts, USA), using the Berkeley Advanced Reconstruction Toolbox (BART)(91). The reconstructed images were exported as DICOM files and analysed

on reporting workstations. Flow and volumetric data CMR data were time-registered to the CPET data. All statistical analyses were performed using R (version 3.2.0, The R Foundation for Statistical Computing, Vienna, Austria).

11. RESULTS - COMPARING THE MECHANISMS OF EXERCISE LIMITATION IN SYSTEMIC SCLEROSIS, SYSTEMIC SCLEROSIS-ASSOCIATED PULMONARY HYPERTENSION AND NON-CONNECTIVE TISSUE-ASSOCIATED PULMONARY HYPERTENSION

This chapter is based on the publication below:

Brown JT, Kotecha T, Steeden JA, Fontana M, Denton CP, Coghlan JG, Knight DS, Muthurangu. Reduced exercise capacity in patients with systemic sclerosis is associated with lower peak tissue oxygen extraction: a cardiovascular magnetic resonance-augmented cardiopulmonary exercise study. Journal of Cardiovascular Magnetic Resonance. 2021 Oct 28;23(1):118

My contribution to this work was recruiting subjects, designing the exercise protocol, conducting all exercise tests, analysing clinical, CPET and CMR data, performing statistical analysis and writing the manuscript.

The study was approved by national ethics committee (IRAS project ID 226101; REC reference 17/LO/1499, National Health Service Health Research Authority UK CRN 058274). All subjects provided written informed consent.

11.1 Introduction

Exercise intolerance is common in systemic sclerosis (SSc), due to lung disease, myocardial involvement, pulmonary artery hypertension (PAH) or anaemia. A relatively under-investigated cause of reduced exercise capacity in these patients is skeletal muscle dysfunction.

It has been shown that SSc patients have skeletal muscle inflammation, fibrosis and vasculopathy(92), all of which can reduce tissue oxygen extraction. Reduced oxygen extraction leads to reduced energy production, skeletal muscle dysfunction and ultimately exercise intolerance.

Understanding the relative importance of these factors is vital for targeting therapy. Unfortunately, this is difficult with conventional cardiopulmonary exercise testing (CPET) as only oxygen consumption (VO_2) is *directly* measured; *other measurements are inferred.* A recently developed a novel technique that combines exercise cardiovascular magnetic resonance (CMR) with conventional CPET(58) has been described. This method (CMR-CPET) provides quantitative assessment of exercise capacity through combined direct measurement of both VO_2 and cardiac output. The CMR measurements of cardiac output are considered gold-standard, eliminating some of the assumptions made by other non-invasive methods (e.g. Doppler echocardiography). Importantly, combining VO_2 and cardiac output allows calculation of arteriovenous oxygen content gradient (ΔavO_2), a robust marker of tissue oxygen extraction(93). CMR-CPET also enables accurate evaluation of ventricular function during exercise, providing a reference standard measure of contractile reserve. Finally, T1 and T2 mapping can also be performed in order to assess myocardial fibrosis and oedema/inflammation, which may be particularly pertinent in SSc patients.

The aim of this study was to use CMR-CPET to comprehensively investigate exercise capacity in patients with SSc. To achieve this, I investigated SSc patients with and without PAH. Furthermore, I included both a healthy control group and a disease control group consisting of patients with PH not due to connective tissue disease (NC-PH). The specific aims of this study were to:

(1) Compare CMR-CPET metrics in the 4 groups

(2) Correlate CMR-CPET metrics to clinical characteristics (6-min walk distance, lung function tests and haemoglobin)

(3) Compare CMR-CPET metrics to myocardial T1 and T2 to identify associations with myocardial fibrosis and oedema/inflammation.

11.2 Methods

11.2.1 Study population

Sixty subjects were recruited between March 2019 and January 2021:

(1) Systemic sclerosis (SSc) - 15 subjects
(2) Systemic sclerosis-associated pulmonary arterial hypertension (SSc-PAH) - 15 subjects
(3) Non-connective tissue disease pulmonary hypertension (NC-PH: either idiopathic pulmonary arterial hypertension—IPAH, or chronic thromboembolic pulmonary arterial hypertension—CTEPH) - 15 subjects
(4) Healthy controls - 15 subjects

Patients were recruited from specialist clinics at a tertiary referral centre for connective tissue disease (CTD) and PAH.

Inclusion criteria were:

(1) confirmed clinical diagnosis for patient groups

(2) age 18–80 years.

In SSc patients, PAH was excluded by either right heart catheterisation (5/15 patients) or by clinical evaluation and risk assessment with a validated risk-assessment tool(75) including, where necessary, echocardiography (10/15 patients). In the 2 PH groups, PH diagnosis was confirmed by right heart catheterisation.

Exclusion criteria were:

(1) general contraindications to CMR scanning

(2) contraindications to performing exercise test (unstable symptoms, including angina, exertional syncope, WHO class IV symptoms, and musculoskeletal disease preventing exercise)

(3) previous symptomatic ischemic heart disease or moderate to severe valvular disease

(4) changes in targeted PH therapy within 3 months

(5) significant lung parenchymal disease that may confound CPET results, such as interstitial lung disease (significant being defined as > 20% lung volume on computed tomography, using a qualitative visual assessment by an experienced computed tomography radiologist at our institution's multi-disciplinary meeting).

Clinical measures from the last outpatient appointment (including 6-min walk test in PH groups) and the most recent lung function test data were collected in all patient groups. In addition, the most recent cardiac catheterisation data were also collected in the 2 PH groups.

11.2.2 CMR-augmented cardiopulmonary exercise testing

Imaging was performed on a 1.5T CMR scanner (Magnetom Aera, Siemens Healthineers, Erlangen, Germany) using two 6-element coils (one spinal matrix, one body matrix). The scanning room was temperature controlled. Full resuscitation facilities were available. Each subject's electrocardiogram (ECG) was monitored continuously using the in-built system in the CMR scanner. This system allowed assessment of rate and rhythm but is not suitable for identification of ischemia. All patients had peripheral venous access during testing for use in resuscitation protocols in the event of clinical instability.

11.2.3 CMR imaging techniques (real-time flow and volume imaging)

Before exercise, subjects underwent a routine CMR with long- and short-axis cine imaging, myocardial native T1 and T2 mapping as previously described(94, 95).

See Chapter 10 (Methods) for description of phase contrast CMR and ventricular volume assessments and CPET.

11.2.4 Exercise protocol

Subjects performed exercise on a supine CMR-compatible cycle ergometer (MR Cardiac Ergometer Pedal, Lode, Groningen, Netherlands). This ergometer allowed exercise workload (power measured in Watts, W) to be controlled by altering resistance. Subjects were briefed before their scan and familiarised with the equipment and exercise protocol. Baseline resting aortic flow and ventricular volumes were acquired before commencing the ramped exercise protocol.

The first minute consisted of exercise against zero resistance, with subjects asked to cycle at 60–70 rpm. Thereafter, the protocol was split in 2-min stages. During each stage, workload was increased at 0, 30 and 60 s with acquisition of aortic flow and ventricular volumes commenced at 90 s. Workload increments at 0, 30 and 60 s varied by stage as follows:

- Stages 1–3: 3 W
- Stages 4–6: 5 W
- Stage 7–8: 7 W
- Stages 9–10: 9 W
- Stages 11–12: 11 W

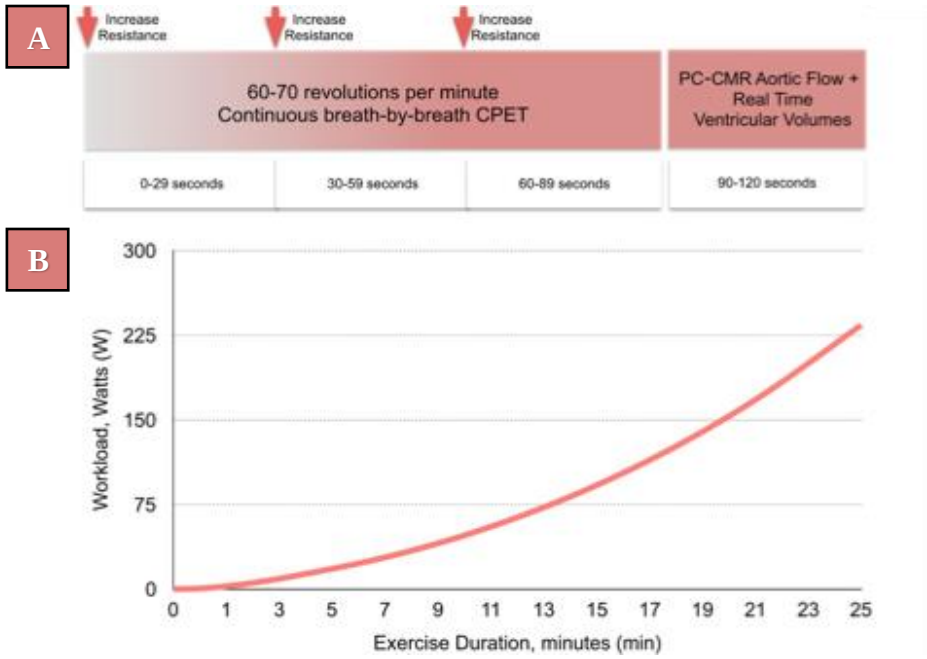

Figure 20. Exercise protocol

Panel A: Exercise and scanning protocol
Panel B: Cumulative workload

The smaller increments at the start of the protocol ensured that even subjects with significant exercise intolerance were able to complete at least 2 exercise stages. This protocol was followed until exhaustion, and at the onset of exhaustion (defined as an inability to maintain cadence or a verbal indication from the subject) the subject was encouraged to maintain cycling while peak aortic flow and ventricular volumes were acquired. Exercise was then stopped, followed by a 15-min recovery period with monitoring of vital signs in the CMR room.

11.2.5 Data analysis

All post-processing of the reconstructed images was performed using 'in-house' plug-ins for the open-source OsiriX DICOM software version 9.0.1 (OsiriX Foundation, Geneva, Switzerland)(96-98).

PC-CMR flow data of the ascending thoracic aorta was segmented using a semi-automatic vessel edge detection algorithm with manual operator correction if required. Stroke volume (SV) was calculated by integrating the flow curve across a single R-R interval. Cardiac output was given by SV x heart rate (HR).

LV and RV endocardial borders were traced manually on the short-axis images at end diastole and end systole, identified by visual assessment of the largest and smallest cavity areas, respectively. Papillary muscle and trabeculae were excluded from the blood pool. Biventricular stroke volumes were calculated as the difference between the end diastolic volume (EDV) and end systolic volume (ESV), and ejection fraction (EF) was determined as (SV/EDV)×100. All measurements were reported by an experienced clinical CMR specialist (DK) blinded to the clinical information. All volumetric data and cardiac output were indexed to body surface area (BSA) and denoted by the suffix "i".

VO_2 and respiratory exchange ratio (RER) measurements were co-registered to CMR data. The VO_2 was indexed to body weight and denoted by the prefix "i". Arteriovenous oxygen content gradient was calculated as $\Delta avO_2 = VO_2/CO$ (using non-indexed data). These calculations were performed at rest and at peak-exercise for all subjects.

11.2.6 Statistical analysis

All statistical analyses were performed using R (version 3.2.0, The R Foundation for Statistical Computing, Vienna, Austria). Data were examined for normality using the Shapiro–Wilk normality test.

Descriptive statistics were expressed as mean (±standard deviation) for normally distributed data, or median (range) for non-normally distributed data.

Main effects of disease type and exercise, and an interaction term representing disease multiplied by exercise for CMR-CPET metrics, were assessed using repeated measures ANOVA (normal data) or aligned rank repeated measures ANOVA (non-normal data). Between-group differences (at rest and exercise) were assessed using 1-way analysis of variance (ANOVA) for normal data, or the Kruskal-Wallis 1-way analysis of variance for non-normal data.

Post hoc comparisons were performed using pairwise *t* tests (normal data) and Mann Whitney tests (non-normal data) with Benjamini-Hochberg correction for multiple comparisons.

Sex distribution between the groups was assessed using the Chi-squared test.

Correlation between metrics corrected for diagnosis was computed using multi-level Spearman's rank partial correlation coefficient.

A p value<0.05 was considered statistically significant.

11.3 Results

11.3.1 Demographics and clinical data

There were no significant differences in age, sex, height, weight or BSA. (Table 2). In both the SSc and SSc-PAH groups, 14 patients (93%) had limited cutaneous systemic sclerosis, while the remaining patient in each group had a diagnosis of diffuse cutaneous systemic sclerosis. (Autoantibody profiles detailed in Table 3). In the NC-PH group, 10 (67%) patients had IPAH and 5 (33%) had CTEPH. Medications for all patients are shown in Table 3.

	SSc	**SSc-PAH**	**NC-PH**	**Control**	***p* value**
Age (yrs)	52.5±14.0	59.7±8.4	51.1±18.1	51.3±4.2	0.19
Height* (m)	1.6 (1.6-1.8)	1.6 (1.5-1.9)	1.6 (1.5-1.9)	1.6 (1.6-1.8)	0.95
Weight (kg)	66.2±14.5	68.6±14.3	75.7±18.4	70.4±13.0	0.38
BSA (m^2)	1.7±0.2	1.8±0.2	1.8±0.2	1.8±0.2	0.72
M/F	2/13	3/12	7/8	3/12	0.15

Table 2. Subject demographics.

BSA=Body Surface Area
NC-PH=Non-Connective Tissue Disease Pulmonary Hypertension
SSc=Systemic Sclerosis
SSc-PAH=Systemic Sclerosis-associated Pulmonary Arterial Hypertension
**denotes non-normally distributed, data shown as median (interquartile range).*

	SSc	SSc-PAH	NC-PH
Antibody Profile			
ACA	7	13	-
ANA	1	-	-
Anti-RNA polymerase III	1	-	-
Anti-RNP	1	2	-
Anti-Scl70	5	-	-
Vasodilator Medications			
Phosphodiesterase-5 inhibitor	-	13	11
Endothelin receptor antagonist	-	11	9
Intravenous epoprostenol	-	2	1
Selective prostacyclin receptor agonist	-	1	1
Soluble guanylate cyclase stimulator	-	1	1

Table 3. Subject characteristics.

ACA = Anti-Centromere Antibodies
ANA = Anti-Nuclear Antibodies
NC-PH = Non-Connective Tissue Disease Pulmonary Hypertension
RNA = Ribonucleic Acid
RNP = Ribonucleoprotein
SSc = Systemic Sclerosis
SSc-PAH = Systemic Sclerosis-associated Pulmonary Arterial Hypertension.

Clinical characteristics (including haemoglobin) from the most recent clinic visit (32 days, interquartile range 6–60 days) and lung function test data [199 days, inter-quartile range (IQR) 13–425 days] are shown in Table 4. The most recent cardiac catheterization (218 days, IQR 57–839 days) and 6 min walk test (6MWT) (32 days, IQR 6–60 days) data from the 2 PH groups are also shown in Table 4.

	SSc	SSc-PAH	NC-PH	*p* value
Hemoglobin (g/L)	121.9±11.4	123.5±14.2	133.3±22.2	0.14
FEV1 (%predicted)	95.5±17.5	85.5±13.2	88.9±14.7	0.20
FVC (%predicted)	98.0±19.8	91.8±15.6	98.1±18.3	0.56
DLCO (%predicted)	67.4±14.7	39.4±14.1‡§	64.3±16.9	<0.001
PVR* (dynes/sec/cm^{-5})	-	346 (146-1373)	444 (180- 1358)	0.17
mPAP* (mmHg)	-	32 (20-80)	39 (25-64)	0.17
PAWP (mmHg)	-	8.9 (6.5 -11.2)	9.7 (7.2-12.3)	0.34
6MWT (m)	-	372±105	451±94	0.042

Table 4. Hemodynamic measurements for pulmonary hypertension groups, clinical measurements for all patient groups.

6MWT=6-Minute Walk Test
DLCO=Diffusion capacity of the Lung for Carbon Monoxide
FEV1=Forced Expiratory Volume in 1 second
FVC=Forced Vital Capacity
mPAP=mean Pulmonary Arterial Pressure
PAWP=Pulmonary Arterial Wedge Pressure
PVR=Pulmonary Vascular Resistance
**denotes non-normally distributed, data shown as median (interquartile range)*
‡significant difference between SSc and SSc-PAH groups
§significant difference between NC-PH and the indicated SSc groups.

The main findings were that:

(1) 6MWT was significantly shorter in the SSc-PAH group compared to NC- PH group (p=0.042)

(2) the measured transfer factor (diffusion capacity of the lung for carbon monoxide, DLCO) as a percentage of the predicted value was significantly lower in the SSc-PAH group compared to the other 2 patient groups (p<0.001).

There were no other significant differences in clinical characteristics (including predicted forced expiratory volume in one second (FEV1), predicted forced vital capacity (FVC), and Hb). Pulmonary haemodynamics were not significant different between the two PH groups.

11.3.2 Resting CMR-CPET

Resting CMR metrics for each of the groups are shown in Table 5. The main difference in functional metrics was a significantly higher cardiac index in the patient groups compared to healthy controls (p≤0.023). In SSc patients this was associated with higher stroke volume index (p=0.017) compared to healthy controls whilst in NC-PH patients, higher HR was observed compared to healthy controls (p=0.005). There were no group differences in biventricular function. Myocardial T2 was higher in the SSc and SSc-PAH groups compared to both controls and NC-PH patients (p<0.006). Myocardial T1 was higher in all patient groups compared to healthy controls (p<0.006) and was higher in SSc-PAH compared to NC-PH patients (p=0.042). There were no group differences in resting iVO_2 but resting ΔavO_2 was significantly lower in the SSc patients (p<0.001) and NC-PH patients (p=0.049) compared to healthy controls.

	SSc	SSc-PAH	NC-PH	Control	*p* value
iVO_2* (ml/min/kg)	3.3 (2.6-4.7)	3.4 (2.9-5.0)	3.1 (1.7-5.3)	3.1 (2.6-4.2)	0.14
COi (L/min/m^2)	3.1±0.7†	3.0±0.8†	3.0±0.7†	2.3±0.4	0.0075
avO_2*(mlO_2/100ml)	4.3 (2.3-6.7) †	4.3 (3.3 - 9.2)	4.4 (3.0-6.6) †	5.4 (4.0-7.2)	0.0068
SVi (ml/m^2)	45.5±7.7†§	41.4±9.7	37.3±10.1	35.4±7.5	0.014
HR (bpm)	69.5±9.1§	72.5±9.0	80.6±10.1†	67.0±13.4	0.0053
RVEDVi (ml/m^2)	70.2±12.1	71.7±13.9	69.7±14.5	61.4±16.2	0.21
RVESVi* (ml/m^2)	24.5 (10.5-40.9)	27.7 (19.0-47.8)	29.1 (12.7-64.8)	23.6 (14.9-58.9)	0.20
RVSVi (ml/m^2)	44.0±7.2†§	40.2±9.4	34.9±9.0	34.8±7.2	0.0076
LVEDVi (ml/m^2)	67.7±11.4§	63.7±12.9	54.7±16.3	58.0±9.9	0.037
LVESVi (ml/m^2)	23.7±8.3	22.9±7.6	19.6±10.5	22.8±5.9	0.54
LVSVi (ml/m^2)	44.1±7.2†§	40.8±9.7	35.1±8.8	35.3±6.7	0.0079
LVEF (%)	66±8	64±9	66±10	61±7	0.38
RVEF* (%)	64 (53-81)	59 (30-66)	56 (22-73)	59 (42-67)	0.10
T2* (msec)	51 (44-57) †§	50 (47-62) †§	48 (43-52)	46 (42-49)	<0.001
T1 (msec)	1076±44†	1079±50†§	1043±46†	994±23	<0.001

Table 5. Resting CPET and CMR metrics.

avO_2=tissue oxygen extraction
COi=cardiac output indexed to BSA
HR=heart rate
iVO_2=oxygen consumption indexed to body surface area (BSA)
LVEDVi= indexed left ventricular end diastolic volume
LVEF=left ventricular ejection fraction
LVESVi=indexed left ventricular end systolic volume
LVSVi=indexed left ventricular stroke volume
RVEDVi/RVEF/RVESVi/RVSVi=right ventricular measurements as per LV
SVi=indexed stoke volume
**denotes non-normally distributed, data shown as median (interquartile range)*
†significant difference between controls and indicated patient group
§significant difference between NC-PH and the indicated SSc groups.

11.3.3 Exercise feasibility

All subjects successfully completed the exercise protocol and no subjects required medical intervention. The peak-exercise RER≥1.0 in 59/60 patients, with 1 SSc- PAH patient, who exercised to exhaustion, achieving an RER of 0.97. Comparisons of exercise duration and peak workload are shown in Table 6. The SSc-PAH group had the lowest peak workload and shortest exercise duration (significantly different from controls and SSc patients — $p<0.003$ for peak work- load, $p<0.006$ for exercise duration). Peak workload was also lower in NC-PH patients compared to controls ($p<0.002$).

Variable	SSc	SSc-PAH	NC-PH	Control	*p* value
Exercise Duration (s)	706±150†	503±166†‡	592±256†	913±158	<0.001
Peak Workload* (W)	62 (27-107) †	37 (21-107) †‡	52 (18-141) †	100 (62-168)	<0.001
Maximum RER*	1.4 (1.1-1.6) †§	1.2 (1.0-1.4) †‡	1.2 (1.0-1.6) †	1.5 (1.1-2.1)	<0.001

Table 6. Exercise metrics for all groups.

RER=Respiratory Exchange Ratio
**denotes non-normally distributed, data shown as median (interquartile range)*
†significant difference between controls and indicated patient groups.
‡significant difference between SSc and SSc-PAH groups
§significant difference between NC-PH and the indicated SSc groups.

11.3.4 Exercise CMR-CPET metrics

CMR-CPET metrics at peak exercise are shown in Table 7. All patient groups had significantly lower peak iVO_2 than healthy controls (p<0.022) as seen in Figure 20.

	SSc	SSc-PAH	NC-PH	Control	*p* value
iVO_2* (ml/min/kg)	14.2 (7.6-26.2) †	9.2 (5.2-15.7) †‡	10.8 (6.6-19.9) †	20.1 (12.8-28.7)	<0.001
COi (L/min/m^2)	5.5±1.2§	4.2±1.0†‡	4.3±1.1†	5.6±0.8	<0.001
avO_2*(mlO_2/100ml)	10.3 (4.6-11.8) †	7.7 (6.1-12.9) †	10.9 (6.9-17.5)	15.0 (7.1-18.7)	0.0028
SVi (ml/m^2)	44.8±10.2	41.6±8.2	37.0±9.7†	47.1±10.2	0.034
HR (bpm)	124.0±16.5	102.7±14.0†‡§	118.4±22.4	122.1±18.8	0.0087
LVEF (%)	72±12	76±8	78±10	77±7	0.24
RVEF* (%)	71 (43-84) §	66 (42-79) †	59 (24-81) †	74 (62-89)	0.0028

Table 7. Peak exercise CPET and CMR metrics.

avO_2=tissue oxygen extraction
COi=cardiac output indexed to BSA
HR=heart rate
iVO_2=oxygen consumption indexed to body surface area (BSA)
LVEF=left ventricular ejection fraction
RVEF=right ventricular ejection fraction
SVi=indexed stoke volume
**denotes non-normally distributed, data shown as geometric mean+/-geometric standard deviation*
†significant difference between controls and indicated patient groups
‡significant difference between SSc and SSc-PAH groups
§significant difference between NC-PH and the indicated SSc groups.

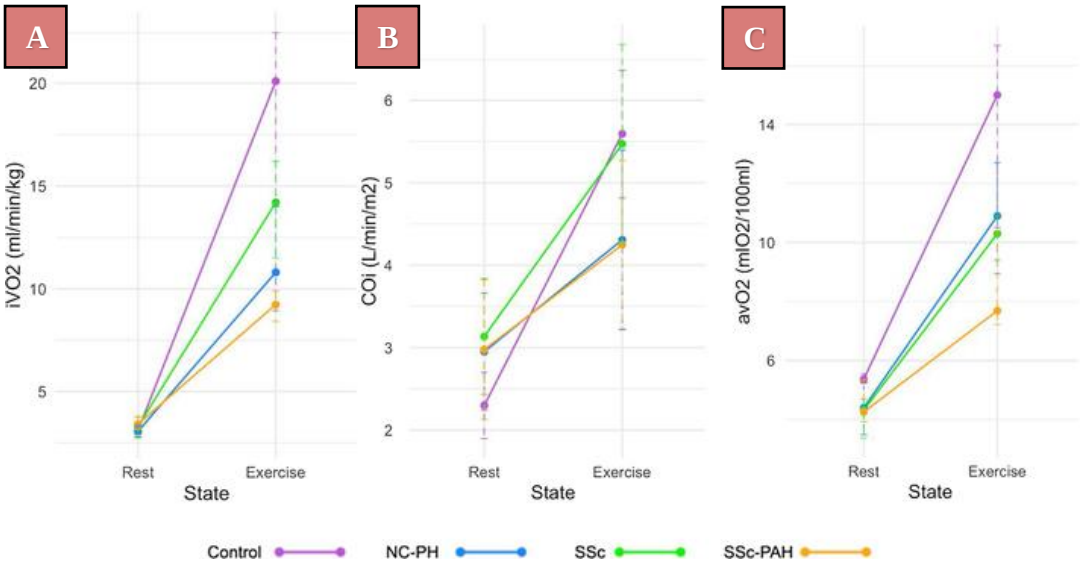

Figure 21. CMR-CPET Metrics at rest and peak-exercise for each subject group.

Systemic Sclerosis (SSc); Systemic Sclerosis-associated Pulmonary Arterial Hypertension (SSc-PAH); Non-Connective Tissue Disease Pulmonary Hypertension (NC-PH); Healthy Controls (Control).
Panel A. Oxygen consumption indexed to weight (iVO_2).*
Panel B. Cardiac output indexed to body surface area.
Panel C. Arteriovenous oxygen gradient (ΔavO_2).*
Normally distributed data displayed as mean ± SD.
**Denotes non-normally distributed data shown as median (interquartile range)*

The SSc-PAH group had the lowest peak iVO_2 (significantly different from both healthy controls and SSc patients — $p<0.01$). This was associated with lower peak cardiac index compared to both healthy controls and SSc patients ($p\leq0.004$) and lower ΔavO_2 than healthy controls ($p=0.003$) — Figure 20-B and Figure 20-C. The lower peak cardiac index during exercise was due to a failure to augment SV and lower peak HR compared to healthy controls ($p=0.015$)—Figure 21-A and Figure 21-B. The SSc-PAH group also had a lower peak RVEF compared to healthy controls ($p=0.042$)—Figure 21-C.

SSc patients had lower peak iVO_2 and ΔavO_2 ($p=0.03$) compared to healthy controls. However, they did have significantly higher peak iVO_2 than SSc- PAH patients ($p=0.01$). SSc patients failed to augment stroke index during exercise (Figure 21-A) but peak stroke index was similar to healthy controls, due to higher resting stroke index. This also resulted in a similar peak

cardiac index compared to healthy controls. All other peak functional metrics were not statistically different from healthy controls.

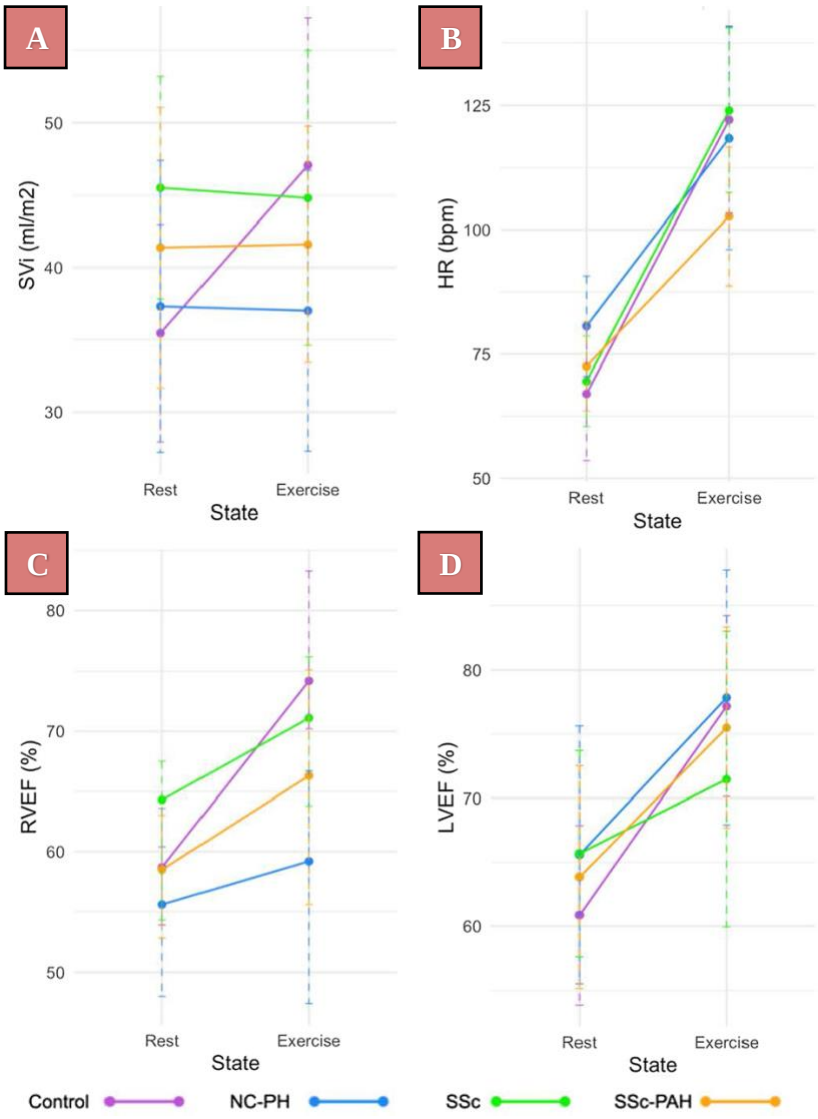

Figure 22. Stroke volume, heart rate and ventricular ejection fraction at rest and peak-exercise for each subject group.

Panel A. Stroke volume indexed to body surface area.
Panel B. Heart rate (HR)
Panel C. Right ventricular ejection fraction (RVEF).*
Panel D. Left ventricular ejection fraction (LVEF).
SSc = Systemic Sclerosis
SSc-PAH = Systemic Sclerosis-associated Pulmonary Arterial Hypertension
NC-PH = Non-Connective Tissue Disease Pulmonary Hypertension
Control = Healthy controls
Normally distributed data displayed as mean ± SD
**Denotes non-normally distributed data shown as median (range).*

The NC-PH group was characterized by significantly lower peak cardiac index compared to both healthy controls and SSc patients ($p \leq 0.005$)—Figure 20-B. The NC-PH group also had the lowest peak stroke index (significantly different to healthy controls—$p=0.034$) and RVEF (statistically significant versus healthy controls and SSc patients—$p \leq 0.042$)—Figure 21-A and 21-C.

Peak iVO_2, cardiac index and ΔavO_2 all correlated with 6MWT after adjusting for diagnosis ($p \leq 0.043$). There was no correlation bet tween 6MWT and peak RVEF, LVEF, stroke index or HR.

11.3.5 Relationship between exercise metrics and lung function and haemoglobin

There was no correlation between predicted FVC and FEV1 and any peak-exercise metrics. There was a correlation (adjusted for diagnosis) between DLCO and peak RVEF and LVEF (peak RVEF *rho*=0.37, *p*=0.015; peak LVEF *rho*=0.31, *p*=0.040). In addition, there was a significant correlation (adjusted for diagnosis) between peak ΔavO_2 and Hb (*rho*=0.33, p=0.025)

11.3.6 Relationship between exercise metrics and myocardial T1 and T2

There were no significant associations between CMR-CPET metrics and myocardial T2 after adjusting for diagnosis. Myocardial T1 correlated (adjusted for diagnosis) with peak stroke volume index (*rho*=−0.33, *p*=0.011) and HR (*rho*=0.31, *p*=0.020). There were no other significant associations.

11.4 Discussion

It is well recognised that systemic sclerosis causes reduced exercise capacity(99), which is often attributed to lung disease or PAH(100). However, patients without lung disease also experience exercise intolerance, and PAH only affects a minority of patients with SSc (8–12% prevalence)(101). Thus, other factors must be important, and I used CMR-CPET to better determine the causes of exercise intolerance in SSc. To investigate the separate contributions of SSc and PH to exercise intolerance, I compared SSc patients (with and without PAH) to healthy controls and NC-PH patients. The main findings of the study were:

(1) All patient groups had reduced peak iVO_2 compared to healthy controls,

(2) SSc and SSc-PAH had reduced peak ΔavO_2 compared to healthy controls and NC-PH patients,

(3) SSc-PAH and NC-PH patients had reduced peak cardiac index compared to healthy controls and SSc patients,

(4) Higher haemoglobin was associated with higher peak ΔavO_2 independent of disease type,

(5) Higher myocardial T1 was associated with lower peak SV.

The defining exercise feature of SSc and SSc-PAH patients was reduced peak VO_2, associated with lower peak ΔavO_2 in both groups. It is well recognized that ΔavO_2 is a marker of skeletal muscle oxygen extraction, and my data suggest that reduced oxygen extraction is a ubiquitous problem in SSc. The ability of skeletal muscle to extract oxygen is vital for normal aerobic respiration and thus cellular function. From these data, I propose the following in SSc patients during exercise:

(1) reduced muscle oxygen extraction,

(2) reduced aerobic respiration and ATP production,

(3) reduced skeletal muscle sarcomeric contraction,

(4) resultant exercise intolerance.

This chain of events has previously been suggested for left-sided heart failure(102) and paediatric PAH(39) and I believe is equally important in SSc. The aetiology of reduced peak ΔavO_2 in these patients is probably generalised skeletal muscle dysfunction/sarcopenia. Sarcopenia is common in SSc(103), and disease specific causes include small vessel vasculopathy(92, 104), muscle fibrosis and inflammation (105). These factors not only cause sarcopenia, but also directly limit oxygen extraction through reduced regional O_2 delivery, intramuscular shunting and mitochondrial dysfunction(106). In this study, I did not explore the exact nature of skeletal muscle involvement in SSc. However, this will be an important feature of future studies, particularly identifying causes amenable to therapeutic interventions.

Interestingly, I found a strong relationship between haemoglobin and peak ΔavO_2. There were no group differences in haemoglobin and, therefore, this finding cannot explain the group differences in oxygen extraction but may contribute to within-group variance. Several animal studies have shown that low haemoglobin causes reduced oxygen extraction through impaired oxygen delivery. There is also some evidence that anaemia lowers muscle oxidative capacity(107) and this may further contribute to lower oxygen extraction(108). Anaemia and iron deficiency are well described in chronic diseases such as PAH. However, iron supplementation has a limited effect on exercise capacity in these patients(109). On the other hand, anaemia in SSc may have a more inflammatory component and anti-inflammatory drugs have been shown to increase Hb(110-113), which might improve exercise capacity.

In addition to reduced peak ΔavO_2, patients with SSc-PAH also had lower peak cardiac index. This 'dual pathology' probably explains why SSc-PAH patients had the lowest peak VO_2 and a lower 6MWT than NC-PH patients. Reduced peak cardiac index was also seen in NC-PH patients, and in both groups, this was largely due to an inability to augment stroke index during exercise. Interestingly, SSc patients also failed to augment stroke index, but higher resting stroke index resulted in normal peak values. Higher baseline stroke index in SSc patients may simply be a response to a systemic inflammatory disease, but this requires more investigation. The failure to augment stroke index can be explained by poor RV contractile reserve and this is reflected by lower peak RVEF in both PAH groups. Reduced contractile reserve is well recognized in PAH(114, 115) due to both RV dysfunction(116) and increased afterload(117). In addition, autonomic failure and reduced inotropy maybe a factor, which is in keeping with the reduced peak HR seen in SSc-PAH patients. Interestingly, I also found that peak stroke index was associated with increased myocardial native T1 but not T2. This suggests that fibrotic changes in the myocardium (secondary to raised afterload and/ or burnt-out myocarditis) may partly underlie the loss of contractile reserve.

Another possible cause of reduced ΔavO_2 in SSc is lung disease, which is why I excluded patients with radiological evidence of extensive parenchymal lung disease. I did not find any association between lung function metrics and peak ΔavO_2, implying that reduced pulmonary O_2 uptake was not the cause of lower ΔavO_2. However, there was an association between predicted DLCO and peak biventricular EF, but the direction of causation is unclear, and the exact cause is to be determined.

In this study, I used CMR-augmented CPET to investigate exercise intolerance. The benefit of this relatively novel technology is that it allows simultaneous quantification of peak iVO_2 and cardiac index and subsequent calculation of ΔavO_2. I used PC-CMR to measure aortic flow as

this provides accurate quantification of cardiac output even in the presence of left-sided valvar regurgitation and shunts. This contrasts with measurement of cardiac output from ventricular volumetric data. Aortic flow can also be estimated using Doppler echocardiography, but this method is often unreliable(118) and difficult to perform during exercise. In addition, CMR also provides reference standard ventricular volumetric and mapping data. My findings demonstrate that CMR-CPET can help develop a better understanding of the causes of exercise dysfunction in different types of disease. In particular, quantification of ΔavO_2 provides new insights into the role of skeletal muscle in reduced exercise capacity. Due to the comprehensive evaluation that CMR-CPET provides, I believe this technique may have a future role in clinical diagnosis, risk stratification and follow-up, as well as providing end-points for clinical trials.

11.5 Limitations

The main limitation of this study is that achieving true peak-exercise using a supine exercise protocol is challenging. This form of supine exercise is not directly comparable with conventional CPET, and this should be considered when interpreting the results. Nevertheless, good correlation between peak iVO_2 obtained during CMR-CPET and conventional CPET has been demonstrated previously (58). Furthermore, even though peak VO_2 and HR during supine exercise are lower than for upright exercise, RER>1 was achieved in most subjects. Therefore, I believe that CMR-CPET metrics measured during supine exercise remain good markers of exercise capacity.

Another limitation was the significant time interval between clinical measures (i.e., lung function tests) and CMR- CPET. This may affect the robustness of correlations between these

markers and future, larger studies should endeavour to assess clinical characteristics at the same time as CMR-CPET.

Finally, skeletal muscle biopsy could have answered some of the questions regarding the cause of reduced oxygen extraction (fibrosis/inflammation/capillary rarefaction). However, this is highly invasive and would have been difficult to perform. Thus, future studies could evaluate skeletal muscle mass, perfusion, T2 and extra- cellular volume as a non-invasive alternative.

11.6 Conclusions

Patients with SSc and SSc-PAH have reduced peak iVO_2. In SSc patients, this appears related to reduced peak ΔavO_2; in SSc-PAH patients, it is related to both reduced peak cardiac index *and* ΔavO_2. This suggests that tissue oxygen extraction is an important determinant of exercise intolerance in SSc and could be used as a biomarker of disease and response to therapy.

12. RESULTS - COMPARING THE MECHANISMS OF ONGOING EXERCISE INTOLERANCE IN COVID-19 PATIENTS.

This chapter is based on the publication below:

> **Brown JT,** Saigal A, Karia N, Patel RK, Razvi Y, Constantinou N, Steeden JA, Mandal S, Kotecha T, Fontana M, Goldring J, Muthurangu V, Knight DS. "Ongoing Exercise Intolerance Following COVID-19: A Magnetic Resonance-Augmented Cardiopulmonary Exercise Test Study". Journal of the American Heart Association. 2022 May 3;11(9)

My contribution to this work was recruiting subjects, designing the exercise protocol, conducting all exercise tests, analysing clinical, CPET and CMR data, performing statistical analysis and writing the manuscript.

The study was approved by national ethics committee (IRAS project ID 226101; REC reference 17/LO/1499, National Health Service Health Research Authority UK CRN 058274). All subjects provided written informed consent.

12.1 Introduction

Ongoing exercise intolerance is recognised following COVID-19, with a significant proportion of hospitalized patients reporting reduced exercise capacity after discharge(82). In addition, reduced peak oxygen consumption (VO_2) has been demonstrated after resolution of acute COVID-19 infection(119). This can partly be explained by residual lung parenchymal damage, myocardial injury, or sequelae from pulmonary thromboembolic disease(120-123). However,

exercise intolerance is also described in patients without clearly identifiable post viral complications(124). In this group, possible causes include:

(1) failure to augment cardiac output (CO) attributable to reduced contractile or preload reserve,

(2) impaired skeletal muscle oxygen extraction caused by skeletal muscle dysfunction.

Unfortunately, identifying and understanding the relative importance of these potential mechanisms is difficult with conventional cardiopulmonary exercise testing (CPET) as only VO_2 is directly measured.

A novel technique has been developed that combines exercise cardiovascular magnetic resonance (MR) with CPET (CMR-CPET), allowing the simultaneous measurement of VO_2 and CO during exercise(58, 125). These data can then be used to calculate arteriovenous oxygen content gradient (ΔavO_2), a recognized marker of tissue oxygen extraction(93). CMR-CPET provides a comprehensive evaluation of the cardiopulmonary exercise response, affording a better understanding of exercise intolerance. In addition, CMR-CPET also allows the accurate evaluation of biventricular volumes and function during exercise. These data can be useful in understanding CO augmentation in terms of both contractile and preload reserve.

The aim of this study was to use CMR-CPET to investigate exercise capacity in patients hospitalized due to COVID-19 infection, with and without self-reported exercise intolerance, through comparison with a healthy control group.

12.2 Methods

12.2.1 Study Population

Sixty subjects were prospectively recruited into this single-centre prospective observational case-control study, and split into 3 equally sized groups:

(1) self-reported reduced exercise capacity following COVID-19 infection ($COVID_{reduced}$)

(2) normal exercise capacity following COVID-19 infection ($COVID_{normal}$)

(3) age- and sex-matched normal controls.

Patients who had recovered from COVID-19 were recruited from the Royal Free London NHS Foundation Trust COVID-19 Follow-up Clinic between January and May 2021. Patients in the post–COVID-19 groups were matched for age, sex, and the presence of diabetes and hypertension.

Inclusion criteria for patients following COVID-19 were:

(1) previous hospitalization with COVID-19 diagnosed by positive combined oro/ nasopharyngeal swab for severe acute respiratory syndrome coronavirus 2 by reverse-transcriptase polymerase chain reaction

(2) age 18 to 80 years.

Exclusion criteria were:

(1) radiological evidence of residual lung parenchymal disease due to COVID-19

(2) troponin positivity during hospital admission

(3) admission to an intensive care unit for invasive ventilation

(4) diagnosis of pulmonary embolism during acute COVID-19 illness

(5) impaired left ventricular (LV) or right ventricular (RV) systolic function on resting cardiovascular magnetic resonance (CMR)

(6) general contraindications to MR scanning

(7) pre-existing contraindications to performing exercise (eg, unstable symptoms including angina, exertional syncope)

(8) previous known cardiovascular disease (including ischemic, non-ischaemic, and moderate or severe valvular disease)

(9) significant lung parenchymal disease that may confound CPET results, such as emphysema or interstitial lung dis- ease (defined as >20% lung volume on computed tomography imaging).

We also recruited 20 uninfected age- and sex- matched healthy control subjects who had no history of COVID-19 infection and no history of cardiovascular disease, hypertension, or diabetes through advertisement by our institution. Fourteen (70%) control subjects underwent MR-CPET before the pandemic. The 6 post-pandemic controls had not experienced any prior symptoms consistent with, or previously been diagnosed as having, COVID-19.

12.2.2 Clinical Assessment

All patients underwent a patient symptom perception questionnaire, 6-minute walk test, blood tests, and spirometry. Patients gave an overall percentage score of how they felt at the time of

CMR-CPET study compared with premorbid baseline. Patient clinical histories, comorbidities, and in-patient blood test results were obtained from patient electronic records systems. Physician-determined severity of acute COVID-19 disease was defined by World Health Organization guidelines.

12.2.3 MR-Augmented Cardiopulmonary Exercise Testing

Imaging was performed on a 1.5 Tesla MR scanner (Magnetom Aera, Siemens Healthcare, Erlangen, Germany) in a temperature-controlled suite. Full resuscitation facilities were available with peripheral venous access sited for emergency and ECG continuously monitored on the MR scanner. Systolic blood pressure was recorded at rest and peak using a MR-compatible blood pressure monitor (Expression MR400, Philips Healthcare, Best, The Netherlands).

12.2.4 MR Imaging Techniques (Real-Time Flow and Volume Imaging)

Before exercise, subjects underwent routine CMR with long- and short-axis cine imaging and myocardial native T1 and T2 mapping(94, 95). T1 mapping used the modified Look-Locker inversion recovery sequence after regional shimming with 5s(3s)3s sampling(126). T2 mapping used single-shot T2-prepared images with varying T2 preparation(127).

All exercise CMR was performed with real-time sequences and was acquired during free breathing. Aortic flow was measured using real-time phase-contrast MR at baseline and at peak exercise using a uniform-density golden-angle spiral sequence, with a compressive sensing reconstruction(85). The CMR parameters used were identical to previous descriptions(125), see Chapter 10 – Methods.

Aortic flow and short-axis image data were reconstructed offline (MATLAB R2018a, MathWorks Inc, Natick, MA), using the Berkeley Advanced Reconstruction Toolbox(91). Reconstructed images were exported as Digital Imaging and Communications in Medicine files and analysed on reporting workstations.

12.2.5 Respiratory Gas Analysis

Breath-by-breath gas exchange analysis was performed using a commercial CPET system (Ultima, MedGraphics, St Paul, MN). The analyser was placed in the MR control room and attached to the face-mask (Hans Rudolph, Kansas City, KS) via bespoke MR-compatible sampling tubes passed through the waveguide. The sampling tubes were modified as previously described(58, 125) and were manufacturer-tested to meet all quality control standards. Gas and flow calibrations were performed before each test and at least 30 minutes after system initiation, as per manufacturer recommendations. All measurements were taken at body temperature and ambient pressure.

12.2.6 Exercise Protocol

Subjects exercised on a supine MR-compatible cycle ergometer (MR Cardiac Ergometer Pedal, Lode, Groningen, the Netherlands). Exercise workload (power measured in watts) was controlled by altering resistance depending on cadence. The exercise protocol (Figure 22) was followed until exhaustion (peak exercise) with CMR measurements performed at rest and peak and VO_2 measured continuously.

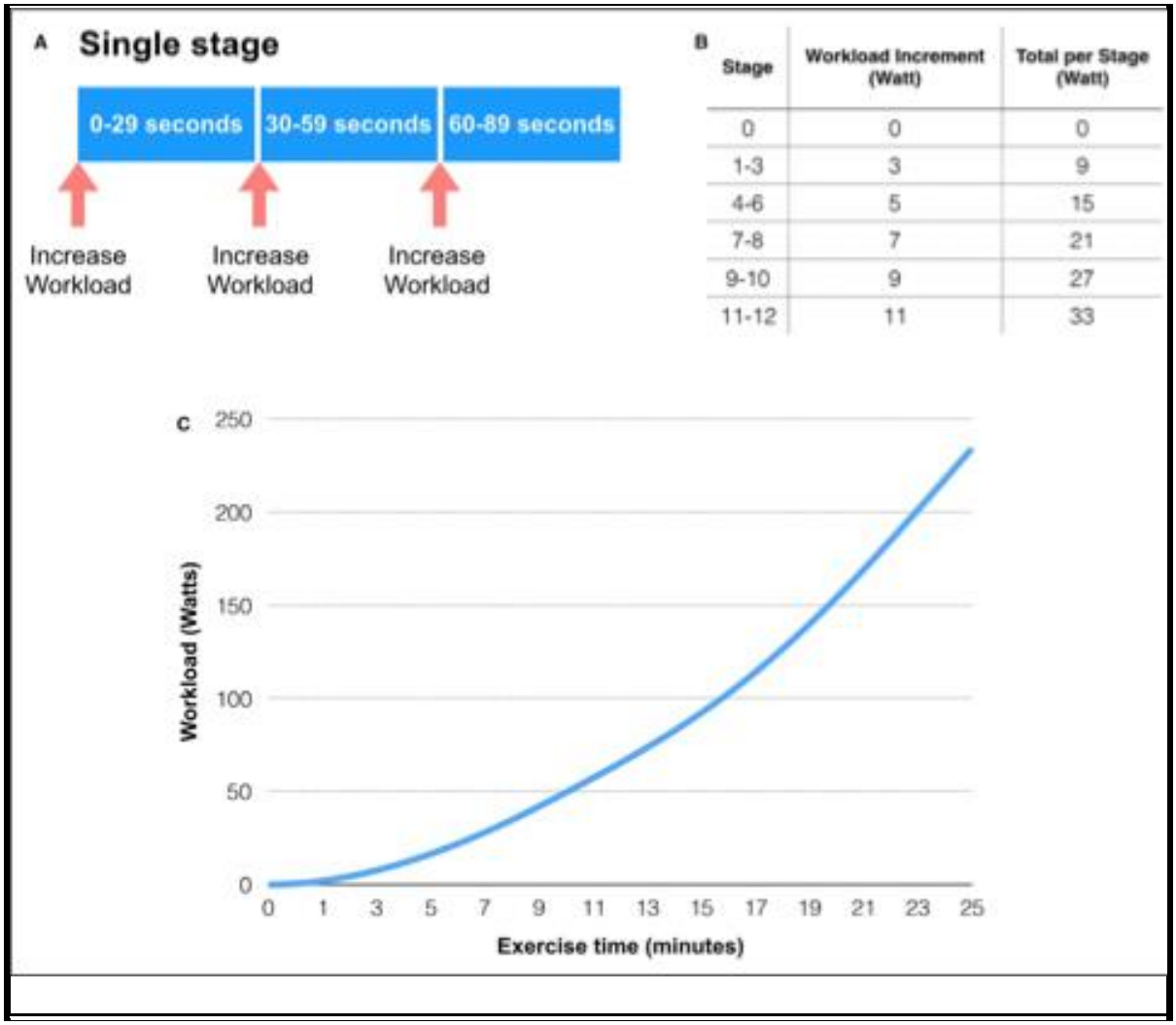

Figure 23. Exercise protocol and cumulative workload.

12.2.7 Data Processing

All post-processing of reconstructed images was performed using "in-house" plug-ins for OsiriX DICOM software version 9.0.1 (OsiriX Foundation, Geneva, Switzerland)(96-98). Aortic phase-contrast MR flow data was segmented using a semiautomatic method with manual operator correction. Stroke volume (SV) was calculated by integrating the flow curve across a single R-R interval; cardiac output was given by stroke volume×heart rate (CO=SV×HR). Biventricular endocardial borders were traced manually on short-axis images at end diastole and end systole, identified by visual assessment of the largest and smallest cavity

areas, respectively. Biventricular SV, ejection fraction, and mass were calculated as previously described, with papillary muscles and trabeculae excluded from the blood pool(125). Postprocessing of SV data obtained by aortic phase-contrast MR flow imaging and by volumetry of cine images was performed in tandem to maintain internal consistency as suggested by Society for Cardiovascular Magnetic Resonance Task Force recommendations(90). Atrial areas were traced on a 4-chamber cine image at end systole. Native myocardial T1 and T2 relaxation times were measured by drawing a single region of interest within the midportion of the interventricular septum on the mid-cavity short-axis maps(95). All measurements were reported by an experienced clinical CMR specialist (D.K.) blinded to clinical information. All volumetric data and CO were indexed to body surface area and denoted by the suffix "i".

VO_2 and respiratory exchange ratio measurements were time registered to corresponding CMR data. The VO_2 was indexed to body weight and denoted by the prefix "i". Arteriovenous oxygen content gradient was calculated as $\Delta avO_2 = VO_2/CO$ (using non-indexed data) at rest and peak exercise for all subjects.

12.2.8 Statistical Analysis

All statistical analysis was performed using R version 3.2.0 (R Foundation for Statistical Computing, Vienna, Austria). Data were examined for normality using the Shapiro-Wilk normality test.

Descriptive statistics were expressed as mean (±SD) for normally distributed data and median (interquartile range) for non-normally distributed data.

Between-group differences in demographic data, clinical metrics, and CMR-CPET metrics (at rest and exercise) were assessed using either 1-way ANOVA for normal data, or the Kruskal-Wallis test for non-normal data.

Post hoc comparisons were performed using pairwise *t* tests (normal data) and Mann-Whitney tests (non-normal data) with Benjamini Hochberg correction for multiple comparisons.

When only comparing post–COVID-19 groups, *t* tests (normal data) and Mann-Whitney tests (non-normal data) were used.

Sex distribution between the groups was assessed using the Chi-squared test.

Correlation between metrics corrected for diagnosis was computed using multilevel Spearman's rank partial correlation coefficient.

A p value <0.05 was considered statistically significant.

12.3 Results

12.3.1 Demographics and Clinical Data

There were no differences in age, sex, height, weight, or body surface area among the 3 groups and no differences in comorbidities between post–COVID-19 patient groups (Table 8).

	Control	$COVID_{reduced}$	$COVID_{normal}$	*p* value
Age (years)	51±4	52±14	52±8	0.98
Weight (kg)	73±13	79±13	80±20	0.23
Height (m)	1.7±0.1	1.7±0.1	1.7±0.1	0.87
BSA (m^2)	1.8±0.2	1.9±0.2	1.9±0.3	0.19
Female, n (%)	12 (60)	11 (55)	11 (55)	1.00
Diabetes mellitus, n (%)	-	1 (5)	1 (5)	1.00
Hypertension, n (%)	-	6 (30)	3 (15)	0.45
No regular medications, n (%)	-	8 (40)	9 (45)	1.00

Table 8. Subject characteristics.

BSA=Body Surface Area
Normally distributed data displayed as mean±SD.

Clinical data for the post–COVID-19 groups are shown in Table 9. The only differences were significantly lower perceived functional recovery (70% of baseline [Interquartile range (IQR), 60–80] versus 98% [IQR, 90–100]; $p<0.001$) and 6-minute walk test (470±87meters versus 560±117 meters; $p=0.009$) in the $COVID_{reduced}$ group. There were no differences in any markers of disease severity between post–COVID-19 patient groups. There were also no significant differences in blood biomarkers at the time of CMR-CPET between patient groups. However, there was a trend toward a greater length of time from discharge to CMR-CPET in the $COVID_{normal}$ group (115 days [IQR, 96–151] versus 97 days [IQR, 80–116]; $p=0.07$).

There were no significant differences in spirometry metrics at the time of CMR-CPET between the 2 post–COVID-19 patient groups. Two patients in the $COVID_{reduced}$ group and 4 patients in the $COVID_{normal}$ group had normal index chest radiographs. As per clinical patient follow-

up protocol, they did not have follow-up chest imaging. The remaining 34 (85%) patients had outpatient follow-up chest radiographs, all of which were normal.

	$COVID_{reduced}$	**$COVID_{normal}$**	***p* value**
Perception of recovery* (% of normal)	70 (60-80)	98 (90-100)	**<0.001**
6-minute walk distance	470±87	560±117	**0.0089**
Duration from discharge to MR-CPET* (days)	97 (80-116)	115 (96-151)	0.068
Severity of acute COVID-19 illness			
Length of admission* (days)	3.5 (1.0-5.2)	4.0 (0.8-5.0)	0.87
Severity score*	4.0 (2.0-4.0)	4.0 (2.0-4.0)	0.69
Peak D-dimer* (ng/mL)	576 (373-1160)	496 (463-1020)	0.91
Peak CRP* (mg/L)	64 (21-116)	45 (23-133)	0.95
Current investigations			
FEV1* (% predicted)	97 (91-102)	93 (88-100)	0.49
FVC* (% predicted)	88 (79-93)	80 (76-93)	0.39
Hemoglobin (g/L)	141±13	137±16	0.42
Creatinine (µmol/L)	73±13	67±15	0.16
CK* (units/L)	93 (71-110)	107 (73-157)	0.29
NT-proBNP* (ng/L)	49 (49-122)	49 (49-64)	0.38

Table 9. Clinical data for patient groups.

CK= creatine kinase
CRP= C-reactive protein
FEV1=Forced Expiratory Volume in 1 second
FVC=Forced Vital Capacity
MR-CPET= magnetic resonance-augmented cardiopulmonary exercise test
NT-proBNP= N-terminal pro B-type natriuretic peptide
Normally distributed data displayed as mean±SD
**denotes non-normally distributed, data shown as median (interquartile range).*

12.3.2 Resting CMR-CPET

Resting CMR metrics are shown in Table 10. The main differences in functional metrics between the 2 post-COVID-19 patient groups and controls were:

(1) Higher LV ejection fraction ($COVID_{reduced}$ 68%±7% versus $COVID_{normal}$ 69%±6% versus controls 61%±7%; $p \leq 0.004$)

(2) Higher RV mass ($COVID_{reduced}$ 25±5 g versus $COVID_{normal}$ 27±5 g versus controls 21±6 g; $p \leq 0.02$).

Variable	Control	$COVID_{reduced}$	$COVID_{normal}$	*p* value
iVO_2 (ml/min/kg)	3.2±0.5	3.1±0.8	3.6±0.7	0.14
COi* (L/min/m^2)	2.4 (2.2-2.8)	2.5 (2.3-3.0)	2.9 (2.4-3.2)	0.14
avO_2 (mlO_2/100ml)	5.2±1.0	4.8±1.2	5.1±0.9	0.44
SVi (mL/min/m^2)	39±9	36±7	40±7	0.35
Heart rate (bpm)	67±12	73±12	73±13	0.21
RVEDVi* (mL/m^2)	65 (54-75)	59 (52-69)	64 (56-69)	0.52
RVESVi* (mL/m^2)	24 (21-30)	20 (18-30)	22 (20-28)	0.29
RVSVi (mL/m^2)	38±9	37±7	40±8	0.48
LVEDVi (mL/m^2)	64±15	56±11	59±10	0.13
LVESVi (mL/m^2)	25±7	18±6†	19±4.6†	**0.0026**
LVSVi (mL/m^2)	39±9	37±7	40±7	0.55
LVEF (%)	61±7	68±7†	69±6†	**<0.001**
RVEF (%)	58±7	62±8	63±6	0.087
Septal T2* (ms)	46 (44-46)	46 (44-47)	46 (45-48)	0.58
Septal T1 (ms)	994±22	1007±29	1016±25†	**0.045**
LV mass (g/m^2)	56±15	54±9	58±10	0.61
RV mass (g/m^2)	21±6	25±5†	27±5†	**0.003**
LA area (cm/m^2)	11±2	10±2	11±2	0.14
RA area* (cm/m^2)	11 (9-12)	9 (8-11)	10 (8-11)	0.17

Table 10. Resting CMR-CPET data.

avO_2=tissue oxygen extraction
COi=cardiac output indexed to body surface (BSA)
iVO_2=oxygen consumption indexed to weight
LA=left atrial
LVEDVi=BSA indexed left ventricular end diastolic volume
LVEF=left ventricular ejection fraction
LVESVi=BSA indexed left ventricular end systolic volume
LVSVi=BSA indexed left ventricular stroke volume
RA=right atrial
RVEDVi/RVEF/RVESVi/RVSVi=right ventricular measurements as per LV
SVi=BSA indexed stoke volume
Normally distributed data displayed as mean±SD
**denotes non-normally distributed data shown as median (interquartile range)*
†significant difference between controls and indicated patient groups.

There was also higher native myocardial T1 in the $COVID_{normal}$ group versus controls ($COVID_{normal}$ 1016±25 ms versus controls 994±22ms; p=0.04). There were no significant group differences in systolic blood pressure , bi-ventricular size, bi-atrial size, indexed stroke volume (SVi), heart rate, indexed oxygen uptake (iVO_2), or tissue oxygen extraction (ΔavO_2) at rest.

12.3.3 Exercise Feasibility

All subjects successfully completed the exercise protocol. No subjects required medical intervention. All subjects achieved maximal respiratory exchange ratio ≥1.0. Comparisons of exercise duration and peak workload are shown in Table 11. The $COVID_{reduced}$ group had the lowest peak workload, which was significantly different from controls ($COVID_{reduced}$ 79W [IQR, 65–100] versus controls 104W [IQR, 86–148]; p=0.01) and shortest exercise duration ($COVID_{reduced}$ 13.3±2.8 minutes versus controls 16.6±3.5 minutes; p=0.008). There were no differences in peak workload or exercise duration patients between patients with $COVID_{normal}$ and controls.

	Control	**$COVID_{reduced}$**	**$COVID_{normal}$**	***p* value**
Exercise duration (minutes)	16.6±3.5	13.3±2.8†	15.1±3.8	**0.01**
Peak workload* (W)	104 (86-148)	79 (65-100)†	104 (71-134)	**0.017**
Maximum RER	1.6±0.2	1.4±0.2†	1.5±0.2	**0.043**

Table 11. Metrics of exercise performance.

RER=Respiratory Exchange Ratio
Normally distributed data displayed as mean±SD
**denotes non-normally distributed data shown as median (interquartile range)*
†*significant difference between controls and indicated patient groups.*

12.3.4 Exercise MR-CPET Metrics

CMR-CPET metrics at peak exercise are shown in Table 12 and Figure 23. The $COVID_{reduced}$ group had the lowest peak iVO_2 (14.9 mL/min per kg [IQR, 13.1– 16.2]), significantly different from healthy controls (22.3 mL/min/kg [16.9–27.6]; p=0.003) and patients with $COVID_{normal}$ (19.1 mL/min/kg [IQR, 15.4– 23.7]; p=0.04). The $COVID_{reduced}$ group also had lower peak indexed cardiac output (COi) (4.7±1.2 L/min/m^2) compared with controls (6.0±1.2 L/min/m^2; p=0.004) and patients with $COVID_{normal}$ (5.7±1.5 L/min/m^2; p=0.02). Lower peak COi during exercise was associated with lower indexed SV in patients with $COVID_{reduced}$ (39±10 mL/min/m^2) compared with controls (48±10 mL/min/m^2; p=0.02). Patients with $COVID_{reduced}$ also had lower body surface area indexed LV end diastolic volume than controls (52±11 mL/min/m^2 versus 62±13 mL/min/m^2; p=0.02) and a trend toward lower indexed RV end diastolic volume (52 mL/min/m^2 [IQR, 50–56] versus 59 mL/min/m^2 [53–66]; p=0.1). There were no differences in peak ΔavO_2, systolic blood pressure, heart rate, LV ejection fraction, or RV ejection fraction between groups.

Variable	Control	$COVID_{reduced}$	$COVID_{normal}$	*p* value
iVO_2* (ml/min/kg)	22.3 (16.9-27.6)	14.9 (13.1-16.2)†‡	19.1 (15.4-23.7)‡	**0.0037**
COi (L/min/m^2)	6.0±1.2	4.7±1.2†‡	5.7±1.5‡	**0.0041**
avO_2 (mlO_2/100ml)	14.8±3.9	13.5±3.4	13.8±2.8	0.46
SVi (mL/min/m^2)	47.7±10.4	39.1±10.0†	43.2±7.4	**0.02**
Heart rate (bpm)	130±22	122±22	132±24	0.35
LVEF (%)	76±8	74±10	78±8	0.31
RVEF* (%)	76 (69-84)	75 (70-79)	76 (72-81)	0.55

Table 12. Exercise CMR-CPET data.

avO_2=tissue oxygen extraction
COi=cardiac output indexed to body surface (BSA)
iVO_2=oxygen consumption indexed to weight
LVEF=left ventricular ejection fraction
RVEF=right ventricular ejection fraction.
SVi=BSA indexed stoke volume
Normally distributed data displayed as mean±SD
**denotes non-normally distributed data shown as median (interquartile range)*
†significant difference between controls and indicated patient groups
‡significant difference between COVID patient groups.

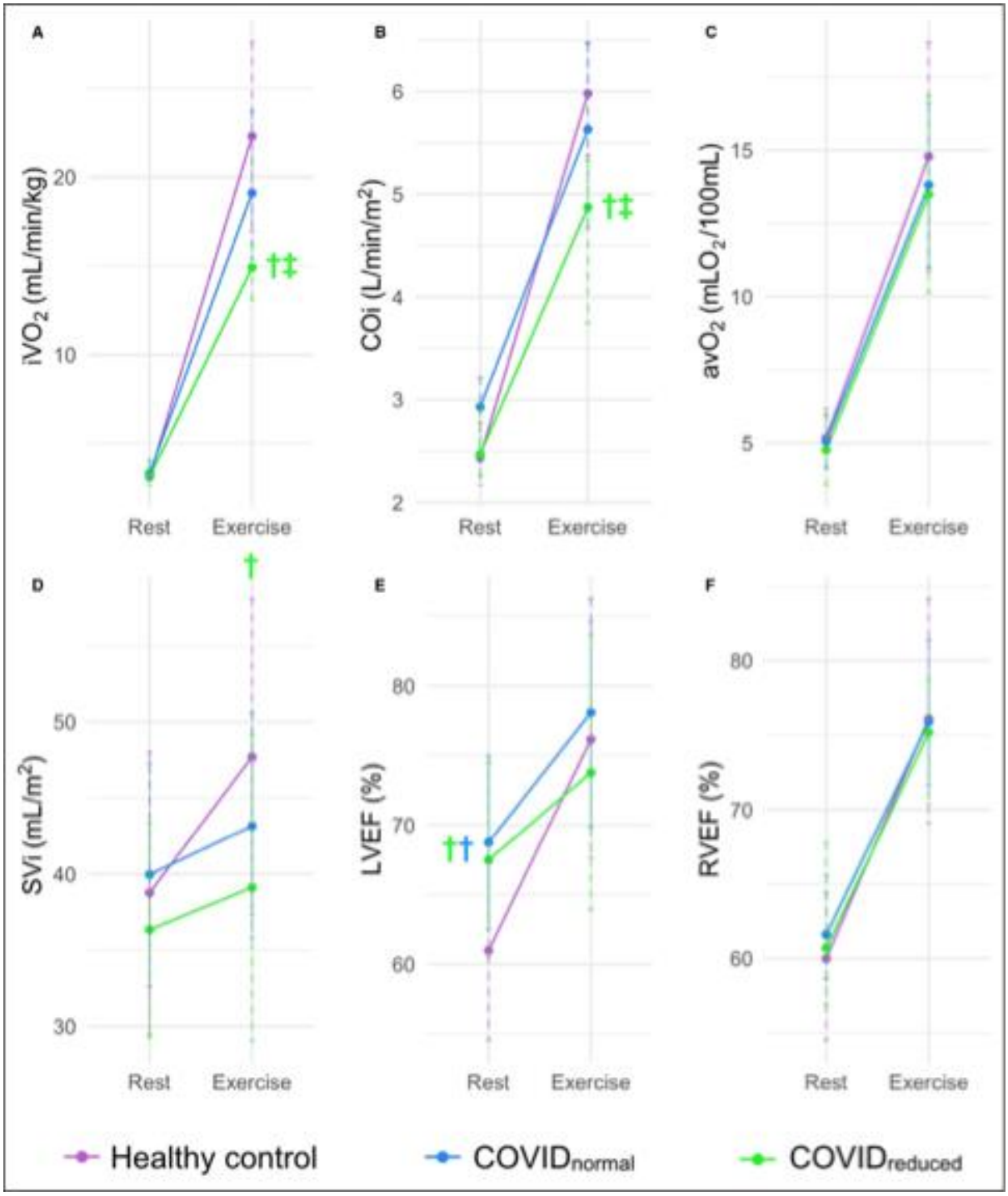

Figure 24. CMR-CPET metrics at rest and peak exercise for each subject group.

Panel A. Oxygen consumption indexed to weight (iVO_2)
Panel B. Cardiac output indexed to body surface area (COi)
Panel C. Arteriovenous oxygen gradient (ΔavO_2)
Panel D. Stroke volume indexed to body surface area (SVi)
Panel E. Left ventricular ejection fraction (LVEF)
Panel F. Right ventricular ejection fraction (RVEF)
† Significant difference between the color-coded group and controls
‡ Significant difference between COVID patient groups.
$COVID_{normal}$ indicates normal exercise capacity following COVID-19, $COVID_{reduced}$ indicates reduced exercise capacity following COVID-19.

12.3.5 Current Clinical Status and CMR-CPET Metrics

Peak iVO (*rho*=0.73, *p*<0.001), COi (*rho*=0.41, *p*=0.008), ΔavO_2 (*rho*=0.46, *p*=0.003), and heart rate (*rho*=0.49, *p*=0.001) all correlated with the 6-minute walk test after adjusting for diagnosis. There were no significant correlations between the 6-minute walk test and peak RV ejection fraction, LV ejection fraction, or indexed SV. There were also no significant correlations between predicted forced vital capacity or forced expiratory volume during the first second and any peak-exercise CMR-CPET metrics.

12.3.6 Disease Severity and CMR-CPET Metrics

There was no association between measures of acute COVID-19 illness severity (length of admission and disease severity score) and any peak exercise CMR-CPET metrics. However, peak iVO_2 (*rho*=0.37, *p*=0.02), COi (*rho*=0.37, *p*=0.02) and indexed SV (*rho*=0.32, *p*<0.05) all correlated with length of time from discharge to CMR-CPET.

12.4 Discussion

The COVID-19 pandemic has caused significant mortality and morbidity worldwide(128). Following resolution of acute infection, ongoing exercise intolerance and failure to return to functional baseline are commonly described(119, 120). However, many patients have no obvious causes to account for these symptoms(124).I used CMR-CPET to evaluate potential mechanisms of exercise limitation in patients previously hospitalized with COVID-19 and

without obvious resting cardiopulmonary pathological sequelae. The main findings of this study were:

(1) the $COVID_{reduced}$ patient group had significantly lower peak iVO_2 than the $COVID_{normal}$ group and healthy controls

(2) this was attributable to lower peak COi during exercise, resulting from a failure to augment SV

(3) there were no abnormalities in cardiac contractile reserve, lung function, or ΔavO_2 to account for lower peak iVO_2 in $COVID_{reduced}$ patients

(4) the deleterious effect on exercise capacity was unrelated to acute COVID-19 illness severity and lessened over time.

Peak VO_2 is an objective marker of exercise capacity that is determined by lung capacity, cardiac function, and peripheral tissue oxygen extraction. Studies have demonstrated reduced peak VO_2 in patients who have recovered from acute COVID-19 infection(119, 129).Although residual cardiovascular and pulmonary damage could explain these findings(120, 121), this study was designed to investigate exercise intolerance in patients without immediately attributable causes. Thus, I hoped to identify "subclinical" pathophysiology that might explain decreased exercise capacity in $COVID_{reduced}$ patients. I demonstrated no differences in spirometry metrics between the 2 post–COVID-19 patient groups, implying that persistent lung damage was not the cause of exercise limitation. I also found no difference in peak ΔavO_2 between any of the groups, suggesting that skeletal muscle function was normal in patients following COVID-19. This contrasts with a recent invasive CPET study that demonstrated impaired ΔavO_2 in a group of patients who were exercise intolerant following COVID-19(129). However, there were some notable differences between the studied cohorts. First, most patients in the invasive CPET study had not been hospitalized during their acute COVID-19 illness.

Second, the time from illness to examination was markedly longer in the invasive CPET study (≈11 months) compared with my medium-term follow-up cohort (≈3 months). Nevertheless, the differences suggest heterogeneity in the pathophysiology of persistent exercise intolerance following COVID-19. This is in keeping with the finding of different exercise phenotypes in patients with post-viral chronic fatigue syndrome, characterized as either low flow (with underlying low biventricular filling) or high flow (associated with impaired systemic oxygen extraction)(130). Finally, while both studies use a cycle ergometer, CMR-CPET is performed supine rather than conventional upright cycling. This affects exercise physiology, such as aerobic work efficiency and muscle deoxygenation response(131, 132), and may account for some differences between study findings.

In this study, reduced iVO_2 in $COVID_{reduced}$ patients appeared to be attributable to a failure to augment CO. This was caused by an inability to increase SV during exercise, with no evidence of chronotropic incompetence. The most obvious reason for reduced SV augmentation is impaired contractile reserve. This is particularly pertinent considering the high prevalence of post–COVID-19 CMR abnormalities, including myocarditis(133). However, I excluded patients with evidence of troponin positivity during their hospital admission. It is worth noting that both patient groups had the higher resting LV ejection fraction, RV mass, and native myocardial T1. While these metrics were in keeping with reference ranges in the general population(90, 121), the differences versus the controls indicate that the patient groups did not have completely "normal" hearts. This might represent the background health status of these previously hospitalised patients and could possibly be suggestive of subclinical cardiovascular disease. Nevertheless, peak exercise biventricular ejection fractions were the same in all groups, and there were no differences in RV mass and T1 between the patients with and without exercise intolerance. These findings go against the idea of contractile dysfunction being the cause of reduced CO augmentation in $COVID_{reduced}$ patients. Another reason for failure to

augment SV on exertion could be diastolic dysfunction, but the similar left atrial sizes and LV masses among all the groups make this less likely. In the absence of abnormalities of systolic or diastolic function, I propose that inadequate preload could be a remaining cause of reduced SV augmentation to consider in the $COVID_{reduced}$ patient group.

Factors that control ventricular filling (not directly assessed in this study) include blood volume and venous compliance. Indeed, blood volume is one of the most important factors in maintaining ventricular filling. Blood volume depletion is known to reduce exercise capacity(134), is depleted in post-viral chronic fatigue syndrome, and correlates with exercise symptoms(135, 136). Furthermore, volume expansion in these patients results in improved exercise tolerance(134). It is possible that similar mechanisms could occur in some patients following COVID-19, reducing ventricular filling during exercise and contributing to exercise intolerance. Similar mechanistic origins of disease would perhaps be unsurprising given the symptom overlap between post-viral chronic fatigue syndrome and patients following COVID-19. Possible causes of reduced blood volume following COVID-19 that could be evaluated in future studies include detraining after severe illness, abnormal renal regulation of fluid balance, and reduced fluid or salt intake(137, 138). Although these causes require further investigation, they do raise the possibility of interventions tailored to volume expansion, such as increased hydration and salt intake. The other important contributor to preload is venous compliance, which controls the proportion of the total blood volume that is "stressed." It is stressed that blood volume that directly contributes to preload and dynamic reduction of venous compliance is required to increase preload during exercise. Venous compliance is controlled by the autonomic system, and there is some evidence of dysautonomia in patients with post-viral chronic fatigue syndrome(138) along with small studies demonstrating dysautonomia in patients following COVID-19(139, 140). Thus, an inability to dynamically reduce compliance

may contribute to reduced exercise capacity in the $COVID_{reduced}$ group and also requires further investigation.

Irrespective of the cause of reduced SV and CO at peak exercise, I did show that exercise capacity appears to improve with time since discharge. This suggests that reduced exercise capacity following COVID-19 is not permanent and that a return to baseline is possible. Of course, this requires long-term surveillance, as well as identification of interventions that may hasten recovery. In this regard, future work should include the longitudinal serial assessment of exercise capacity over a sufficient time period to ensure adequate time for recovery (eg, at 1 year). Interestingly, I also showed no association between exercise capacity and disease severity, which is consistent with other studies of patients with previous COVID-19 infection(141). This strengthens the idea that exercise intolerance is not simply the result of residual organ damage but a specific response to COVID-19 infection.

One of the unique aspects of this study is the use of CMR-CPET. This technique enables simultaneous quantification of peak VO_2 and CO, with subsequent calculation of ΔavO_2, but is dependent on real-time MR sequences. These can be challenging to use and require optimization to ensure robustness, particularly during exercise. I have previously shown that one of the most important factors in determining the reproducibility of real-time MR is spatial and temporal resolution(57, 96). Thus, I used highly accelerated spiral acquisitions, reconstructed using compressed sensing. These techniques provide spatial and temporal resolution only slightly lower than clinical sequences. Accelerated real-time spiral sequences with compressed sensing reconstruction for assessment of aortic flow and ventricular volumes have previously been validated(85, 86). Unfortunately, validation at peak exercise with conventional gated breath-hold or respiratory averaged MR is not possible. It should also be noted that these techniques are not widely available and can be challenging to use, meaning

that CMR-CPET cannot be considered a clinical tool at the moment. Nevertheless, CMR-CPET does allow more sophisticated investigation of pathophysiology enabling generation of important new hypotheses. Furthermore, high-resolution real-time sequences are starting to become more clinically available(142), opening the possibility of CMR-CPET being used as a clinical test. Of course, this will require further validation both of real-time sequences (at peak exercise) and CMR-CPET in general. Simultaneous right heart catheterization and CPET (invasive CPET) is the reference standard direct method of measuring of ΔavO_2 .(129, 134) Furthermore, invasive CPET can be performed using conventional metabolic carts and upright exercise ergometers, and allows traditional catheter-based estimation of CO. It has been previously shown that VO_2 measured during MR-CPET correlates well with VO_2 measured during conventional CPET(58). In addition, resting CO by phase-contrast MR correlates well with CO measured invasively(143). However, CMR-CPET measurements of exercise CO and ΔavO_2 have not been directly compared with invasive CPET. This is mainly attributable to the significant difficulties in performing simultaneous MR and invasive CPET. Nevertheless, validating this novel technique is desirable, and future work should investigate a way of overcoming the logistical barriers to a direct comparison.

There are limitations of the study to consider. The $COVID_{reduced}$ and $COVID_{normal}$ groups, but not the control group, were matched for hypertension and diabetes. While this is an important limitation, it does not account for the differences in MR-CPET metrics between the 2 post–COVID-19 patient groups given their matching for these comorbidities. Furthermore, there were no differences in peak iVO_2 and peak COi between the $COVID_{normal}$ group and healthy controls. These results suggest that the absence of comorbidity matching in the control group did not significantly affect the results. As patients with significant cardiac and respiratory diseases were excluded, I only matched post–COVID-19 patient groups by age, sex,

hypertension, and diabetes. I believe that this covers most confounders of exercise capacity, but in future studies with larger recruitment, it may be beneficial to more extensively match groups. Neither of the patient groups were matched for pre–COVID-19 exercise history because of the difficulty in ascertaining accurate exercise histories. Future studies may be able to overcome this problem by excluding subjects who are unable to provide an accurate exercise history, although this does risk introducing a significant selection bias. I did not have spirometry data for the healthy control group to compare against patient groups. However, this cohort was particularly advantageous as most data were acquired before the pandemic and, therefore, would not have been confounded by prior COVID-19 infection. We have presented CMR-derived data of left atrial size and LV mass but no specific measures of diastolic function, which should also be evaluated in future work. Further studies should also include the assessment of exercise capacity in response to intravenous fluid challenge, as I propose blood volume depletion as a potential cause of impaired SV augmentation.

This CMR-CPET study emphasizes the importance of SV augmentation in the normal response to exercise. There were no differences in contractile reserve, left atrial size or LV mass (suggestive of diastolic impairment), or peak afterload that could explain reduced SV augmentation in $COVID_{reduced}$ patients. Therefore, I propose that inadequate preload could be a possible mechanism of reduced SV augmentation and, consequently, of exercise intolerance in these patients. However, this is a hypothesis of exclusion, and larger, more statistically powered studies are required to fully understand the origin of exercise intolerance in these patients. These data show no relationship between disease severity and peak CMR-CPET metrics and, reassuringly, that abnormalities in peak CMR-CPET metrics may improve with time from the acute illness. I believe that the comprehensive evaluation of unexplained dyspnoea and exercise intolerance is pivotal to help correctly identify potential therapeutic targets in these patients.

13. RESULTS - THE PROGNOSTIC UTILITY OF EXERCISE CMR IN INTERMEDIATE RISK SYSTEMIC SCLEROSIS ASSOCIATED PULMONARY HYPERTENSION

This chapter is based on the publication below:

Brown JT, Virsinskaite R, Kotecha T, Steeden J, Fontana M, Karia N, Schreiber BE, Ong VH, Denton CP, Coghlan JG, Muthurangu V, Knight DS. "Prognostic utility of exercise CMR in intermediate risk patients with systemic sclerosis-associated pulmonary arterial hypertension". European Heart Journal – Cardiovascular Imaging. 2024 Aug **00**, 1-9

My contribution to this work was recruiting subjects, designing the exercise protocol, conducting all exercise tests, analysing clinical, CPET and CMR data, performing statistical analysis and writing the manuscript.

The study was approved by national ethics committee (IRAS project ID 226101; REC reference 17/LO/1499, National Health Service Health Research Authority UK CRN 058274). All subjects provided written informed consent.

13.1 Introduction

Cardiovascular magnetic resonance (CMR) is a key imaging modality in the assessment of pulmonary hypertension (PH). Metrics of right ventricular (RV) size and function by CMR are accurate, reproducible and prognostic in PH(144, 145). Consequently, CMR-derived metrics of RV size and function have been used to augment clinical PH risk stratification tools and as end-points in trials of targeted PH therapy(146, 147). This is reflected by international guidelines that now incorporate CMR metrics into the comprehensive risk assessment of

patients with pulmonary arterial hypertension (PAH)(62). Cardiovascular MR is particularly useful in patients with systemic sclerosis-associated pulmonary arterial hypertension (SSc-PAH) where it also helps to identify additional relevant SSc-specific cardiovascular pathology(148).

Evaluating disease severity through standardised risk of death assessment is pivotal to the clinical management of patients with PAH, facilitating a systemic approach to treatment escalation decisions as well as enabling prognostication(62). The majority of patients with PAH, including those with SSc-PAH, are categorised as intermediate risk(149, 150). In the 2022 European Society of Cardiology/European Respiratory Society (ESC/ERS) PH guidelines, this category is further subdivided into intermediate-low and intermediate-high risk strata based upon a composite score of functional class (FC), 6 minute walk distance (6MWD) and N-terminal pro-B-type natriuretic peptide (NT-proBNP)(62). This was done to provide better discrimination of risk and direction of treatment strategies during follow-up using routinely collected clinical data. However, the additional role of CMR is less clear in these two intermediate groups as they have less overtly abnormal right ventricles, particularly when compared with idiopathic PAH (IPAH)(151). One potential solution could be exercise CMR (Ex-CMR), which has been used to unmask pathophysiology in a range of cardiovascular diseases and can predict outcome in patients with heart muscle disease.(152, 153). Recently, I have combined exercise CMR with cardiopulmonary exercise testing (CMR-CPET) to provide truly comprehensive evaluation of the determinants of exercise capacity. I have previously used CMR-CPET to better understand mechanisms of exercise intolerance in patients with SSc with and without PH(125) and believe that it could be used to better evaluate risk in SSc-PAH. The aim of this study was to assess if Ex-CMR metrics are more predictive of outcome in patients with intermediate risk SSc-PAH compared with resting CMR.

13.2 Methods

13.2.1 Patient population

I performed a prospective, single centre, observational study of fifty patients with a confirmed diagnosis of SSc-PAH categorised as intermediate PH risk who underwent CMR-CPET between March 2019 and March 2022. Patients were recruited from the National PH Service at the Royal Free Hospital, one of seven UK specialist centres for the management of adult PH.

Inclusion criteria were:

1. a confirmed diagnosis of PAH by right heart catheterisation (RHC) according to contemporaneous international guidelines(60)
2. a diagnosis of SSc (including those with a concomitant overlap syndrome diagnosis) fulfilling the American College of Rheumatology/European League Against Rheumatism 2013 classification criteria(68)
3. PH categorised as intermediate risk according to the 2022 ESC/ERS PH guidelines based upon average risk score of N-terminal pro-B-type natriuretic peptide (NT-proBNP, obtained on the day of testing), functional class (FC) and 6-minute walk distance (6MWD), as obtained at the last outpatient clinic appointment)(154)
4. age 18–80 years.

Exclusion criteria were:

1. general contraindications to CMR scanning
2. contraindications to performing an exercise test (unstable symptoms, including angina, exertional syncope, World Health Organization (WHO) FC IV symptoms, and musculoskeletal disease preventing exercise),

3. previous symptomatic ischemic heart disease or moderate-to-severe valvular disease,

4. changes in targeted PH therapy within 3 months

5. significant lung parenchymal disease that may confound CPET results, such as interstitial lung disease (significant being defined as > 20% lung volume on computed tomography, using a qualitative visual assessment by an experienced computed tomography radiologist at our institution's multi-disciplinary meeting).

13.2.2 Clinical data

Patients were subdivided into intermediate-low and intermediate-high risk categories using the current European Society of Cardiology/European Respiratory Society (ESC/ERS) guidelines.(154) Functional class and 6MWD were obtained from the most recent out-patient clinic encounter on the PH service database. Blood tests for full blood count (FBC) and NT-proBNP were obtained on the day of CMR-CPET, prior to the exercise scan. The most recent lung function test data and the most recent cardiac catheterization data were obtained from patient electronic records systems and specialist services databases by clinicians blinded to the patient outcomes. Outcome was ascertained by checking the patient summary care record on the National Health Service (NHS) spine portal on 15th November 2023.

13.2.3 CMR-augmented cardiopulmonary exercise testing

Cardiovascular magnetic resonance-augmented CPET was performed as previously described (125). Imaging was performed on a 1.5T CMR scanner (Magnetom Aera, Siemens, Erlangen, Germany) using two 6-element coils (one spinal matrix, one body matrix). The scanning room was temperature controlled. Full resuscitation facilities were available. Each subject's electrocardiogram (ECG) was monitored continuously using the in-built system in the CMR scanner. This system allowed assessment of rate and rhythm but is not suitable for

identification of ischemia. All patients had peripheral venous access during testing for use in resuscitation protocols in the event of clinical instability.

13.2.4 CMR imaging techniques (real-time flow and volume imaging)

Before exercise, subjects underwent a routine CMR with long- and short-axis cine imaging, myocardial native T1 and T2 mapping as previously described(95, 125). At rest and peak exercise, aortic flow was measured using real-time phase-contrast (PC) CMR (PC-CMR). PC-CMR was performed using a uniform density golden-angle spiral sequence, with a compressive sensing (CS) reconstruction(85). Real-time assessment of biventricular volumes was performed at rest and peak exercise, immediately after each real-time flow acquisition using a 2D multi-slice real-time tiny golden-angle spiral CS balanced steady state free precession (bSSFP) sequence(86). All real-time imaging was acquired during free breathing with parameters as previously described(125). The aortic flow and short-axis image data were reconstructed off-line (MATLAB R2018a, MathWorks Inc, Natick, Massachusetts, USA), using the Berkeley Advanced Reconstruction Toolbox (BART).

13.2.5 Respiratory gas analysis

Breath-by-breath gas exchange analysis was performed using a commercial CPET system (Ultima, MedGraphics, St Paul, Minnesota, USA). The analyser was placed in the CMR control room and attached to the facemask (Hans Rudolph, Kansas City, USA) via a set of CMR-compatible sampling tubes (umbilicus) passed through the waveguide. This bespoke umbilicus was modified as previously described increasing overall length from the standard 234–1000 cm and removing ferromagnetic components(58). It was thoroughly tested by the manufacturer, meeting all quality control standards. Gas and flow calibrations were performed

before each test and at least 30 min after system initiation. All measurements were taken at body temperature and ambient pressure.

13.2.6 Exercise protocol

Subjects performed exercise on a supine CMR-compatible cycle ergometer (MR Cardiac Ergometer Pedal, Lode, Groningen, Netherlands) as previously described(125). The first minute of the protocol consisted of exercise against zero resistance, with subjects asked to cycle at 60–70 rpm. Thereafter, the protocol was split in 2-minute stages, each containing three workload increments introduced at 0, 30 and 60 seconds into the stage as follows - stages 1–3: 3 Watts (W), stages 4–6: 5 W, stage 7–8: 7 W, stages 9–10: 9 W and stages 11–12: 11 W. The smaller increments at the start of the protocol ensured that even subjects with significant exercise intolerance were able to complete at least two exercise stages. This protocol was followed until exhaustion. At the onset of exhaustion (defined as an inability to maintain cadence or a verbal indication from the subject), the subject was encouraged to maintain cycling while peak aortic flow and ventricular volumes were acquired, after which exercise was stopped.

13.2.7 Data analysis

All CMR studies were reported by experienced clinical CMR observers (J.B., D.S.K.). blinded to patient outcomes and analysed using ‘in-house’ plug-ins for OsiriX MD version 9.0.1 (Pixmeo Sarl, Bernex, Switzerland)(96-98). PC-CMR flow data of the ascending thoracic aorta was segmented using a semi-automatic vessel edge detection algorithm with manual operator correction if required. Stroke volume (SV) was calculated by integrating the flow curve across a single R-R interval. Cardiac output (CO) was given by SV x heart rate (HR). End diastole and end systole were defined per short-axis slice by visual assessment of cavity areas and

segmentation was performed manually. Papillary muscles and trabeculae were excluded from the blood pool. Left and right ventricular (LV and RV) stroke volumes were calculated as the difference between the end diastolic volume (EDV) and end systolic volume (ESV). Ejection fraction (EF) was determined as (SV/EDV) × 100. Bi-atrial areas were traced at end systole on a 4-chamber cine image acquired at rest. All volumetric data, area data and cardiac output were indexed to body surface area (BSA) and denoted by the suffix -i. Native myocardial T1 and T2 relaxation times were measured by drawing a region of interest (ROI) within the interventricular septum on the mid-cavity short-axis maps remote from the insertion points(95).

Oxygen uptake (VO_2) and respiratory exchange ratio (RER) measurements were time-registered to CMR data. The VO_2 was indexed to body weight and denoted by the prefix -i. Arteriovenous oxygen content gradient was calculated as $\Delta avO_2 = VO_2/CO$ (using non-indexed data). These calculations were performed at rest and peak-exercise for all subjects. Ventilatory efficiency was evaluated as the slope of the minute ventilation carbon dioxide production (VE/VCO_2) plot in the portion where there was a linear relationship.

13.2.8 Statistics

All statistical testing was performed using R (RStudio 2021.09.2 using R 4.1.2). Data were examined for normality using the Shapiro–Wilk normality test. Descriptive statistics were expressed as mean (± standard deviation) for normally distributed data and median (interquartile range) for non-normally distributed data. Differences between dead and alive groups performed were performed using *t* tests (normal data) and Mann-Whitney tests (non-normal data). Univariable survival analysis was performed using Cox Proportional Hazards (CPH) regression with hazard ratio (HR) reported per standard deviation change in continuous metrics. Due to collinearity and the small population size, bidirectional stepwise Cox

regression was used to select the most parsimonious model with all significant CMR metrics from univariable analysis being entered.

Optimal cut-offs for prognostic metrics from stepwise Cox were identified using maximally selected rank statistics. These defined reduced and normal RV contractile reserve groups that were then additionally combined with intermediate-low and intermediate-high risk groups. Survival differences were assessed using Kaplan-Meier plots with both omnibus and pairwise Log-Rank tests (Benjamini and Hochberg adjustment for multiple comparisons performed using).

For all tests, a p value <0.05 was considered statistically significant.

13.3 Results

13.3.1 Study population

Clinical details of the study population and targeted PH therapies are shown in Table 13. The median age was 65 (full range 29-76) years and patients were predominantly female (48, 96%). As expected, the majority of patients had limited (44, 88%) rather than diffuse (6, 12%) SSc disease. Four (8%) patients had an overlap connective tissue disease diagnosis. There were 30 (60%) patients in the intermediate-low PH risk category and 20 (40%) in the intermediate-high PH risk category. The majority of patients (44, 88%) were prevalent for their PAH diagnosis. Nine (18%) patients died during a median follow-up period of 2.1 years (range 0.1-4.6 years). Compared to survivors, patients who died during follow-up had significantly higher NT-proBNP (p=0.033), but similar 6MWD (p=0.70) and FC (p=0.77).

	SSc-PAH patients (n = 50)
Demographics and co-morbidities	
Female, n (%)	48 (96)
Age* (median [full range]), years	65 (29-76)
Incident/Prevalent PAH diagnosis, n (%)	6/44 (12/88)
Intermediate-low/intermediate-high risk, n (%)	30 (60) / 20 (40)
Background haemodynamic and clinical measurements	
PVR* (dynes/s/cm^{-5})	291 (214-400)
mPAP* (mmHg)	31 (24-36)
FVC (%predicted)	94.9±18.9
FEV1 (%predicted)	86.7±16.4
DLCO (%predicted)	40.6±10.2
Targeted PH therapies (n=44, 88%)	
PDE5I, n (%)	39 (78)
ERA, n (%)	37 (74)
SGCS, n (%)	2 (4)
Prostanoids (IV/oral IP receptor agonist), n (%)	1 (2) / 4 (8)
SSc details	
Limited/diffuse SSc, n (%)	44/6 (88/12)
Overlap syndromes, n (%)	4 (8)
- Myositis, n (%)	2 (4)
- SLE, n (%)	2 (4)

Table 13. Clinical details of the study cohort.

DLCO=diffusion capacity of the lung for carbon monoxide
ERA=endothelin receptor antagonist
FEV1=forced expiratory volume in one second
FVC=forced vital capacity
IP=prostacyclin
IV=intravenous
mPAP=mean pulmonary arterial pressure
PAH=pulmonary arterial hypertension
PDE5I=phosphodiesterase type 5 inhibitor
PVR=pulmonary vascular resistance
SGCS=soluble guanylate cyclase stimulator
SLE=systemic lupus erythematosus
SSc=scleroderma/systemic sclerosis
Normally distributed data displayed as mean±SD
**Denotes non-normally distributed data shown as median (interquartile range) unless otherwise specified.*

13.3.2 Resting CMR-CPET

Resting CMR-CPET data are shown in Table 14. Compared to published normal values(90) (88), 8% of patients had abnormal RVEDVi, 24% had abnormal RVESVi and 36% had abnormal RVEF. The only significant differences in resting CMR metrics between dead and alive patients were indexed right atrial area (RAi, p=0.034) and septal T2 (p=0.040), which were both higher in patients who died during follow-up. Importantly, there were no significant differences in resting biventricular size or function between dead and alive patients. Patients who died during follow-up also had higher resting VO_2 p=0.040).

	Total cohort (n = 50)	Alive (n = 41)	Dead (n = 9)	*p*- value
Clinical data and PAH risk stratification data				
Age* (years)	65 (58-71)	64 (58-69)	69 (65-71)	0.18
6MWD (m)	361±99	363±103	349±82	0.70
NT-proBNP* (ng/L)	378 (154-685)	256 (127-616)	1590 (207-2230)	**0.033**
WHO FC*	3 (2-3)	3 (2-3)	3 (2-3)	0.77
PAH risk score*	2 (2-3)	2 (2-3)	3 (3-3)	**0.011**
Hb* (g/L)	120 (113-129)	120 (111-129)	119 (117-122)	0.88
Resting CMR metrics				
RVEDVi (mL/m^2)	75±18	73±17	82±17	0.16
RVESVi* (mL/m^2)	29 (22-41)	28 (22-36)	44 (34-46)	0.098
RVSVi (mL/m^2)	41±11	41±11	44±8	0.48
RVEF (%)	56±11	57±11	54±10	0.56
LVEDVi (mL/m^2)	65±15	65±16	67±13	0.77
LVESVi* (mL/m^2)	23 (16-28)	22 (16-28)	23 (14-31)	0.85
LVSVi (mL/m^2)	42±11	41±12	44±7	0.60
LVEF* (mL/m^2)	66 (59-72)	66 (58-72)	68 (62-76)	0.54
HR (bpm)	74±12	74±13	74±9	0.99
CO (L/min)	3.1±0.8	3.0±0.9	3.3±0.6	0.41
RAi area (cm^2/m^2)	13±3	13±3	15±4	**0.034**
LAi area (cm^2/m^2)	14±3	13±3	15±3	0.23
Native myocardial T1 (ms)	1082±55	1078±53	1096±63	0.37
Myocardial T2 (ms)	52±4	52±4	55±5	**0.04**
Resting CPET metrics				
iVO_2* (mL/min/kg)	3.4 (3.0-4.0)	3.2 (3.0-4.0)	3.8 (3.5-5.0)	**0.040**
avO_2* (mLO_2/100mL)	4.2 (3.9-5.0)	4.2 (3.9-5.0)	4.2 (3.9-4.3)	0.85

Table 14. Differences in clinical data, PAH risk stratification data and resting CMR-CPET in dead compared to alive patients.

6MWD=six-minute walk distance
avO_2=tissue oxygen extraction
CMR=cardiovascular magnetic resonance
CO=cardiac output

CPET=cardiopulmonary exercise test
FC=functional class
Hb=haemoglobin
HR=heart rate
iVO_2=oxygen consumption indexed to weigh
LAi=left atrial area indexed to body surface area (BSA)
NT-proBNP=N-terminal pro-B-type natriuretic peptide
PAH=pulmonary arterial hypertension
RAi=right atrial area indexed to BSA
RVEDVi/RVEF/RVESVi/RVSVi=right ventricular measurements as per LV
WHO=World Health Organization
Normally distributed data displayed as mean±SD
**Denotes non-normally distributed data shown as median (interquartile range) unless otherwise specified.*

13.3.3 Exercise feasibility

All subjects successfully completed the exercise protocol without complication; no subjects required medical intervention. Peak-exercise RER ≥1.0 was achieved in 44 (88%) patients; of the six patients who exercised to exhaustion but did not reach anaerobic threshold, the lowest peak RER was 0.88.

Changes in CMR-CPET metrics with exercise are shown in Table 15. There were significant decreases of RVEDV (p=0.014), LVEDV (p<0.001) and LVESV (p<0.001) on exercise along with significant increases in LVEF (p=0.034), COi (p<0.001), iVO_2 (p<0.001) and ΔavO_2 (p<0.001). There was no significant difference in RVEF between rest and peak exercise (p=0.36).

Variable	Rest	Exercise	*p* value
CMR metrics			
RVEDVi* (mL/m^2)	75 (44-124)	68 (40-118)	0.014
RVESVi (mL/m^2)	32±12	30±14	0.11
RVSVi (mL/m^2)	41±11	39±12	0.10
RVEF (%)	56±11	58±14	0.36
LVEDVi (mL/m^2)	65±15	58±14	<0.001
LVESVi (mL/m^2)	23±9	19±9	<0.001
LVSVi (mL/m^2)	42±11	39±12	0.061
LVEF (%)	65±10	68±12	0.034
CO (L/min)	3.1±0.8	4.1±1.1	<0.001
CPET metrics			
iVO_2 (mL/min/kg)	3.7±0.9	9.7±1.8	<0.001
avO_2* (mLO_2/100mL)	4.2 (3.0-9.7)	8.7 (5.9-19.5)	<0.001

Table 15. Changes in CMR-CPET metrics with exercise.

avO_2=tissue oxygen extraction
CMR=cardiovascular magnetic resonance
CO=cardiac output
CPET=cardiopulmonary exercise test
iVO_2=oxygen consumption indexed to weight
LVEDVi=BSA-indexed left ventricular end diastolic volume
LVEF=left ventricular ejection fraction
LVESVi=BSA-indexed left ventricular end systolic volume
LVSVi= BSA-indexed left ventricular stroke volume
RVEDVi/RVEF/RVESVi/RVSVi=right ventricular measurements as per LV
Normally distributed data displayed as mean ± SD
**Denotes non-normally distributed data shown as median (interquartile range) unless otherwise specified.*

The only significant difference in either rest or exercise CMR metrics between the intermediate-low and intermediate-high risk groups, shown in Table 16, was exercise RVESV, which was lower in the intermediate-low risk patients (p=0.043).

	Total cohort (n = 50)	Intermediate-low risk (n = 30)	Intermediate-high risk (n = 20)	*p* value
Age (years)	65 (58-71)	65 (59-69)	67 (58-72)	0.43
Resting CMR metrics				
RVEDVi (mL/m^2)	75±18	72±18	78±17	0.27
RVESVi* (mL/m^2)	29 (22-41)	27 (21-36)	35 (26-44)	0.13
RVSVi (mL/m^2)	41±11	40±10	43±12	0.48
RVEF (%)	56±11	57±10	55±12	0.59
LVEDVi (mL/m^2)	65±15	64±13	67±18	0.52
LVESVi* (mL/m^2)	23 (16-28)	21 (16-28)	23 (18-29)	0.62
LVSVi (mL/m^2)	42±11	41±10	43±13	0.68
LVEF* (mL/m^2)	66 (59-72)	66 (60-71)	66 (56-72)	0.63
Exercise CMR metrics				
RVEDVi (mL/m^2)	69±17	67±18	73±16	0.23
RVESVi* (mL/m^2)	26 (19-39)	22 (18-35)	37 (23-43)	0.043
RVSVi* (mL/m^2)	37 (32-44)	40 (32-46)	36 (33-39)	0.46
RVEF (%)	58±14	61±14	53±14	0.071
LVEDVi (mL/m^2)	58±14	57±12	59±18	0.79
LVESVi* (mL/m^2)	16 (12-24)	14 (12-21)	19 (12-29)	0.46
LVSVi (mL/m^2)	39±12	40±10	38±14	0.61
LVEF* (mL/m^2)	73 (60-77)	73 (68-78)	71 (58-76)	0.28

Table 16. Differences between intermediate-low risk and intermediate-high risk patients in rest and exercise CMR metrics.

LVEDVi=BSA-indexed left ventricular end diastolic volume
LVEF=left ventricular ejection fraction
LVESVi=BSA-indexed left ventricular end systolic volume
LVSVi=BSA-indexed left ventricular stroke volume
RVEDVi/RVEF/RVESVi/RVSVi=right ventricular measurements as per LV
Normally distributed data displayed as mean±SD
**Denotes non-normally distributed data shown as median (interquartile range) unless otherwise specified.*

Differences in exercise CMR-CPET metrics in dead compared to alive patients are shown in Table 17. The only significant differences were higher peak RVESVi (p=0.017), lower peak RVEF (p=0.044) and higher VE/VCO_2 (p=0.011) in patients who died during follow-up.

	Total cohort (n = 50)	**Alive (n = 41)**	**Dead (n = 9)**	***p* value**
Exercise CMR metrics				
RVEDVi (mL/m^2)	69±17	68±17	76±17	0.17
RVESVi* (mL/m^2)	26 (19-39)	23 (18-36)	44 (27-45)	0.017
RVSVi* (mL/m^2)	37 (32-44)	39 (32-44)	35 (33-37)	0.57
RVEF (%)	58±14	59±14	49±8	0.044
LVEDVi (mL/m^2)	58±14	59±15	55±13	0.48
LVESVi* (mL/m^2)	16 (12-24)	16 (12-24)	14 (11-23)	0.70
LVSVi (mL/m^2)	39±12	40±12	36±8	0.42
LVEF* (mL/m^2)	73 (60-77)	73 (65-77)	76 (59-77)	0.79
HR (bpm)	108±15	108±16	104±10	0.47
CO (L/min)	4.1±1.1	4.2±1.2	3.6±0.6	0.16
Exercise CPET metrics				
iVO_2 ($mL/min/kg$)	9.7±1.8	9.9±1.9	9.0±1.5	0.20
avO_2* ($mLO_2/100mL$)	8.7 (7.5-10.9)	8.7 (7.5-11.3)	9.0 (7.5-10.2)	0.85
VE/VCO_2	45.2±10.2	43.5±10.0	52.8±7.7	0.011

Table 17. Differences in exercise CMR-CPET metrics in dead compared to alive patients.

avO_2=tissue oxygen extraction
CMR=cardiovascular magnetic resonance
CO=cardiac output
CPET=cardiopulmonary exercise test
HR=heart rate
iVO_2=oxygen consumption indexed to weight
LVEDVi=BSA-indexed left ventricular end diastolic volume
LVEF=left ventricular ejection fraction
LVESVi=BSA-indexed left ventricular end systolic volume
LVSVi=BSA-indexed left ventricular stroke volume
RVEDVi/RVEF/RVESVi/RVSVi=right ventricular measurements as per LV
VE/VCO_2=ventilatory equivalents for carbon dioxide
Normally distributed data displayed as mean±SD
**Denotes non-normally distributed data shown as median (interquartile range) unless otherwise specified.*

13.3.4 Predictors of mortality

Resting univariable CMR predictors of all-cause mortality (Figure 24) included RVESVi (p=0.048), myocardial T2 (p=0.040) and RAi (p=0.033).

CMR-CPET parameter	Hazard ratio	*P* value
Rest RVEDVi	1.78	0.11
Rest RVESVi	2.04	0.048*
Rest RVSVi	1.22	0.57
Rest RVEF	0.69	0.32
Rest LVEDVi	1.12	0.75
Rest LVESVi	0.98	0.97
Rest LVSVi	1.15	0.70
Rest LVEF	1.29	0.56
Rest heart rate	1.06	0.88
Rest COi	1.28	0.46
Rest iVO_2	1.83	0.036*
Rest avO_2	1.00	1.00
T1	1.45	0.29
T2	2.17	0.04*
RAi area	2.18	0.033*
LAi area	1.45	0.28
Age	1.90	0.19

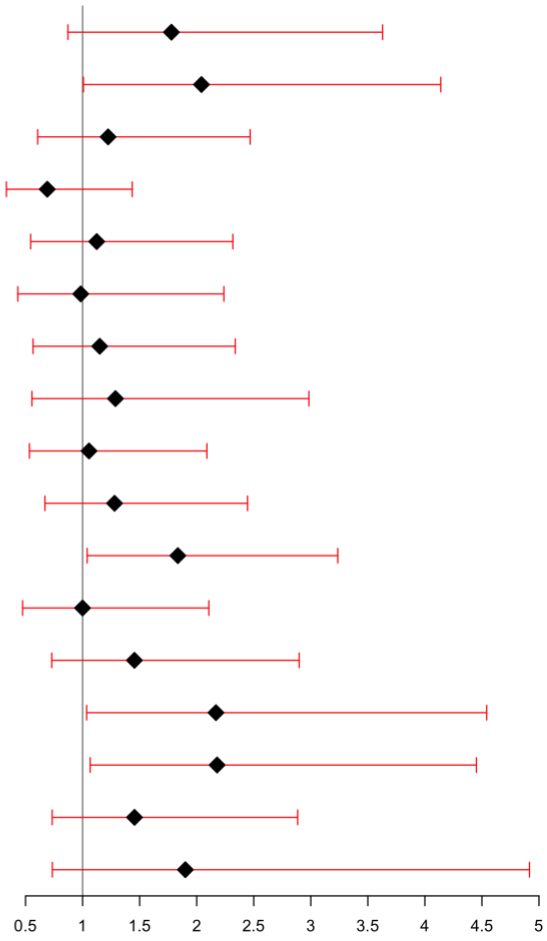

Figure 25. Forest plot of resting CMR and CPET variables to predict all-cause mortality on univariable Cox regression analysis.

** denotes statistically significant metrics (p <0.05).*

Peak Exercise-CMR predictors of all-cause mortality (Figure 25) included RVESVi (p=0.014) and RVEF (p=0.026).

CMR-CPET parameter	Hazard ratio	*P* value
Peak RVEDVi	1.74	0.096
Peak RVESVi	2.33	0.014*
Peak RVSVi	0.74	0.46
Peak RVEF	0.46	0.026*
Peak LVEDVi	0.79	0.58
Peak LVESVi	1.16	0.68
Peak LVSVi	0.65	0.30
Peak LVEF	0.81	0.53
Peak heart rate	0.88	0.70
Peak COi	0.56	0.17
Peak iVO_2	0.55	0.17
Peak avO_2	0.72	0.46
VE/VCO_2	3.31	0.012*

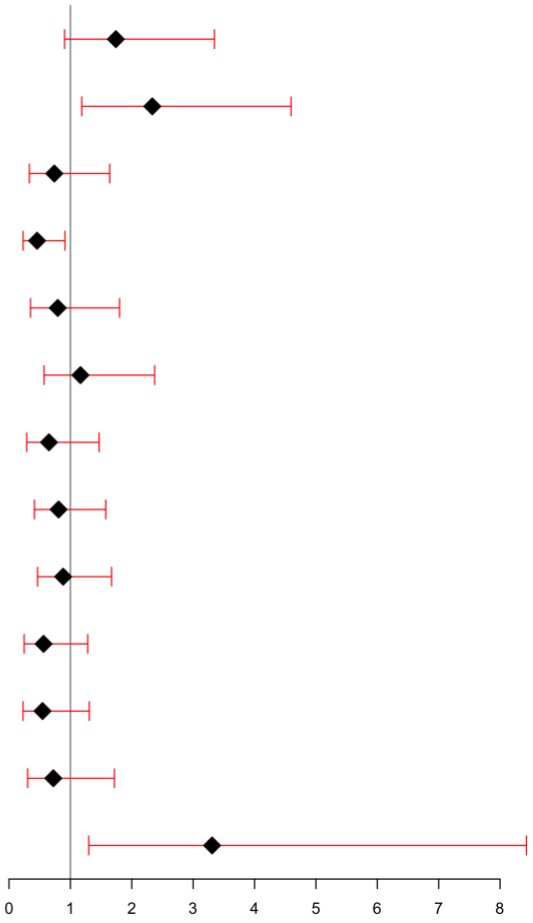

Figure 26. Forest plot of peak exercise CMR and CPET variables to predict all-cause mortality on univariable Cox regression analysis.

**denotes statistically significant metrics (p <0.05).*

Neither rest nor exercise CMR metrics of LV size and function was prognostic in this study cohort.

On stepwise analysis including all these variables, only peak RVESVi (p=0.039) was selected. The optimal threshold of peak RVESVi was <39mL/m^2 (p=0.0015) and dichotomised survival curves based on this cut-off show clear separation (Figure 26-A). When combined with intermediate-low or intermediate-high risk status, intermediate-low risk patients with peak RVESVi <39mL/m^2 had significantly better survival than all other groups (Figure 26-B),

including intermediate-low risk patients with peak RVESVi ≥39mL/m^2 (p=0.0067). There were no significant survival differences between the other 3 groups.

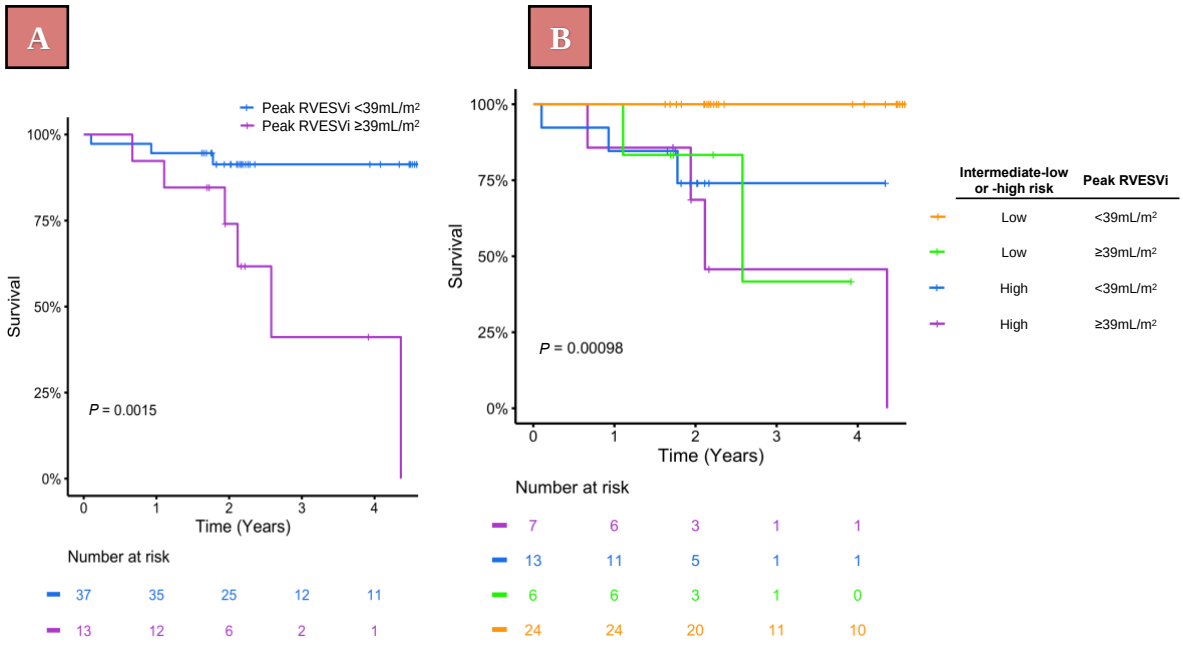

Figure 27. Kaplan-Meier plots

Panel A. Survival curves for reduced and normal right ventricular contractile reserve groups, as defined by a peak RVESVi threshold of <39mL/m2
Panel B. Survival curves for 4 groups defined by all combinations of reduced and normal RV contractile reserve and intermediate-low/-high risk.

13.4 Discussion

The main findings of this CMR-CPET study of a cohort of intermediate risk patients with SSc-PAH were:

(i) the majority of patients had normal CMR-defined resting measures of RV size and function

(ii) peak RVESVi was the only CMR metric to predict prognosis on stepwise Cox regression analysis, with an optimal threshold <39mL/m^2 to predict a favourable outcome

(iii) intermediate-low risk patients with peak RVESVi <39mL/m^2 had significantly better survival than all other combinations of intermediate-low/-high risk status and peak RVESV

(iv) VE/VCO_2 and resting VO_2 were predictive of all-cause mortality in this cohort, but not peak VO_2, peak CO or peak ΔavO_2.

Although Ex-CMR has been shown to be predictive of cardiac decompensation and arrhythmia in dilated cardiomyopathy (153), to my knowledge this is the first mortality-driven study demonstrating the prognostic capacity of Ex-CMR.

It is well known that the response of the RV to elevated afterload is the major determinant of outcome in PAH(155), hence CMR is well placed to aid risk stratification in these patients. However, the majority of studies demonstrating the relationship between resting CMR-derived RV metrics and survival in PAH included sicker patients, as evidenced by more severely deranged RV function(144, 145). Thus, the role of CMR in risk stratifying patients with less abnormal RV function, such as in this cohort, is not as well defined. This is particularly pertinent in patients with SSc-PAH, who tend to have more favourable pulmonary haemodynamics and RV function(151) as well as being more likely to be classified as intermediate risk (149, 150). In fact, resting RVESVi was only just predictive of prognosis in this study, suggesting that resting CMR metrics may be less sensitive in this important sub-population. Conversely, both peak exercise RVEF and RVESVi were strongly predictive of all-cause mortality.

Additionally, peak RVESVi <39mL/m^2 combined with intermediate-low risk status identified a subgroup of patients with significantly better prognosis. Thus, while resting RVESV has been shown to augment clinically utilised risk score calculators(146) these results show that RV

contractile reserve might better predict outcome in intermediate risk SSc-PAH patients. This is analogous to LV contractile reserve (measured using echocardiography with either pharmacological or exercise stressors) predicting outcome in non-ischaemic heart muscle disease(156). However, robust non-invasive assessment of RV contractile reserve requires reliable and reproducible measures that I believe only CMR can currently provide. Furthermore, exercise stress is preferable to pharmacological agents, both because it is more physiological and causes less side-effects. This finding, if corroborated by future studies, would have some implications for risk stratification, which is central to treatment choices and management strategies in PAH(62). Current metrics such as FC, 6MWD and BNP enable quick risk stratification in PAH patients in the out-patient clinic setting. However, my results suggest that intermediate-low risk patients (defined by FC, 6MWD and BNP) with RVESVi$\geq$39mL/m^2 have similar outcome to intermediate-high risk patients. Furthermore, there is no mortality in intermediate-low risk patients with RVESVi<39mL/m^2. Thus, inclusion of peak RVESVi allows the intermediate-low risk group to be subdivided in a prognostically important way, demonstrating the additive value of Ex-CMR with clinically derived risk strata.

Interestingly, I found that VE/VCO_2 slope and resting VO_2 were predictive of all-cause mortality in SSc-PAH stratified as intermediate risk. However, neither peak VO_2, peak CO nor peak ΔavO_2 were prognostic. Resting VO_2 reflects basal metabolic rate which is increased in patients with congestive heart failure and is also independently related to mortality(157, 158). Thus, it is not surprising that this is predictive of outcome in this population. Similarly, VE/VCO_2 has been shown to be prognostic in IPAH, although its predictive utility is less clear in studies of patients with PAH with associated conditions (APAH), such as SSc(8, 159, 160). The poor predictive capabilities of peak VO_2, COi and ΔavO_2 may be surprising as these are well-established markers of cardiovascular fitness and are known to be severely impaired in

SSc-PAH(125). However, peak VO_2 has previously been shown to not be predictive of outcome in study cohorts including patients with APAH(8, 160). Thus, this study supports the suggestion that CPET-derived metrics might be more variable in APAH subcategories, particularly in multisystem disorders such as SSc, and require further dedicated evaluation. This also highlights the utility of Ex-CMR to directly evaluate the response of the RV to exercise in these patients.

13.4.1 Limitations

Although fifty patients with confirmed SSc-PAH stratified as intermediate risk is a reasonable sized cohort relative to the rarity of the condition, this is nevertheless a single-centre study of a small patient cohort. Additionally, the optimal threshold for peak exercise RVESVi to predict outcome is specific to the CMR-CPET protocol that I used. Thus, future studies should be directed at developing reproducible protocols to aid dissemination to other centres and increasing the study population size. This would help validate these findings of additive prognostic benefit, and thus incorporation into routine SSc-PAH management. Achieving true peak exercise using a supine bicycle ergometer is also challenging and not directly comparable with conventional CPET. However, the majority of patients reached RER and good correlation between CMR-CPET and conventional CPET in achieving peak iVO_2 has been demonstrated previously (58). Another limitation of the study was the lack of contemporaneous invasive pressure data with the median time between the last catheterisation and Ex-CMR being 426 days. This meant that risk stratification based on invasive pressures could not be performed and prevented comparison of the prognostic utility of exercise RV data compared with resting pressure data. One possible solution is to leverage CMR-guided right heart catheterisation, which is increasingly becoming feasible in the clinical environment in patients with PAH(161). In patients undergoing this procedure, it would be relatively easy to add an Ex-CMR study,

enabling contemporaneous invasive pressures to be fully integrated into risk models. Furthermore, it would also be possible to measure invasive stress haemodynamics, which could provide even more granular prognostic information.

13.5 Conclusions

Peak exercise assessment of RV size and function may help identify patients with poorer prognosis amongst intermediate risk cohorts of patients with SSc-PAH, even when resting CMR measurements and conventional clinical risk stratification appear relatively reassuring. Thus, Ex-CMR could offer added value to clinical PH risk stratification in SSc-PAH, particularly in intermediate risk patients, and may provide an additional investigative strategy when considering optimisation of targeted PH therapies.

14. DISCUSSION AND CONCLUSIONS

The combination of CMR and CPET allows comprehensive and simultaneous assessment of the mechanisms that contribute to exercise dysfunction, through measurement of cardiac output and oxygen consumption which allows non-invasive tissue oxygen extraction metrics to be calculated.

In this thesis, I have performed a series of studies which employed this technique to better understand the limitations in populations where exercise intolerance is a key feature. As a result of this work, I have demonstrated that CMR-CPET can be carried out safely in a wide range of patients, and that a symptom-led, maximal (as evidenced by the vast majority of participant attaining an RER>1) exercise test is feasible and well tolerated.

Whilst direct comparisons with the upright CPET used in clinical practice are not possible, nevertheless there is correlation between the techniques, and CMR-CPET derived CPET indices are of clinical relevance (see VE/VCO_2 slope in intermediate SSc-PAH patients).

What was not possible to ascertain in these studies was the extent to which exercise would unmask left heart disease, for instance diastolic dysfunction. It is known that overt diastolic dysfunction occurs in at least 15% of patients with SSc(162), and indeterminate diastolic function in up to a further 40%. It is possible that this also applies to the SSc-PAH population and may confound some of the assumptions made in this thesis. Additional imaging sequences, e.g. to assess atrial areas or volumes during exercise (see Future Work point 4 below) may help clarify this issue, as would exercise RHC in the CMR environment.

Whilst the imaging sequences and exercise protocols developed for these studies were specific to the department in which I did my PhD, there is no conceptual barrier to them being employed in other centres. This would enable validation of the technique in different populations and larger cohorts.

Further limitations of this work included a lack of automation for assessing cardiac volumes and aortic flows (See Future Work point 3 below), which would address some of the problems associated with lack of inter-reader repeatability with this time-consuming technique by removing the human component of the variability. Clearly any machine learning algorithms would need appropriate training data sets and human oversight.

14.1 Mechanisms of exercise limitation in systemic sclerosis, systemic sclerosis-associated pulmonary arterial hypertension and non-connective tissue associated pulmonary hypertension.

In Chapter 11, I show that CMR-CPET identifies reduced peak cardiac index as mechanism for exercise intolerance for both pulmonary hypertension groups, and that reduced peak tissue oxygen extraction is feature of both systemic sclerosis groups. With further work, the precise site or sites responsible for the reduction in tissue oxygen extraction in the skeletal muscle of SSc patients might be identified, and treatment targets postulated. CMR-CPET would then provide a useful non-invasive biomarker, avO_2, for assessing response to treatment. Finally, the finding that peak stroke index was inversely associated with native myocardial T1 across

the patient groups in this study suggests that myocardial fibrosis is a common pathway in the inflammatory condition SSc and in the pulmonary hypertension groups where RV afterload is important, and if there is a causal association there may be role for antifibrotic therapy for these conditions.

14.2 Mechanisms of ongoing exercise intolerance in COVID-19 patients

In Chapter 12, using exercise CMR, I identify another mechanism of exercise intolerance. In patients with self-reported exercise intolerance after COVID-19 infection, CMR-CPET metrics showed whilst peak VO_2 was reduced in these patients, tissue oxygen extraction was not responsible. The reduced cardiac output was not due to chronotropic incompetence, but due to failure of stroke volume augmentation. The exercise CMR metrics showed that ventricular systolic function (and contractile reserve) was not implicated, and in the absence of evident diastolic dysfunction, I hypothesise that the venous preload is reduced in these patients. This is mechanistically plausible in light of similar studies investigating chronic post-viral fatigue syndromes and suggests a potentially therapeutic intervention in the form of volume expansion with increased fluid and electrolyte intake. Length of hospital admission and the severity of infection were not correlated with metrics of exercise intolerance, and reassuringly I show that the degree of exercise intolerance decreases with time from hospital admission.

14.3 Prognostic utility of exercise CMR in intermediate risk systemic sclerosis associated pulmonary arterial hypertension

In Chapter 13, I show the prognostic utility of Exercise CMR in systemic sclerosis-associated pulmonary artery hypertension. By assessing right ventricular systolic volume at peak exercise, “intermediate risk” patients (which constitute the majority of SSc-PAH) can be risk-stratified

more precisely, and I define the threshold for indexed RVESV of greater than 39ml/m^2 as being associated with poorer prognosis. Furthermore, this finding remains even when patients are stratified as “intermediate-low” or “intermediate-high” risk. Exercise CMR therefore has the ability to add to contemporary risk-stratification tools with exercise provoking a non-invasive correlate of pulmonary artery to right ventricular uncoupling, earlier in the disease process than current investigations that are performed at rest are able to. This finding can allow earlier identification of patients for treatment escalation, and RVESVi measured by exercise CMR could be used a biomarker to assess response to treatment in this group of patients.

14.4 Future Work

Further work in this area would involve four main areas:

1. Understanding the limitation of tissue oxygen extraction in systemic sclerosis:

   Muscle biopsy with microscopy could identify the architectural changes in muscle fibres and capillaries that may explain the finding of reduced avO_2 in SSc, and assessment of mitochondrial density and function, together with metabolomic studies could provide correlates with the physiological findings from this CMR-CPET research.
2. Producing less expensive equipment for exercise in CMR environment:

   With simpler, less expensive exercise modalities, validated against the ergometer used in these CMR-CPET studies, the technique could be more widely disseminated for use in other CMR departments that scan pulmonary hypertension populations. The application of exercise may be similarly useful for risk-stratification in pulmonary hypertension due to causes other than systemic sclerosis. Finally, simpler exercise

modalities would permit simultaneous exercise CMR and right heart catheterisation with the insights this could provide in terms of pressure/volume loop and pulmonary vascular resistance assessment not just at rest, but during the conditions were symptoms are evident. It is plausible that exercise metrics may be more important in terms of prognosis and response to treatment than resting metrics, and these questions could be explored with wider access to exercise CMR.

3. Automation of aortic flow and ventricular volume assessment:

   In this research, aortic flow and ventricular volume measurements were performed manually after reconstruction of the images off-line from the CMR scanner. With advancement of the available technology, image reconstruction can be performed in real-time and machine learning algorithms could give real-time outputs for cardiac output and bi-ventricular volumes. Not only would this give important clinical information in a timely manner in its own right, but the combination of exercise CMR and right heart catheterisation could give real-time assessment of other important metrics including pulmonary vascular resistance.

4. Incorporating further assessments of cardiac function during exercise:

   Although I focussed necessarily on aortic flow and ventricular volumes as the essential assessment of cardiac function during this research, there are other potential metrics that the imaging sequences could be adapted to provide, including atrial sizes (eg 4 chamber view) and volumes (atrial short axis views), pulmonary artery distensibility and ventricular septal curvature. Correlation of such metrics with simultaneous right heart catheterisation during exercise may identify novel biomarkers for non-invasive assessment of pulmonary haemodynamics for serial assessment of patients with pulmonary hypertension.

Finally, the techniques used in this research were heretofore observational. Serial assessment of patients using Exercise CMR +/- CPET, validated with simultaneous right heart catheterisation in pulmonary hypertension patients, both before and after treatment targeted to the cause of exercise limitation, would identify if the technique could be used for serial, non-invasive, assessment of such patients.

15. PUBLICATIONS

15.1 Publications Arising from Research Fellowship

1. **Brown JT**, Kotecha T, Steeden JA, Fontana M, Denton CP, Coghlan JG, Knight DS, Muthurangu. Reduced exercise capacity in patients with systemic sclerosis is associated with lower peak tissue oxygen extraction: a cardiovascular magnetic resonance-augmented cardiopulmonary exercise study. Journal of Cardiovascular Magnetic Resonance. 2021 Oct 28;23(1):118
2. **Brown JT,** Saigal A, Karia N, Patel RK, Razvi Y, Constantinou N, Steeden JA, Mandal S, Kotecha T, Fontana M, Goldring J, Muthurangu V, Knight DS. Ongoing Exercise Intolerance Following COVID-19: A Magnetic Resonance-Augmented Cardiopulmonary Exercise Test Study. Journal of the American Heart Association. 2022 May 3;11(9)
3. **Brown JT,** Virsinskaite R, Kotecha T, Steeden JA, Fontana M, Karia N, Schreiber BE, Ong VH, Denton CP, Coghlan JG, Muthurangu V, Knight DS. Prognostic utility of exercise cardiovascular magnetic resonance in patients with systemic sclerosis-associated pulmonary arterial hypertension. European Heart Journal – Cardiovascular Imaging. 2024 Aug 19;00, 1-9
4. Patel RK, Ioannou A, Razvi Y, Chacko L, Venneri L, Bandera F, Knight D, Kotecha T, Martinez-Naharro A, Masi A, Porcari A, **Brown J,** Patel K, Manisty C, Moon J, Rowczenio D, Gilbertson JA, Sinagra G, Lachmann H, Wechalekar A, Petrie A, Whelan C, Hawkins PN, Gillmore JD, Fontana. Sex differences among patients with transthyretin amyloid cardiomyopathy - from diagnosis to prognosis. European Journal of Heart Failure. 2022 Dec;24(12):2355-2363

5. Jaubert O, Montalt-Tordera J, **Brown J,** Knight D, Arridge S, Steeden J, Muthurangu V. FReSCO: Flow Reconstruction and Segmentation for low-latency Cardiac Output monitoring using deep artifact suppression and segmentation. Magnetic Resonance in Medicine. 2022 Nov;88(5):2179-2189
6. Ioannou A, Patel RK, Razvi Y, Porcari A, Sinagra G, Venneri L, Bandera F, Masi A, Williams GE, O'Beara S, Ganesananthan S, Massa P, Knight D, Martinez-Naharro A, Kotecha T, Chacko L, **Brown J,** Rauf MU, Manisty C, Moon J, Lachmann H, Wechelakar A, Petrie A, Whelan C, Hawkins PN, Gillmore JD, Fontana M. Impact of Earlier Diagnosis in Cardiac ATTR Amyloidosis Over the Course of 20 Years. Circulation. 2022 Nov 29;146(22):1657-1670
7. Chacko L, Karia N, Venneri L, Bandera F, Passo BD, Buonamici L, Lazari J, Ioannou A, Porcari A, Patel R, Razvi Y, **Brown J,** Knight D, Martinez-Naharro A, Whelan C, Quarta CC, Manisty C, Moon J, Rowczenio D, Gilbertson JA, Lachmann H, Wechelakar A, Petrie A, Moody WE, Steeds RP, Potena L, Riefolo M, Leone O, Rapezzi C, Hawkins PN, Gillmore JD, Fontana M. Progression of echocardiographic parameters and prognosis in transthyretin cardiac amyloidosis. European Journal of Heart Failure. 2022 Sep;24(9):1700-1712
8. Rosmini S, Seraphim A, Knott K, **Brown JT**, Knight DS, Zaman S, Cole G, Sado D, Captur G, Gomes AC, Zemrak F, Treibel TA, Cash L, Culotta V, O'Mahony C, Kellman P, Moon JC, Manisty. Non-invasive characterization of pleural and pericardial effusions using T1 mapping by magnetic resonance imaging. European Heart Journal Cardiovascular Imaging. 2022 Jul 21;23(8):1117-1126
9. Knight DS, Karia N, Cole AR, Maclean RH, **Brown JT**, Masi A, Patel RK, Razvi Y, Chacko L, Venneri L, Kotecha T, Martinez-Naharro A, Kellman P, Scott-Russell AM, Schreiber BE, Ong VH, Denton CP, Fontana M, Coghlan JG, Muthurangu V. Distinct

cardiovascular phenotypes are associated with prognosis in systemic sclerosis: a cardiovascular magnetic resonance study. European Heart Journal Cardiovascular Imaging. 2022 Jul 1

10. Bandera F, Martone R, Chacko L, Ganesananthan S, Gilbertson JA, Ponticos M, Lane T, Martinez-Naharro A, Whelan C, Quarta C, Rowczenio D, Patel R, Razvi Y, Lachmann H, Wechelakar A, **Brown J,** Knight D, Moon J, Petrie A, Cappelli F, Guazzi M, Potena L, Rapezzi C, Leone O, Hawkins PN, Gillmore JD, Fontana M. Clinical Importance of Left Atrial Infiltration in Cardiac Transthyretin Amyloidosis. Journal of the American College of Cardiology Cardiovasc Imaging. 2022 Jan;15(1):17-29
11. Thornton GD, Shetye A, Knight DS, Knott K, Artico J, Kurdi H, Yousef S, Antonakaki D, Razvi Y, Chacko L, **Brown J**, Patel R, Vimalesvaran K, Seraphim A, Davies R, Xue H, Kotecha T, Bell R, Manisty C, Cole GD, Moon JC, Kellman P, Fontana M, Treibel TA. Myocardial Perfusion Imaging After Severe COVID-19 Infection Demonstrates Regional Ischemia Rather Than Global Blood Flow Reduction. Cardiovascular Medicine. 2021 Dec 7;8:764599
12. Joy G, Artico J, Kurdi H, Seraphim A, Lau C, Thornton GD, Oliveira MF, Adam RD, Aziminia N, Menacho K, Chacko L, **Brown JT,** Patel RK, Shiwani H, Bhuva A, Augusto JB, Andiapen M, McKnight A, Noursadeghi M, Pierce I, Evain T, Captur G, Davies RH, Greenwood JP, Fontana M, Kellman P, Schelbert EB, Treibel TA, Manisty C, Moon JC; COVIDsortium Investigators. Prospective Case-Control Study of Cardiovascular Abnormalities 6 Months Following Mild COVID-19 in Healthcare Workers. JACC Cardiovasc Imaging. 2021 Nov;14(11):2155-2166
13. Kotecha T, Knight DS, Razvi Y, Kumar K, Vimalesvaran K, Thornton G, Patel R, Chacko L, **Brown JT**, Coyle C, Leith D, Shetye A, Ariff B, Bell R, Captur G, Coleman M, Goldring J, Gopalan D, Heightman M, Hillman T, Howard L, Jacobs M, Jeetley PS,

Kanagaratnam P, Kon OM, Lamb LE, Manisty CH, Mathurdas P, Mayet J, Negus R, Patel N, Pierce I, Russell G, Wolff A, Xue H, Kellman P, Moon JC, Treibel TA, Cole GD, Fontana. Patterns of myocardial injury in recovered troponin-positive COVID-19 patients assessed by cardiovascular magnetic resonance. European Heart Journal. 2021 May 14;42(19):1866-1878

14. Aimo A, Chubuchny V, Vergaro G, Barison A, Nicol M, Cohen-Solal A, Castiglione V, Spini V, Giannoni A, Petersen C, Taddei C, Pasanisi E, Chacko L, Martone R, Knight D, **Brown J,** Martinez-Naharro A, Passino C, Fontana M, Emdin M. A simple echocardiographic score to rule out cardiac amyloidosis. European Journal of Clinical Investigations. 2021 May;51(5)
15. Chacko L, Boldrini M, Martone R, Law S, Martinez-Naharrro A, Hutt DF, Kotecha T, Patel RK, Razvi Y, Rezk T, Cohen OC, **Brown JT**, Srikantharajah M, Ganesananthan S, Lane T, Lachmann HJ, Wechalekar AD, Sachchithanantham S, Mahmood S, Whelan CJ, Knight DS, Moon JC, Kellman P, Gillmore JD, Hawkins PN, Fontana M. Cardiac Magnetic Resonance-Derived Extracellular Volume Mapping for the Quantification of Hepatic and Splenic Amyloid. Circulation Cardiovascular Imaging. 2021 Apr 20:
16. Kotecha T, Monteagudo JM, Martinez-Naharro A, Chacko L, **Brown J,** Knight D, Knott KD, Hawkins P, Moon JC, Plein S, Xue H, Kellman P, Lockie T, Patel N, Rakhit R, Fontana M. Quantitative cardiovascular magnetic resonance myocardial perfusion mapping to assess hyperaemic response to adenosine stress. European Heart Journal Cardiovasc Imaging. 2021 Feb 22;22(3):273-281
17. Kotecha T, Chacko L, Chehab O, O'Reilly N, Martinez-Naharro A, Lazari J, Knott KD, Brown J, Knight D, Muthurangu V, Hawkins P, Plein S, Moon JC, Xue H, Kellman P, Rakhit R, Patel N, Fontana M. Assessment of Multivessel Coronary Artery Disease

Using Cardiovascular Magnetic Resonance Pixelwise Quantitative Perfusion Mapping. JACC Cardiovasc Imaging. 2020 Dec;13(12):2546-2557

18. Knight DS, Kotecha T, Martinez-Naharro A, **Brown JT**, Bertelli M, Fontana M, Muthurangu V, Coghlan JG. Cardiovascular magnetic resonance-guided right heart catheterization in a conventional CMR environment - predictors of procedure success and duration in pulmonary artery hypertension. Journal of Cardiovascular Magnetic Resonance. 2019 Sep 9;21(1):57

15.2 Presentations and Posters

1. **Poster:** Dark blood imaging: shedding light on myocardial disease. J. Brown, L. Chacko, A. Martinez-Naharro, T. Kotecha, A. Steriotis, H. Xue, P. Kellman, DS. Knight, M. Fontana. EuroCMR May 2019, Venice.
2. **Poster:** Subclinical myocardial abnormalities in systemic sclerosis-associated versus non-connective tissue disease pulmonary hypertension by CMR multiparametric mapping. .J Brown, K. Norrington, T. Kotecha, A. Martinez-Naharro, H. Fayed, L. Teresi, C. Denton, B. Schreiber, M. Fontana, P. Kellman, J. Coghlan, DS. Knight ESC Congress 2019, Paris.
3. **Poster:** Reduced peripheral tissue oxygen extraction in systemic sclerosis-associated pulmonary arterial hypertension demonstrated by MR-augmented CPET. J Brown, T Kotecha, M Fontana, C Denton, G Coghlan, J Steeden, D Knight, V Muthurangu. Society of Cardiovascular Magnetic Resonance, Orland USA 2020
4. **Oral Presentation:** Harnessing the potential of CMR-CPET in Scleroderma Associated Pulmonary Arterial Hypertension. National Pulmonary Hypertension Research Forum, November 2019.

16. BIBLIOGRAPHY

1. Kitzman DW, Groban L. Exercise intolerance. Heart Fail Clin. 2008;4(1):99-115.
2. McCoy J, Bates M, Eggett C, Siervo M, Cassidy S, Newman J, et al. Pathophysiology of exercise intolerance in chronic diseases: the role of diminished cardiac performance in mitochondrial and heart failure patients. Open Heart. 2017;4(2):e000632.
3. Del Buono MG, Arena R, Borlaug BA, Carbone S, Canada JM, Kirkman DL, et al. Exercise Intolerance in Patients With Heart Failure: JACC State-of-the-Art Review. J Am Coll Cardiol. 2019;73(17):2209-25.
4. Babu AS, Arena R, Myers J, Padmakumar R, Maiya AG, Cahalin LP, et al. Exercise intolerance in pulmonary hypertension: mechanism, evaluation and clinical implications. Expert Rev Respir Med. 2016;10(9):979-90.
5. Alvarez P, Hannawi B, Guha A. Exercise And Heart Failure: Advancing Knowledge And Improving Care. Methodist Debakey Cardiovasc J. 2016;12(2):110-5.
6. Bol E, de Vries WR, Mosterd WL, Wielenga RP, Coats AJ. Cardiopulmonary exercise parameters in relation to all-cause mortality in patients with chronic heart failure. Int J Cardiol. 2000;72(3):255-63.
7. Badagliacca R, Papa S, Poscia R, Valli G, Pezzuto B, Manzi G, et al. The added value of cardiopulmonary exercise testing in the follow-up of pulmonary arterial hypertension. J Heart Lung Transplant. 2019;38(3):306-14.
8. Deboeck G, Scoditti C, Huez S, Vachiéry JL, Lamotte M, Sharples L, et al. Exercise testing to predict outcome in idiopathic versus associated pulmonary arterial hypertension. Eur Respir J. 2012;40(6):1410-9.
9. Wensel R, Francis DP, Meyer FJ, Opitz CF, Bruch L, Halank M, et al. Incremental prognostic value of cardiopulmonary exercise testing and resting haemodynamics in pulmonary arterial hypertension. Int J Cardiol. 2013;167(4):1193-8.
10. Guazzi M, Cahalin LP, Arena R. Cardiopulmonary exercise testing as a diagnostic tool for the detection of left-sided pulmonary hypertension in heart failure. J Card Fail. 2013;19(7):461-7.
11. Arnold JMO, Liu P, Howlett J, Ignaszewski A, Leblanc M-H, Kaan A, et al. Ten year survival by NYHA functional class in heart failure outpatients referred to specialized multidisciplinary heart failure clinics 1999 to 2011. European Heart Journal. 2013;34(suppl_1).
12. Kim NH, Fisher M, Poch D, Zhao C, Shah M, Bartolome S. Long-term outcomes in pulmonary arterial hypertension by functional class: a meta-analysis of randomized controlled trials and observational registries. Pulmonary Circulation. 2020;10(4):2045894020935291.
13. Arena R, Myers J, Williams MA, Gulati M, Kligfield P, Balady GJ, et al. Assessment of Functional Capacity in Clinical and Research Settings. Circulation. 2007;116(3):329-43.
14. Dolgin M, Committee NYHAC. Nomenclature and Criteria for Diagnosis of Diseases of the Heart and Great Vessels: Little, Brown; 1994.
15. Kubo SH, Schulman SP, Starling RC, Jessup M, Wentworth D, Burkhoff D. Development and validation of a patient questionnaire to determine New York Heart Association classification. Journal of cardiac failure. 2004;10 3:228-35.
16. Agarwala P, Salzman SH. Six-Minute Walk Test: Clinical Role, Technique, Coding, and Reimbursement. Chest. 2020;157(3):603-11.

17. Chapter 5 - Macromolecular Assembly. In: Pollard TD, Earnshaw WC, Lippincott-Schwartz J, Johnson GT, editors. Cell Biology (Third Edition): Elsevier; 2017. p. 63-74.
18. Guzmán Mentesana G, Báez AL, Lo Presti MS, Domínguez R, Córdoba R, Bazán C, et al. Functional and structural alterations of cardiac and skeletal muscle mitochondria in heart failure patients. Arch Med Res. 2014;45(3):237-46.
19. Murray AJ, Edwards LM, Clarke K. Mitochondria and heart failure. Curr Opin Clin Nutr Metab Care. 2007;10(6):704-11.
20. Pereira M, Matuszewska K, Glogova A, Petrik J. Mutant p53, the Mevalonate Pathway and the Tumor Microenvironment Regulate Tumor Response to Statin Therapy. Cancers (Basel). 2022;14(14).
21. Higginbotham MB, Morris KG, Williams RS, McHale PA, Coleman RE, Cobb FR. Regulation of stroke volume during submaximal and maximal upright exercise in normal man. Circ Res. 1986;58(2):281-91.
22. Sullivan MJ, Cobb FR, Higginbotham MB. Stroke volume increases by similar mechanisms during upright exercise in normal men and women. Am J Cardiol. 1991;67(16):1405-12.
23. Åstrand P-O, Rodahl K, Dahl HA, Strømme SB, Allen TJ. Textbook of Work Physiology: Physiological Bases of Exercise, Fourth Edition. Physiotherapy Canada. 2003;56:248.
24. Wasserman K, Hansen JE, Sue DY, Whipp BJ, Froelicher VF. Principles of exercise testing and interpretation. Journal of Cardiopulmonary Rehabilitation and Prevention. 1987;7(4):189.
25. Md MA, Parrott CF, Ph DM, Ph DP, Md FY, Md BU. Skeletal muscle abnormalities in heart failure with preserved ejection fraction. Heart Fail Rev. 2022.
26. Ommen SR, Nishimura RA, Appleton CP, Miller FA, Oh JK, Redfield MM, et al. Clinical utility of Doppler echocardiography and tissue Doppler imaging in the estimation of left ventricular filling pressures: A comparative simultaneous Doppler-catheterization study. Circulation. 2000;102(15):1788-94.
27. Skaluba SJ, Litwin SE. Mechanisms of exercise intolerance: insights from tissue Doppler imaging. Circulation. 2004;109(8):972-7.
28. Hadano Y, Murata K, Yamamoto T, Kunichika H, Matsumoto T, Akagawa E, et al. Usefulness of mitral annular velocity in predicting exercise tolerance in patients with impaired left ventricular systolic function. Am J Cardiol. 2006;97(7):1025-8.
29. Ha JW, Oh JK, Pellikka PA, Ommen SR, Stussy VL, Bailey KR, et al. Diastolic stress echocardiography: a novel noninvasive diagnostic test for diastolic dysfunction using supine bicycle exercise Doppler echocardiography. J Am Soc Echocardiogr. 2005;18(1):63-8.
30. Troughton R, Michael Felker G, Januzzi JL, Jr. Natriuretic peptide-guided heart failure management. Eur Heart J. 2014;35(1):16-24.
31. Boucly A, Weatherald J, Savale L, Jaïs X, Cottin V, Prevot G, et al. Risk assessment, prognosis and guideline implementation in pulmonary arterial hypertension. Eur Respir J. 2017;50(2).
32. Guyatt GH, Thompson PJ, Berman LB, Sullivan MJ, Townsend M, Jones NL, et al. How should we measure function in patients with chronic heart and lung disease? J Chronic Dis. 1985;38(6):517-24.
33. Cahalin L, Pappagianopoulos P, Prevost S, Wain J, Ginns L. The relationship of the 6-min walk test to maximal oxygen consumption in transplant candidates with end-stage lung disease. Chest. 1995;108(2):452-9.

34. ATS Statement. American Journal of Respiratory and Critical Care Medicine. 2002;166(1):111-7.
35. Chambers DJ, Wisely NA. Cardiopulmonary exercise testing-a beginner's guide to the nine-panel plot. BJA Educ. 2019;19(5):158-64.
36. Albouaini K, Egred M, Alahmar A, Wright DJ. Cardiopulmonary exercise testing and its application. Postgrad Med J. 2007;83(985):675-82.
37. Mancini DM, Eisen H, Kussmaul W, Mull R, Edmunds LH, Jr., Wilson JR. Value of peak exercise oxygen consumption for optimal timing of cardiac transplantation in ambulatory patients with heart failure. Circulation. 1991;83(3):778-86.
38. Chaudhry S, Kumar N, Behbahani H, Bagai A, Singh BK, Menasco N, et al. Abnormal heart-rate response during cardiopulmonary exercise testing identifies cardiac dysfunction in symptomatic patients with non-obstructive coronary artery disease. Int J Cardiol. 2017;228:114-21.
39. Barber NJ, Ako EO, Kowalik GT, Cheang MH, Pandya B, Steeden JA, et al. Magnetic Resonance-Augmented Cardiopulmonary Exercise Testing: Comprehensively Assessing Exercise Intolerance in Children With Cardiovascular Disease. Circ Cardiovasc Imaging. 2016;9(12).
40. Bandera F, Generati G, Pellegrino M, Garatti A, Labate V, Alfonzetti E, et al. Mitral regurgitation in heart failure: insights from CPET combined with exercise echocardiography. Eur Heart J Cardiovasc Imaging. 2017;18(3):296-303.
41. Coats CJ, Rantell K, Bartnik A, Patel A, Mist B, McKenna WJ, et al. Cardiopulmonary Exercise Testing and Prognosis in Hypertrophic Cardiomyopathy. Circ Heart Fail. 2015;8(6):1022-31.
42. Charalampopoulos A, Gibbs JS, Davies RJ, Gin-Sing W, Murphy K, Sheares KK, et al. Exercise physiological responses to drug treatments in chronic thromboembolic pulmonary hypertension. J Appl Physiol (1985). 2016;121(3):623-8.
43. Francis DP, Shamim W, Davies LC, Piepoli MF, Ponikowski P, Anker SD, et al. Cardiopulmonary exercise testing for prognosis in chronic heart failure: continuous and independent prognostic value from VE/VCO(2)slope and peak VO(2). Eur Heart J. 2000;21(2):154-61.
44. Milani RV, Lavie CJ, Mehra MR, Ventura HO. Understanding the basics of cardiopulmonary exercise testing. Mayo Clin Proc. 2006;81(12):1603-11.
45. Neuberg GW, Friedman SH, Weiss MB, Herman MV. Cardiopulmonary Exercise Testing: The Clinical Value of Gas Exchange Data. Archives of Internal Medicine. 1988;148(10):2221-6.
46. Huang W, Resch S, Oliveira RK, Cockrill BA, Systrom DM, Waxman AB. Invasive cardiopulmonary exercise testing in the evaluation of unexplained dyspnea: Insights from a multidisciplinary dyspnea center. Eur J Prev Cardiol. 2017;24(11):1190-9.
47. Berry NC, Manyoo A, Oldham WM, Stephens TE, Goldstein RH, Waxman AB, et al. Protocol for exercise hemodynamic assessment: performing an invasive cardiopulmonary exercise test in clinical practice. Pulm Circ. 2015;5(4):610-8.
48. Guazzi M, Bandera F, Ozemek C, Systrom D, Arena R. Cardiopulmonary Exercise Testing: What Is its Value? J Am Coll Cardiol. 2017;70(13):1618-36.
49. Pugliese NR, Fabiani I, Santini C, Rovai I, Pedrinelli R, Natali A, et al. Value of combined cardiopulmonary and echocardiography stress test to characterize the haemodynamic and metabolic responses of patients with heart failure and mid-range ejection fraction. European Heart Journal - Cardiovascular Imaging. 2019;20(7):828-36.

50. Guazzi M, Villani S, Generati G, Ferraro OE, Pellegrino M, Alfonzetti E, et al. Right Ventricular Contractile Reserve and Pulmonary Circulation Uncoupling During Exercise Challenge in Heart Failure: Pathophysiology and Clinical Phenotypes. JACC Heart Fail. 2016;4(8):625-35.
51. Nagueh SF, Mikati I, Kopelen HA, Middleton KJ, Quiñones MA, Zoghbi WA. Doppler estimation of left ventricular filling pressure in sinus tachycardia. A new application of tissue doppler imaging. Circulation. 1998;98(16):1644-50.
52. Bellenger NG, Burgess MI, Ray SG, Lahiri A, Coats AJ, Cleland JG, et al. Comparison of left ventricular ejection fraction and volumes in heart failure by echocardiography, radionuclide ventriculography and cardiovascular magnetic resonance; are they interchangeable? Eur Heart J. 2000;21(16):1387-96.
53. Foster EL, Arnold JW, Jekic M, Bender JA, Balasubramanian V, Thavendiranathan P, et al. MR-compatible treadmill for exercise stress cardiac magnetic resonance imaging. Magn Reson Med. 2012;67(3):880-9.
54. Jekic M, Foster EL, Ballinger MR, Raman SV, Simonetti OP. Cardiac function and myocardial perfusion immediately following maximal treadmill exercise inside the MRI room. J Cardiovasc Magn Reson. 2008;10(1):3.
55. Niezen RA, Doornbos J, van der Wall EE, de Roos A. Measurement of aortic and pulmonary flow with MRI at rest and during physical exercise. J Comput Assist Tomogr. 1998;22(2):194-201.
56. La Gerche A, Claessen G, Van de Bruaene A, Pattyn N, Van Cleemput J, Gewillig M, et al. Cardiac MRI: a new gold standard for ventricular volume quantification during high-intensity exercise. Circ Cardiovasc Imaging. 2013;6(2):329-38.
57. Lurz P, Muthurangu V, Schievano S, Nordmeyer J, Bonhoeffer P, Taylor AM, et al. Feasibility and reproducibility of biventricular volumetric assessment of cardiac function during exercise using real-time radial k-t SENSE magnetic resonance imaging. J Magn Reson Imaging. 2009;29(5):1062-70.
58. Barber NJ, Ako EO, Kowalik GT, Steeden JA, Pandya B, Muthurangu V. MR augmented cardiopulmonary exercise testing-a novel approach to assessing cardiovascular function. Physiol Meas. 2015;36(5):N85-94.
59. Ako EO, Barber N, Kowalik GT, Steeden J, Muthurangu V. MR augmented cardiopulmonary exercise testing - a novel method of assessing cardiovascular function. Journal of Cardiovascular Magnetic Resonance. 2015;17(1):Q2.
60. Galiè N, Humbert M, Vachiery J-L, Gibbs S, Lang I, Torbicki A, et al. 2015 ESC/ERS Guidelines for the diagnosis and treatment of pulmonary hypertension: The Joint Task Force for the Diagnosis and Treatment of Pulmonary Hypertension of the European Society of Cardiology (ESC) and the European Respiratory Society (ERS): Endorsed by: Association for European Paediatric and Congenital Cardiology (AEPC), International Society for Heart and Lung Transplantation (ISHLT). European Heart Journal. 2015;37(1):67-119.
61. Condon DF, Nickel NP, Anderson R, Mirza S, de Jesus Perez VA. The 6th World Symposium on Pulmonary Hypertension: what's old is new. F1000Res. 2019;8.
62. Humbert M, Kovacs G, Hoeper MM, Badagliacca R, Berger RMF, Brida M, et al. 2022 ESC/ERS Guidelines for the diagnosis and treatment of pulmonary hypertension. European Respiratory Journal. 2022:2200879.
63. Hoeper MM, Humbert M, Souza R, Idrees M, Kawut SM, Sliwa-Hahnle K, et al. A global view of pulmonary hypertension. Lancet Respir Med. 2016;4(4):306-22.

64. Frost A, Badesch D, Gibbs JSR, Gopalan D, Khanna D, Manes A, et al. Diagnosis of pulmonary hypertension. Eur Respir J. 2019;53(1).
65. Rich S, Dantzker DR, Ayres SM, Bergofsky EH, Brundage BH, Detre KM, et al. Primary pulmonary hypertension. A national prospective study. Ann Intern Med. 1987;107(2):216-23.
66. Frost AE, Badesch DB, Barst RJ, Benza RL, Elliott CG, Farber HW, et al. The changing picture of patients with pulmonary arterial hypertension in the United States: how REVEAL differs from historic and non-US Contemporary Registries. Chest. 2011;139(1):128-37.
67. Hoeper MM, Pausch C, Grünig E, Staehler G, Huscher D, Pittrow D, et al. Temporal trends in pulmonary arterial hypertension: results from the COMPERA registry. Eur Respir J. 2022;59(6).
68. van den Hoogen F, Khanna D, Fransen J, Johnson SR, Baron M, Tyndall A, et al. 2013 classification criteria for systemic sclerosis: an American College of Rheumatology/European League against Rheumatism collaborative initiative. Arthritis Rheum. 2013;65(11):2737-47.
69. Denton CP, Khanna D. Systemic sclerosis. Lancet. 2017;390(10103):1685-99.
70. Elhai M, Meune C, Avouac J, Kahan A, Allanore Y. Trends in mortality in patients with systemic sclerosis over 40 years: a systematic review and meta-analysis of cohort studies. Rheumatology (Oxford). 2012;51(6):1017-26.
71. Solomon JJ, Olson AL, Fischer A, Bull T, Brown KK, Raghu G. Scleroderma lung disease. Eur Respir Rev. 2013;22(127):6-19.
72. Avouac J, Airò P, Meune C, Beretta L, Dieude P, Caramaschi P, et al. Prevalence of pulmonary hypertension in systemic sclerosis in European Caucasians and metaanalysis of 5 studies. J Rheumatol. 2010;37(11):2290-8.
73. Phung S, Strange G, Chung LP, Leong J, Dalton B, Roddy J, et al. Prevalence of pulmonary arterial hypertension in an Australian scleroderma population: screening allows for earlier diagnosis. Intern Med J. 2009;39(10):682-91.
74. Kahan A, Coghlan G, McLaughlin V. Cardiac complications of systemic sclerosis. Rheumatology (Oxford). 2009;48 Suppl 3:iii45-8.
75. Coghlan JG, Denton CP, Grünig E, Bonderman D, Distler O, Khanna D, et al. Evidence-based detection of pulmonary arterial hypertension in systemic sclerosis: the DETECT study. Ann Rheum Dis. 2014;73(7):1340-9.
76. Launay D, Sobanski V, Hachulla E, Humbert M. Pulmonary hypertension in systemic sclerosis: different phenotypes. Eur Respir Rev. 2017;26(145).
77. Boutou AK, Pitsiou GG, Siakka P, Dimitroulas T, Paspala A, Sourla E, et al. Phenotyping Exercise Limitation in Systemic Sclerosis: The Use of Cardiopulmonary Exercise Testing. Respiration. 2016;91(2):115-23.
78. Dumitrescu D, Nagel C, Kovacs G, Bollmann T, Halank M, Winkler J, et al. Cardiopulmonary exercise testing for detecting pulmonary arterial hypertension in systemic sclerosis. Heart. 2017;103(10):774-82.
79. Groepenhoff H, Vonk-Noordegraaf A, Boonstra A, Spreeuwenberg MD, Postmus PE, Bogaard HJ. Exercise testing to estimate survival in pulmonary hypertension. Med Sci Sports Exerc. 2008;40(10):1725-32.
80. Carfì A, Bernabei R, Landi F. Persistent Symptoms in Patients After Acute COVID-19. Jama. 2020;324(6):603-5.
81. Nehme M, Braillard O, Alcoba G, Aebischer Perone S, Courvoisier D, Chappuis F, et al. COVID-19 Symptoms: Longitudinal Evolution and Persistence in Outpatient Settings. Ann Intern Med. 2021;174(5):723-5.

82. Chopra V, Flanders SA, O'Malley M, Malani AN, Prescott HC. Sixty-Day Outcomes Among Patients Hospitalized With COVID-19. Ann Intern Med. 2021;174(4):576-8.
83. Plein S, Greenwood J, Ridgway JP. Cardiovascular MR manual. 2nd ed. ed. Cham: Springer International Publishing; 2015.
84. Caroff J, Bière L, Trebuchet G, Nedelcu C, Sibileau E, Beregi JP, et al. Applications of phase-contrast velocimetry sequences in cardiovascular imaging. Diagnostic and Interventional Imaging. 2012;93(3):159-70.
85. Kowalik GT, Knight D, Steeden JA, Muthurangu V. Perturbed spiral real-time phase-contrast MR with compressive sensing reconstruction for assessment of flow in children. Magn Reson Med. 2020;83(6):2077-91.
86. Steeden JA, Kowalik GT, Tann O, Hughes M, Mortensen KH, Muthurangu V. Real-time assessment of right and left ventricular volumes and function in children using high spatiotemporal resolution spiral bSSFP with compressed sensing. J Cardiovasc Magn Reson. 2018;20(1):79.
87. Schulz-Menger J, Bluemke DA, Bremerich J, Flamm SD, Fogel MA, Friedrich MG, et al. Standardized image interpretation and post-processing in cardiovascular magnetic resonance - 2020 update : Society for Cardiovascular Magnetic Resonance (SCMR): Board of Trustees Task Force on Standardized Post-Processing. J Cardiovasc Magn Reson. 2020;22(1):19.
88. Kawel-Boehm N, Hetzel SJ, Ambale-Venkatesh B, Captur G, Francois CJ, Jerosch-Herold M, et al. Reference ranges ("normal values") for cardiovascular magnetic resonance (CMR) in adults and children: 2020 update. J Cardiovasc Magn Reson. 2020;22(1):87.
89. Kelemen BW, Mathai SC, Tedford RJ, Damico RL, Corona-Villalobos C, Kolb TM, et al. Right ventricular remodeling in idiopathic and scleroderma-associated pulmonary arterial hypertension: two distinct phenotypes. Pulm Circ. 2015;5(2):327-34.
90. Kawel-Boehm N, Maceira A, Valsangiacomo-Buechel ER, Vogel-Claussen J, Turkbey EB, Williams R, et al. Normal values for cardiovascular magnetic resonance in adults and children. J Cardiovasc Magn Reson. 2015;17(1):29.
91. Tamir JI, Ong F, Cheng JY, Uecker M, Lustig M, editors. Generalized magnetic resonance image reconstruction using the Berkeley advanced reconstruction toolbox.
92. Partovi S, Schulte AC, Aschwanden M, Staub D, Benz D, Imfeld S, et al. Impaired skeletal muscle microcirculation in systemic sclerosis. Arthritis Res Ther. 2012;14(5):R209.
93. Mottram RF. The interrelationship of blood flow, oxygen utilization of blood and oxygen consumption of human skeletal muscle. J Physiol. 1958;142(2):314-22.
94. Kramer CM, Barkhausen J, Bucciarelli-Ducci C, Flamm SD, Kim RJ, Nagel E. Standardized cardiovascular magnetic resonance imaging (CMR) protocols: 2020 update. J Cardiovasc Magn Reson. 2020;22(1):17.
95. Messroghli DR, Moon JC, Ferreira VM, Grosse-Wortmann L, He T, Kellman P, et al. Clinical recommendations for cardiovascular magnetic resonance mapping of T1, T2, T2* and extracellular volume: A consensus statement by the Society for Cardiovascular Magnetic Resonance (SCMR) endorsed by the European Association for Cardiovascular Imaging (EACVI). Journal of Cardiovascular Magnetic Resonance. 2017;19(1):75.
96. Muthurangu V, Lurz P, Critchely JD, Deanfield JE, Taylor AM, Hansen MS. Real-time assessment of right and left ventricular volumes and function in patients with congenital heart disease by using high spatiotemporal resolution radial k-t SENSE. Radiology. 2008;248(3):782-91.

97. Odille F, Steeden JA, Muthurangu V, Atkinson D. Automatic segmentation propagation of the aorta in real-time phase contrast MRI using nonrigid registration. J Magn Reson Imaging. 2011;33(1):232-8.
98. Rosset A, Spadola L, Ratib O. OsiriX: an open-source software for navigating in multidimensional DICOM images. J Digit Imaging. 2004;17(3):205-16.
99. Cuomo G, Santoriello C, Polverino F, Ruocco L, Valentini G, Polverino M. Impaired exercise performance in systemic sclerosis and its clinical correlations. Scand J Rheumatol. 2010;39(4):330-5.
100. Owens GR, Follansbee WP. Cardiopulmonary manifestations of systemic sclerosis. Chest. 1987;91(1):118-27.
101. Condliffe R, Kiely DG, Peacock AJ, Corris PA, Gibbs JS, Vrapi F, et al. Connective tissue disease-associated pulmonary arterial hypertension in the modern treatment era. Am J Respir Crit Care Med. 2009;179(2):151-7.
102. Borlaug BA. Mechanisms of exercise intolerance in heart failure with preserved ejection fraction. Circ J. 2014;78(1):20-32.
103. Siegert E, March C, Otten L, Makowka A, Preis E, Buttgereit F, et al. Prevalence of sarcopenia in systemic sclerosis: assessing body composition and functional disability in patients with systemic sclerosis. Nutrition. 2018;55-56:51-5.
104. Abdulle AE, Diercks GFH, Feelisch M, Mulder DJ, van Goor H. The Role of Oxidative Stress in the Development of Systemic Sclerosis Related Vasculopathy. Front Physiol. 2018;9:1177.
105. Corallo C, Fioravanti A, Tenti S, Pecetti G, Nuti R, Giordano N. Sarcopenia in systemic sclerosis: the impact of nutritional, clinical, and laboratory features. Rheumatol Int. 2019;39(10):1767-75.
106. Bueno M, Papazoglou A, Valenzi E, Rojas M, Lafyatis R, Mora AL. Mitochondria, Aging, and Cellular Senescence: Implications for Scleroderma. Curr Rheumatol Rep. 2020;22(8):37.
107. Gregg SG, Willis WT, Brooks GA. Interactive effects of anemia and muscle oxidative capacity on exercise endurance. J Appl Physiol (1985). 1989;67(2):765-70.
108. Skattebo Ø, Calbet JAL, Rud B, Capelli C, Hallén J. Contribution of oxygen extraction fraction to maximal oxygen uptake in healthy young men. Acta Physiol (Oxf). 2020;230(2):e13486.
109. Howard L, He J, Watson GMJ, Huang L, Wharton J, Luo Q, et al. Supplementation with Iron in Pulmonary Arterial Hypertension. Two Randomized Crossover Trials. Ann Am Thorac Soc. 2021;18(6):981-8.
110. Papadaki HA, Kritikos HD, Valatas V, Boumpas DT, Eliopoulos GD. Anemia of chronic disease in rheumatoid arthritis is associated with increased apoptosis of bone marrow erythroid cells: improvement following anti-tumor necrosis factor-alpha antibody therapy. Blood. 2002;100(2):474-82.
111. Doyle MK, Rahman MU, Han C, Han J, Giles J, Bingham CO, 3rd, et al. Treatment with infliximab plus methotrexate improves anemia in patients with rheumatoid arthritis independent of improvement in other clinical outcome measures-a pooled analysis from three large, multicenter, double-blind, randomized clinical trials. Semin Arthritis Rheum. 2009;39(2):123-31.
112. "An official European Respiratory Society statement: pulmonary haemodynamics during exercise." Gabor Kovacs, Philippe Herve, Joan Albert Barbera, Ari Chaouat, Denis Chemla, Robin Condliffe, Gilles Garcia, Ekkehard Grunig, Luke Howard, Marc Humbert,

Edmund Lau, Pierantonio Laveneziana, Gregory D. Lewis, Robert Naeije, Andrew Peacock, Stephan Rosenkranz, Rajeev Saggar, Silvia Ulrich, Dario Vizza, Anton Vonk Noordegraaf and Horst Olschewski. Eur Respir J 2017; 50: 1700578. Eur Respir J. 2018;51(1).
113. Raj DS. Role of interleukin-6 in the anemia of chronic disease. Semin Arthritis Rheum. 2009;38(5):382-8.
114. Houston BA, Tedford RJ. Stressing the stepchild: assessing right ventricular contractile reserve in pulmonary arterial hypertension. Eur Respir J. 2015;45(3):604-7.
115. Blumberg FC, Arzt M, Lange T, Schroll S, Pfeifer M, Wensel R. Impact of right ventricular reserve on exercise capacity and survival in patients with pulmonary hypertension. Eur J Heart Fail. 2013;15(7):771-5.
116. Hsu S, Houston BA, Tampakakis E, Bacher AC, Rhodes PS, Mathai SC, et al. Right Ventricular Functional Reserve in Pulmonary Arterial Hypertension. Circulation. 2016;133(24):2413-22.
117. Ghuysen A, Lambermont B, Kolh P, Tchana-Sato V, Magis D, Gerard P, et al. Alteration of right ventricular-pulmonary vascular coupling in a porcine model of progressive pressure overloading. Shock. 2008;29(2):197-204.
118. Maeder MT, Karapanagiotidis S, Dewar EM, Kaye DM. Accuracy of Echocardiographic Cardiac Index Assessment in Subjects with Preserved Left Ventricular Ejection Fraction. Echocardiography. 2015;32(11):1628-38.
119. Raman B, Cassar MP, Tunnicliffe EM, Filippini N, Griffanti L, Alfaro-Almagro F, et al. Medium-term effects of SARS-CoV-2 infection on multiple vital organs, exercise capacity, cognition, quality of life and mental health, post-hospital discharge. EClinicalMedicine. 2021;31:100683.
120. Huang C, Huang L, Wang Y, Li X, Ren L, Gu X, et al. 6-month consequences of COVID-19 in patients discharged from hospital: a cohort study. Lancet. 2021;397(10270):220-32.
121. Kotecha T, Knight DS, Razvi Y, Kumar K, Vimalesvaran K, Thornton G, et al. Patterns of myocardial injury in recovered troponin-positive COVID-19 patients assessed by cardiovascular magnetic resonance. Eur Heart J. 2021;42(19):1866-78.
122. Poissy J, Goutay J, Caplan M, Parmentier E, Duburcq T, Lassalle F, et al. Pulmonary Embolism in Patients With COVID-19: Awareness of an Increased Prevalence. Circulation. 2020;142(2):184-6.
123. Nalbandian A, Sehgal K, Gupta A, Madhavan MV, McGroder C, Stevens JS, et al. Post-acute COVID-19 syndrome. Nat Med. 2021;27(4):601-15.
124. Lam GY, Befus AD, Damant RW, Ferrara G, Fuhr DP, Stickland MK, et al. Exertional intolerance and dyspnea with preserved lung function: an emerging long COVID phenotype? Respir Res. 2021;22(1):222.
125. Brown JT, Kotecha T, Steeden JA, Fontana M, Denton CP, Coghlan JG, et al. Reduced exercise capacity in patients with systemic sclerosis is associated with lower peak tissue oxygen extraction: a cardiovascular magnetic resonance-augmented cardiopulmonary exercise study. J Cardiovasc Magn Reson. 2021;23(1):118.
126. Kellman P, Hansen MS. T1-mapping in the heart: accuracy and precision. J Cardiovasc Magn Reson. 2014;16(1):2.
127. Giri S, Chung YC, Merchant A, Mihai G, Rajagopalan S, Raman SV, et al. T2 quantification for improved detection of myocardial edema. J Cardiovasc Magn Reson. 2009;11(1):56.
128. Dong E, Du H, Gardner L. An interactive web-based dashboard to track COVID-19 in real time. Lancet Infect Dis. 2020;20(5):533-4.

129. Singh I, Joseph P, Heerdt PM, Cullinan M, Lutchmansingh DD, Gulati M, et al. Persistent Exertional Intolerance After COVID-19: Insights From Invasive Cardiopulmonary Exercise Testing. Chest. 2022;161(1):54-63.
130. Joseph P, Arevalo C, Oliveira RKF, Faria-Urbina M, Felsenstein D, Oaklander AL, et al. Insights From Invasive Cardiopulmonary Exercise Testing of Patients With Myalgic Encephalomyelitis/Chronic Fatigue Syndrome. Chest. 2021;160(2):642-51.
131. Goulding RP, Okushima D, Fukuoka Y, Marwood S, Kondo N, Poole DC, et al. Impact of supine versus upright exercise on muscle deoxygenation heterogeneity during ramp incremental cycling is site specific. Eur J Appl Physiol. 2021;121(5):1283-96.
132. Wehrle A, Waibel S, Gollhofer A, Roecker K. Power Output and Efficiency During Supine, Recumbent, and Upright Cycle Ergometry. Front Sports Act Living. 2021;3:667564.
133. Kim JY, Han K, Suh YJ. Prevalence of abnormal cardiovascular magnetic resonance findings in recovered patients from COVID-19: a systematic review and meta-analysis. J Cardiovasc Magn Reson. 2021;23(1):100.
134. Oldham WM, Lewis GD, Opotowsky AR, Waxman AB, Systrom DM. Unexplained exertional dyspnea caused by low ventricular filling pressures: results from clinical invasive cardiopulmonary exercise testing. Pulm Circ. 2016;6(1):55-62.
135. Hurwitz BE, Coryell VT, Parker M, Martin P, Laperriere A, Klimas NG, et al. Chronic fatigue syndrome: illness severity, sedentary lifestyle, blood volume and evidence of diminished cardiac function. Clin Sci (Lond). 2009;118(2):125-35.
136. Newton JL, Finkelmeyer A, Petrides G, Frith J, Hodgson T, Maclachlan L, et al. Reduced cardiac volumes in chronic fatigue syndrome associate with plasma volume but not length of disease: a cohort study. Open Heart. 2016;3(1):e000381.
137. Miwa K. Down-regulation of renin-aldosterone and antidiuretic hormone systems in patients with myalgic encephalomyelitis/chronic fatigue syndrome. J Cardiol. 2017;69(4):684-8.
138. Natelson BH, Brunjes DL, Mancini D. Chronic Fatigue Syndrome and Cardiovascular Disease: JACC State-of-the-Art Review. J Am Coll Cardiol. 2021;78(10):1056-67.
139. Barizien N, Le Guen M, Russel S, Touche P, Huang F, Vallée A. Clinical characterization of dysautonomia in long COVID-19 patients. Sci Rep. 2021;11(1):14042.
140. Becker RC. Autonomic dysfunction in SARS-COV-2 infection acute and long-term implications COVID-19 editor's page series. J Thromb Thrombolysis. 2021;52(3):692-707.
141. Rinaldo RF, Mondoni M, Parazzini EM, Baccelli A, Pitari F, Brambilla E, et al. Severity does not impact on exercise capacity in COVID-19 survivors. Respir Med. 2021;187:106577.
142. Vermersch M, Longère B, Coisne A, Schmidt M, Forman C, Monnet A, et al. Compressed sensing real-time cine imaging for assessment of ventricular function, volumes and mass in clinical practice. Eur Radiol. 2020;30(1):609-19.
143. Razavi R, Hill DL, Keevil SF, Miquel ME, Muthurangu V, Hegde S, et al. Cardiac catheterisation guided by MRI in children and adults with congenital heart disease. Lancet. 2003;362(9399):1877-82.
144. van de Veerdonk MC, Kind T, Marcus JT, Mauritz GJ, Heymans MW, Bogaard HJ, et al. Progressive right ventricular dysfunction in patients with pulmonary arterial hypertension responding to therapy. J Am Coll Cardiol. 2011;58(24):2511-9.
145. van Wolferen SA, Marcus JT, Boonstra A, Marques KM, Bronzwaer JG, Spreeuwenberg MD, et al. Prognostic value of right ventricular mass, volume, and function in idiopathic pulmonary arterial hypertension. Eur Heart J. 2007;28(10):1250-7.

146. Lewis RA, Johns CS, Cogliano M, Capener D, Tubman E, Elliot CA, et al. Identification of Cardiac Magnetic Resonance Imaging Thresholds for Risk Stratification in Pulmonary Arterial Hypertension. Am J Respir Crit Care Med. 2020;201(4):458-68.
147. Vonk Noordegraaf A, Channick R, Cottreel E, Kiely DG, Marcus JT, Martin N, et al. The REPAIR Study: Effects of Macitentan on RV Structure and Function in Pulmonary Arterial Hypertension. JACC Cardiovasc Imaging. 2022;15(2):240-53.
148. Knight DS, Karia N, Cole AR, Maclean RH, Brown JT, Masi A, et al. Distinct cardiovascular phenotypes are associated with prognosis in systemic sclerosis: a cardiovascular magnetic resonance study. Eur Heart J Cardiovasc Imaging. 2023;24(4):463-71.
149. Boucly A, Weatherald J, Savale L, de Groote P, Cottin V, Prévot G, et al. External validation of a refined four-stratum risk assessment score from the French pulmonary hypertension registry. Eur Respir J. 2022;59(6).
150. Hoeper MM, Pausch C, Olsson KM, Huscher D, Pittrow D, Grünig E, et al. COMPERA 2.0: a refined four-stratum risk assessment model for pulmonary arterial hypertension. Eur Respir J. 2022;60(1).
151. Ramjug S, Hussain N, Hurdman J, Billings C, Charalampopoulos A, Elliot CA, et al. Idiopathic and Systemic Sclerosis-Associated Pulmonary Arterial Hypertension: A Comparison of Demographic, Hemodynamic, and MRI Characteristics and Outcomes. Chest. 2017;152(1):92-102.
152. Craven TP, Tsao CW, La Gerche A, Simonetti OP, Greenwood JP. Exercise cardiovascular magnetic resonance: development, current utility and future applications. J Cardiovasc Magn Reson. 2020;22(1):65.
153. Le TT, Bryant JA, Ang BWY, Pua CJ, Su B, Ho PY, et al. The application of exercise stress cardiovascular magnetic resonance in patients with suspected dilated cardiomyopathy. J Cardiovasc Magn Reson. 2020;22(1):10.
154. Humbert M, Kovacs G, Hoeper MM, Badagliacca R, Berger RMF, Brida M, et al. 2022 ESC/ERS Guidelines for the diagnosis and treatment of pulmonary hypertension. Eur Heart J. 2022;43(38):3618-731.
155. Chin KM, Kim NH, Rubin LJ. The right ventricle in pulmonary hypertension. Coron Artery Dis. 2005;16(1):13-8.
156. Waddingham PH, Bhattacharyya S, Zalen JV, Lloyd G. Contractile reserve as a predictor of prognosis in patients with non-ischaemic systolic heart failure and dilated cardiomyopathy: a systematic review and meta-analysis. Echo Res Pract. 2018;5(1):1-9.
157. Poehlman ET, Scheffers J, Gottlieb SS, Fisher ML, Vaitekevicius P. Increased resting metabolic rate in patients with congestive heart failure. Ann Intern Med. 1994;121(11):860-2.
158. Ruggiero C, Metter EJ, Melenovsky V, Cherubini A, Najjar SS, Ble A, et al. High basal metabolic rate is a risk factor for mortality: the Baltimore Longitudinal Study of Aging. J Gerontol A Biol Sci Med Sci. 2008;63(7):698-706.
159. Wensel R, Opitz CF, Anker SD, Winkler J, Höffken G, Kleber FX, et al. Assessment of survival in patients with primary pulmonary hypertension: importance of cardiopulmonary exercise testing. Circulation. 2002;106(3):319-24.
160. Ferreira EV, Ota-Arakaki JS, Ramos RP, Barbosa PB, Almeida M, Treptow EC, et al. Optimizing the evaluation of excess exercise ventilation for prognosis assessment in pulmonary arterial hypertension. Eur J Prev Cardiol. 2014;21(11):1409-19.

161. Knight DS, Kotecha T, Martinez-Naharro A, Brown JT, Bertelli M, Fontana M, et al. Cardiovascular magnetic resonance-guided right heart catheterization in a conventional CMR environment - predictors of procedure success and duration in pulmonary artery hypertension. J Cardiovasc Magn Reson. 2019;21(1):57.
162. Ross L, Patel S, Stevens W, Burns A, Prior D, La Gerche A, et al. The clinical implications of left ventricular diastolic dysfunction in systemic sclerosis. Clin Exp Rheumatol. 2022;40(10):1986-92.